
Travail de fin d'études et stage[BR]- Travail de fin d'études : Stability of a system with high penetration of power electronic converters: impact of wind events and transmission outages[BR]- Stage d'insertion professionnelle

Auteur : Colot, Antonin

Promoteur(s) : Cornélusse, Bertrand

Faculté : Faculté des Sciences appliquées

Diplôme : Master en ingénieur civil électromécanicien, à finalité spécialisée en énergétique

Année académique : 2020-2021

URI/URL : <http://hdl.handle.net/2268.2/11507>

Avertissement à l'attention des usagers :

Tous les documents placés en accès ouvert sur le site le site MatheO sont protégés par le droit d'auteur. Conformément aux principes énoncés par la "Budapest Open Access Initiative"(BOAI, 2002), l'utilisateur du site peut lire, télécharger, copier, transmettre, imprimer, chercher ou faire un lien vers le texte intégral de ces documents, les disséquer pour les indexer, s'en servir de données pour un logiciel, ou s'en servir à toute autre fin légale (ou prévue par la réglementation relative au droit d'auteur). Toute utilisation du document à des fins commerciales est strictement interdite.

Par ailleurs, l'utilisateur s'engage à respecter les droits moraux de l'auteur, principalement le droit à l'intégrité de l'oeuvre et le droit de paternité et ce dans toute utilisation que l'utilisateur entreprend. Ainsi, à titre d'exemple, lorsqu'il reproduira un document par extrait ou dans son intégralité, l'utilisateur citera de manière complète les sources telles que mentionnées ci-dessus. Toute utilisation non explicitement autorisée ci-avant (telle que par exemple, la modification du document ou son résumé) nécessite l'autorisation préalable et expresse des auteurs ou de leurs ayants droit.



UNIVERSITÉ DE LIÈGE- FACULTÉ DES SCIENCES APPLIQUÉES

Stability of a system with high penetration of power electronic converters: impact of wind events and transmission outages

Travail de fin d'études réalisé en vue de l'obtention du grade de master
"Ingénieur Civil en Electromécanique" par

Colot Antonin

Année académique 2020-2021

Abstract

Nowadays, renewable energy sources take a larger share in energy production. The power systems encounter a significant turn because of the growth of renewable energy sources, which brings more power electronics into the grid. For instance, modern wind farms are equipped with full converter wind turbines to ensure a higher energy yield. Furthermore, HVDC links, equipped with power electronic converters, have become popular because of their controllability and are installed in various power systems. The power electronic converters replace the synchronous machines, and instabilities at higher frequencies may now occur. It thus has led to a reshape in the classification of power system stability. Wind turbines are placed where the wind potential is the highest. They are grouped in wind parks which concentrate large amount of active power production. Variations in wind speeds thus lead to rapid changes in the loading of the system, which may jeopardize its stability.

This thesis aims at assessing the stability of a system mainly composed of power electronic converters. A fictitious network is tested under various scenarios, and solutions are proposed to ensure a secure system for the different tests realized. The simulation tool used applies the phasor approximation method, therefore, the fast interactions that may occur between the converters and the network are not analyzed here.

The thesis is divided into five parts. The first part introduces the stability issues encountered in a power system mainly composed of power electronics. It also describes the classification of wind events and their intensity. The second part illustrates the network studied and the modeling of the converters. It highlights their different control modes. The third part focuses on wind events and their impact on the stability of the system. The evolution of the voltages is studied for two different wind events: the *Ramping event* and the *Storm event*. Those events are combined with operations on HVDC links. Their active power productions are changed according to the rules of the energy market. Solutions are proposed to mitigate the impact of those events on the network voltages. The fourth part focuses on transmission outages. Solutions are proposed to ensure a secure system after the incident occurred. Finally, the last part describes the necessity of having grid forming converters in the system. It shows the evolution of voltage phasors for the system with and without a grid forming converter. Finally, an overall conclusion is drawn.

Résumé

De nos jours, les énergies renouvelables prennent une part plus importante dans la production d'énergie. Les réseaux électriques subissent d'importants changements en raison de leurs croissances. Ces dernières contribuent à amener plus d'électroniques de puissance dans les réseaux. Par exemple, les parcs éoliens modernes sont équipés d'électroniques de puissance pour garantir le meilleur rendement énergétique. De plus, les liaisons HVDC, équipées de convertisseurs électroniques de puissance, sont devenues populaires grâce à leur contrôlabilité et sont à présent installées dans plusieurs réseaux électriques. Les convertisseurs électroniques de puissance remplacent les machines synchrones, et des instabilités à plus hautes fréquences peuvent désormais apparaître. Cela a conduit à une reclassification des instabilités dans les réseaux électriques.

Les éoliennes sont installées aux endroits avec le meilleur potentiel de vent. Elles sont souvent regroupées en parcs, ce qui concentre ainsi une grande partie de la production de puissance active. Les variations dans les vitesses de vent provoquent des changements rapides dans le chargement du réseau, ce qui peut compromettre sa stabilité.

Ce mémoire évalue la stabilité d'un système composé principalement de convertisseurs électroniques de puissance. Un réseau fictif est testé sous différents scénarios et des solutions sont proposées pour assurer l'opération sécurisée du réseau pour les différents tests réalisés. L'outil de simulation utilisé applique l'approximation phaseur, dès lors, les interactions rapides pouvant survenir entre les convertisseurs et le réseau ne sont pas analysées ici.

Le mémoire est divisé en cinq parties. La première partie présente les problèmes de stabilité rencontrés dans un système de puissance majoritairement composé d'électroniques de puissance. Elle décrit également la classification des événements de vent et leur intensité. La deuxième partie discute du réseau étudié et de la modélisation des convertisseurs. Elle met en évidence leurs différents modes de contrôle. La troisième partie se concentre sur les événements de vent et leur impact sur la stabilité du système. L'évolution des tensions du réseau est étudiée pour deux événements de vent différents : le *Ramping event* et le *Storm event*. Ces événements sont combinés avec des opérations sur les liaisons HVDC. L'injection de puissance active des liens HVDC est modifiée selon les règles du marché de l'énergie. Des solutions sont proposées pour atténuer l'impact de ces événements sur les tensions du réseau. La quatrième partie porte sur les incidents dans le réseau électrique. Le système est perturbé par l'événement de vent et est donc opéré loin de son point de fonctionnement optimal. Des solutions sont proposées pour assurer un système opérable après l'incident. Enfin, la dernière partie décrit la nécessité d'avoir des convertisseurs *grid forming* dans le système. Elle montre l'évolution des phaseurs de tension pour le système avec et sans convertisseur *grid forming*. Enfin, une conclusion générale est dressée.

Acknowledgements

I would like to thank ELIA and Mr. *Olivier Bronckart* for allowing me to work on this interesting subject. I had the chance to carry this thesis out as I wanted to. He provided me the information I needed, and his remarks were crucial to give more sense to the work I've done.

I would also like to thank Prof. *Bertrand Cornélusse* for his availability. He was always ready to discuss, and his advice helped me to complete this thesis.

I would like to express my gratitude to Prof. *Thierry Van Cutsem*. He helped me since the beginning, and our long discussions were always fascinating and instructing. His enthusiasm helped me get through this work, and he passed me on his passion for power systems, such that I've never got bored during these past few months. He also gave me the opportunity to work on a complete and detailed model, without which I would not have been able to carry this thesis out.

Finally, I would like to thank my family. They gave me the chance to complete my engineering studies, and they always supported me even though they did not understand a word of what I was doing.

Contents

1	Introduction	1
2	Intermittency of renewable energy sources' production : Importance of wind speed fluctuations	3
2.1	Classification of extreme wind events	3
2.2	Extreme wind events : how to deal with them ?	5
3	Overview of stability issues in a power system with high integration of converter interfaced generation	7
3.1	Frequency stability	7
3.2	Voltage stability	8
3.3	Rotor angle stability	10
3.3.1	Transient stability	10
3.3.2	Small-disturbance stability	11
3.4	Converter-driven stability	11
3.4.1	Fast interactions	12
3.4.2	Slow interactions	12
3.5	Resonance stability	13
4	Network description	14
4.1	Working principle of grid following and grid forming converters	15
4.1.1	Concept of active power control in a simple circuit	15
4.1.2	Modeling of the grid following converters	16
4.1.3	Modeling of the grid forming converters	22
4.2	The simulation tool	26
5	Impact of wind events and HVDC operations on the system stability	27
5.1	From a lightly loaded system to a highly loaded system : The <i>Ramping event</i> scenario	27
5.1.1	Description of the sequence of events	27
5.1.2	Influence of the sequence of events on the power flows and on the network frequency after the network balancing	29
5.1.3	The different types of control available for the reactive power loop of the wind parks	30
5.1.4	Wind parks WP1 and WP2 are in voltage control mode: <i>configuration V</i>	30
5.1.5	Wind parks WP1 and WP2 are in reactive power control mode: <i>Configuration Q</i>	35

5.1.6	Wind parks WP1 are in reactive power control mode and wind parks WP2 are in voltage control mode: <i>Configuration VQ</i>	41
5.2	From a highly loaded system to a lightly loaded system : The <i>Storm event</i> scenario	44
5.2.1	Description of the sequence of events	45
5.2.2	Influence of the sequence of events on the power flows and on the network frequency after balancing	46
5.2.3	The different options available for wind parks after being impacted by the storm.	47
5.2.4	Wind parks WP1 and WP2 are disconnected from the grid: <i>Configuration AllTripped</i>	47
5.2.5	Wind parks WP1 are disconnected from the grid and wind parks WP2 stay connected: <i>Configuration WP1Tripped</i>	50
5.3	Conclusion	51
6	Impact of a transmission outage on the network post wind event	53
6.1	Incident in the network post <i>Ramping event</i> : Loss of the green circuits . . .	53
6.1.1	Description of the incident	53
6.1.2	The different scenarios analysed	53
6.1.3	Scenario 1	54
6.1.4	Scenario 2	59
6.1.5	Global Results	61
6.1.6	Scenario 3	65
6.1.7	Scenario 4	67
6.1.8	Scenario 5 & Scenario 6	68
6.2	Incident in the network post <i>Ramping event</i> : Three-phase short-circuit at TORPAH cleared by the tripping of the green circuits	71
6.2.1	Description of the incident	71
6.2.2	Scenario 1	71
6.2.3	Comparison between scenarios 1 and 2	72
6.2.4	Scenario 5	73
6.2.5	Conclusion	73
6.3	Incident in the network during <i>Storm event</i> : Loss of HVDC-AB before the automaton connects a shunt inductor	74
6.3.1	Description of the incident	74
6.3.2	Results	75
6.4	Conclusion	77
7	HVDC-AC in grid following mode	79
7.1	The different scenarios analyzed	79
7.2	Scenario α	80
7.3	Scenario β	81
7.4	Scenarios γ and γ'	81
7.5	Scenario δ	82
7.6	Conclusion	83
8	Conclusion	84

9	Appendix	i
9.1	Acronyms	i
9.2	Power flows: <i>Ramping event</i>	ii
9.3	Power flows: <i>Storm event</i>	iii
9.4	<i>Configuration Q+Automaton version 2</i> : HVDC-AC power shift variant . .	v
9.5	Influence of the maximum current magnitude of HVDC-AC on the network stability post incident	vi
9.6	<i>Scenario 1</i> : Influence of HVDC-AC synthetic inertia on the active power production and voltage phasors	vii
9.7	<i>Scenario 3</i> : Influence of the maximum ramping rate of HVDC-AB direct current and the value of the synchronous condensers gain on the voltages of the wind parks	viii
9.8	Network post <i>Ramping event</i> : Preventive actions to ensure a safe system .	ix
10	Bibliography	xi

Chapter 1

Introduction

In Europe, wind energy is picking up an important part of electricity production. In 2019, 15.4 GW of additional wind power capacity has been installed, raising the overall capacity to 205 GW ([33]). As wind power has developed, the percentage of electricity demand covered by wind power has increased. Denmark, one pioneer in wind energy, reached a 49% share of wind power in their electricity mix in 2019. As the penetration of wind energy reaches high percentages, the impact on the power system stability should be reviewed.

Wind technology is developing and wind turbines have a bigger rated size. Wind farms are distributed all around the country in special windy sites to maximize the energy yield. In Belgium, as most of the good windy sites onshore have been already exploited, the establishment of large offshore wind farms becomes more common. The tendencies presented in [33] confirmed that in 2019, the biggest part of the new wind capacity was built offshore, further away from the land, attached to the rest of the transmission grid by only a few lines. Furthermore, wind energy is recognized as a decentralized production as the location does not depend on the electricity demand ([19]) and thus, power has to flow over longer paths before reaching load centers. Large offshore wind farms, because they are concentrating an extensive volume of power and, most of the time, because they are far away from any load centers, can jeopardize the system as extensive amount of power has to rush along only a few lines. Another issue stems from the unreliability of wind power production.

Renewable energy sources are unpredictable because they depend on the weather. When all offshore wind capacity is concentrated in a tiny area, weather variations could greatly alter the production of wind parks and the power flows. As, occasionally, those phenomena happen rapidly, the grid operator may not react in time and the electrical network would then be conducted far from its optimal working point. Furthermore, as the system is operated close to its stability limits, an incident could bring instabilities.

Even though forecasting tools are now becoming more accurate, what actions should be taken in case of those events occur to ensure a stable system? This is the question addressed by this Master's thesis.

This thesis is subdivided into three parts. The first part addresses the issues related to strong changes in wind conditions. Those variations affect wind power production, thus, the power flows. The wind events are also combined with HVDC operations. The

HVDC links play a major role as they convey vast amount of power in or out the system. The voltage levels reached after the wind event are then analyzed and solutions are proposed to ensure acceptable voltage levels. The second part aims at analyzing the system dynamics after a transmission outage. The last part introduces the importance of a grid forming converter in the system studied.

In the following, explanations on issues related to wind speed variations are given. Then, an introduction to stability issues provoked by converter interfaced generation is presented. This serves as an overview of the large topic that is power system stability with high integration of renewable energy sources. Finally, the network and the converters' models are described before getting into the simulation results.

Chapter 2

Intermittency of renewable energy sources' production : Importance of wind speed fluctuations

2.1 Classification of extreme wind events

As it has been pointed out, one of the major drawbacks of wind energy is its unpredictability. The wind speeds may vary in a brief time, thus, the wind power also fluctuates following the wind speed variations. Those fluctuations can be reflected on the grid depending on the type of wind turbine used. Several wind speed fluctuations exist. A previous study ([8]) on offshore wind integration from ELIA, the Belgian transmission system operator (TSO), has shown severe issues associated with high wind speed fluctuations that they called *storm events* and *ramping events*. The *storm event*, according to their definition, corresponds to a disconnection of wind capacity because of wind speeds exceeding the limit (cut-out wind speed) followed by a reconnection once the wind speeds have sufficiently decreased. In a short amount of time, the system loses a large fraction of its power production and once the storm passed the wind farm, wind turbines are restarted thus, raising their active power production. Indeed, the typical wind power curve is shown in Figure 2.1 and one can observe that, after a specific wind speed, the wind turbine is shut down and its active power production drops to 0MW. Some wind turbines embed high wind ride through capability ([24]), or storm ride through capability, which makes them able to stay connected and permits them to produce power even though the wind speed is above the cut-out wind speed. Furthermore, as there is no hysteresis loop, once the wind speeds go below the maximum wind speed that the turbine can handle, the turbine can start again.

The research carried out by ELIA showed faster dynamics in the restart causing fluctuations up to 1000MW in 15 minutes (67MW/min) when a total capacity of 2300MW of offshore wind power is considered. *Ramping events* are also extreme scenarios where a rapid power loss or gain results from wind speed fluctuations. In their study, ELIA focused on large power imbalances that occur if no measures are taken. They define a way to deal with a rapid loss or gain of wind power with the help of forecasting tools.

One can get definitions of several extreme wind events in [20]. Among them, the case of the cyclone Xaver that ran over the North Sea in December 2013 is reported. Wind

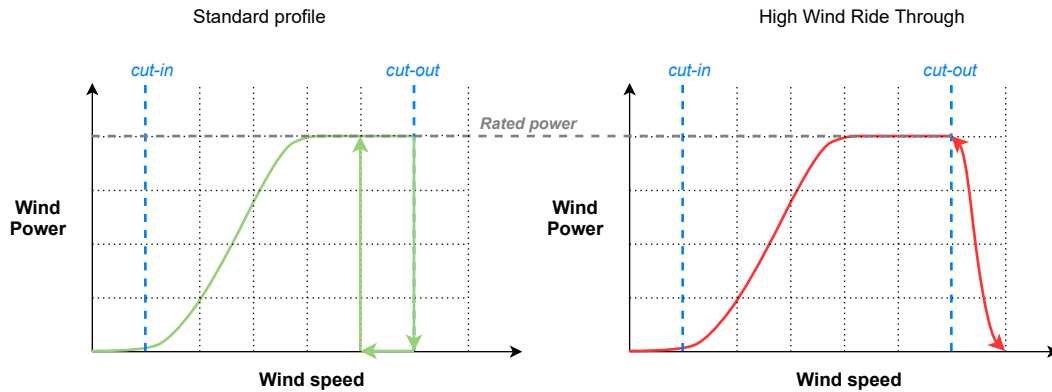


Figure 2.1: Typical profiles for wind power curves. Two profiles are shown, the standard with the hysteresis and the other one when the high wind ride through technology is implemented.

speeds over 25 m/s have been measured for over 30 hours. Those extreme wind speeds would lead to wind parks shut down. The same article also proposes a definition for wind ramps. This definition diverges from the one found in ELIA's study, as it also considers wind direction. Indeed, wind ramps correspond to rapid changes in wind speeds or direction. Those sudden changes in direction lead to the reorientation of the rotor and a sudden drop in the active power production. The time scale for ramp events can range from 5 minutes to 6 hours and the power fluctuations can vary between 10% to 75% given as a percentage of rated power.

In [11] a more detailed definition of ramp events can be found. It is characterized by:

- A magnitude ΔP_r given as a percentage of the rated power,
- a duration Δt_r .

Using those two variables, a ramp rate that corresponds to the quotient of those quantities can reveal the harshness of the phenomenon. An example is shown in Figure 2.2.

One can find more definitions about ramping events in [10], emphasizing the fact that the limits of the phenomenon are hard to determine. The article provides better definitions of upward and downward ramp events. Whereas cyclones, thunderstorms, or wind gusts provoke upward ramp events, characterized by an increase in wind power, downward ramp events can result from other wind conditions. Indeed, it can be a reduction in wind speed leading to a drop in wind power production, but an increase in wind speeds can also provoke power reductions. The wind speeds could override the cut-out wind speed, shutting down the wind turbines to avoid mechanical damages.

As presented in [6], wind ramps can have notable effects even though they can be forecasted. As described in the report, the Electric Reliability Council of Texas (ERCOT) called for an emergency plan because of the large power imbalance due to a large extent to wind power fluctuations in their zone. Even though the ramping event was forecasted, it has been merged with a load ramping and led to serious imbalances in the network. The ramping event causes the system to lose 8MW per minute for 3 hours and a half. This is not an extreme event as the wind power reduction is pretty small. But as the

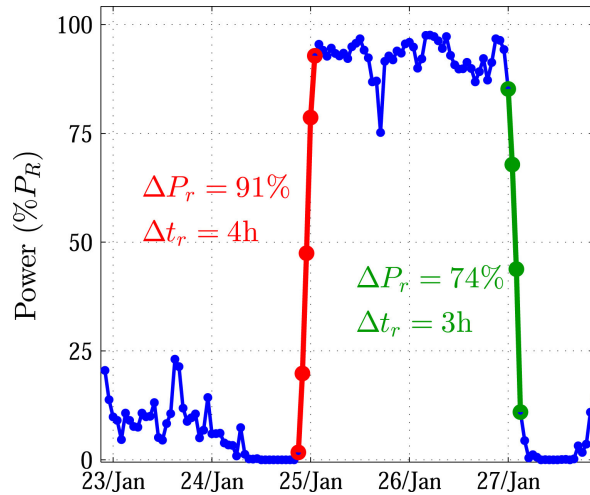


Figure 2.2: Example of two ramp events. Both ramp up and down are represented, and the data has been extracted from a wind park in Spain ([11]).

experience shows, the mix of several factors like load ramping up coupled with wind generation ramp-down can affect the system more than expected. Larger wind ramps would have larger consequences. As stated in the report, ERCOT can expect a wind event with a power reduction of 93MW/min for a wind fleet of 15000MW. This kind of event can arise once a year according to ERCOT.

Finally, article [3] evaluates a scenario for 2030 where 81GW of wind power is installed in the North Sea. It shows that the largest ramping event the system could expect is the loss of 61GW in 340 minutes (179MW/min). The sudden disconnection of wind turbines because of excessive wind speeds would induce this large loss.

As explained in the articles cited in this chapter, weather changes could lead to severe upward or downward ramp events. *Storm events* are a part of those ramp events as they are downward ramp events provoked by the protection of wind turbines against excessive wind speeds. They lead to the largest drop in active power production. On the other hand, the ramp events induce large changes in the power flows in such a short amount of time that it is difficult for an operator to react in time. This chapter aimed to assess the criticality of those wind events to better draw some credible scenarios. It reveals the rapidity of the phenomena for a human being but these are still very slow phenomena for automatic controllers. Those scenarios are analyzed in the pursuing of this thesis.

2.2 Extreme wind events : how to deal with them ?

In the study presented by ELIA and all the papers mentioned in section 2.1, the forecast tool performances are essential. Wind events are of particular importance in a country like Belgium as the offshore wind farms are very close to each other. Therefore, large amounts of wind energy can be lost quickly when such events happen. This situation is specific to Belgium as other countries have offshore wind farms that are disseminated all over their territory. Nevertheless, for countries with a large share of wind power in their electricity mix, changes in wind conditions can create large imbalances. Denmark has a very high penetration of wind energy, sometimes the demand is entirely covered by

wind production ([15]). Even though wind farms are spread all over the country, wind events can jeopardize the Danish system as power imbalances are much harder to handle. Hence, powerful forecasting tools have been developed and some strategies are used to deal with storm events. The method suggested in [4] describes a tool to plan wind farm shut down most efficiently. The wind parks studied are on the west coast of Denmark, where there are strong winds. It is said that a good assessment is of crucial importance. Indeed, if the wind speeds overcome the cut-out wind speed for a short amount of time (wind gust), only a part of the wind parks will shut down, most of the wind turbines could still run. If one has decided, with the help of the forecasting tool, to shut down the wind parks because of the excessive wind speeds, it would lead to useless energy losses. If the wind event, on the other hand, is not a wind gust but a storm that will pass over several wind parks, the preventive shut down of wind parks becomes essential. Indeed, the rapid and unexpected loss of energy can be critical for the system as wind power represents an important part of the electricity production. Thus, if a storm is detected, strategies are applied for a progressive shutting down of wind turbines to avoid a large drop in power production in a brief time. But the forecasting tool has to be accurate enough to detect what wind event the wind parks will encounter. One can notice the same conclusion in the study made by ELIA where specific strategies are defined with the help of forecasting tools.

Even though the wind events are forecasted, they can lead to severe issues, as [6] shows with the ERCOT event. Those events are rapid and can prevent the grid operator from reacting fast enough. The weakened system would become more prone to stability issues.

Chapter 3

Overview of stability issues in a power system with high integration of converter interfaced generation

When power system stability is examined, one can look at different specific issues. The power system stability can be sliced into different branches, as is seen in Figure 3.1. The graph is taken from [18] that reconsiders the stability issues for a high concentration of converter interfaced generation in power systems.

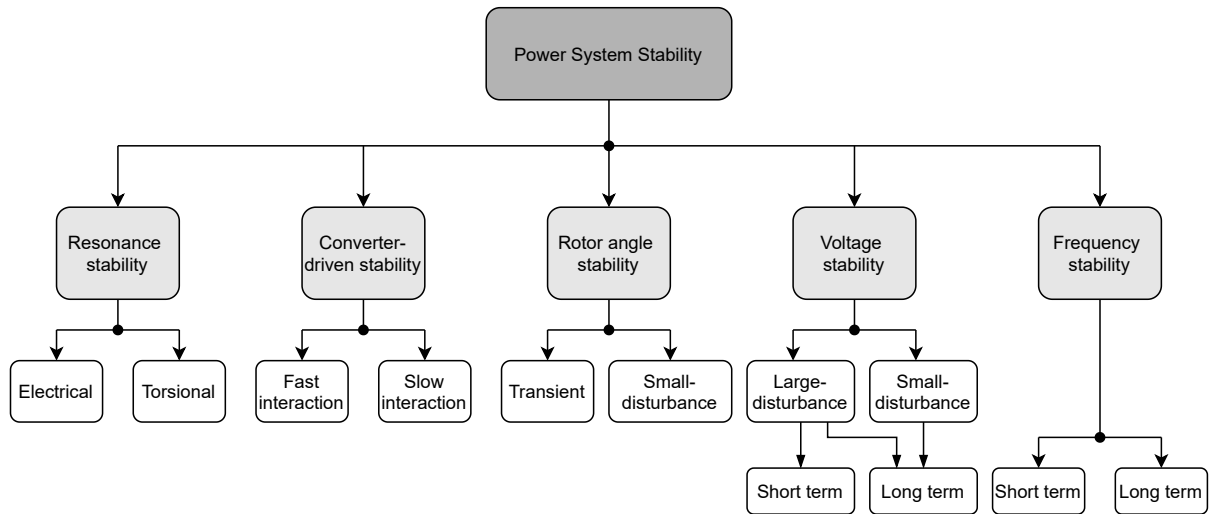


Figure 3.1: Overview of power system stability ([18]).

3.1 Frequency stability

Large power variations in a short amount of time affect the frequency. This is one of the major issues when dealing with system with high wind power penetration. Wind speed fluctuations disturb wind energy production and generate power imbalances that impact the frequency of the network. Therefore, the growing penetration of wind energy in modern power systems involves a larger amount of spinning reserve to oppose the potential loss of large active power injections ([1]). In [12], the amount of spinning reserve to be allocated by the TSO can reach 10% of the wind power installed capacity if the wind

power integration overreaches 10% of the total capacity available.

One other issue related to wind turbines is the potential decrease in the system's inertia. Modern wind turbines are decoupled from the grid (full-converter wind turbines). Therefore, wind turbines' inertia cannot help when encountering large power variations to prevent a too high rate of change of frequency (RoCoF). As wind turbines are replacing synchronous machines that were bringing large inertia to the system, the RoCoF is higher in a system mainly composed of power converters. Because of that, wind turbine manufacturers proposed the principle of synthetic inertia ([13]). In normal operation, wind turbines are equipped with a maximum power point tracking system (MPPT) that always extracts the maximum energy from the wind. Therefore, the wind turbine does not have any reserve of active power that can be used in case of a sudden drop in frequency. When synthetic inertia is implemented, the MPPT is overruled and the kinetic energy stored in the rotor is consumed. It has been shown in [13] that this synthetic inertia is very useful to limit the RoCoF and the frequency nadir. It also leaves more time for synchronous generators to react to the frequency disturbance. Nevertheless, the inertia in the control loop must be correctly tuned, as it can lead to a severe drop in the rotational speed of the machine if it is not correctly set. Furthermore, following the disturbance, the rotor will have to speed up again, thus it will draw active power from the network.

As the total system's inertia is diminished in a power system with high integration of power electronics, the need for fast primary frequency response to arrest the frequency drop is crucial ([18]). This is something that converter interfaced generation can offer as the only limit they have is the response time of power electronics. A good design of a fast-acting controller to arrest frequency drop can troubleshoot the issue caused by the system's inertia decrease.

The subject of the impact on the frequency stability of a low inertia power system has already been largely examined. This problem is not studied in this thesis.

3.2 Voltage stability

Large variations in active power cause not only frequency stability issues but also influence the voltages. To illustrate these phenomena, the following example has been taken from [16]. One assumes that wind turbines have very poor low voltage ride-through capability and their reactive power capability is limited by the use of wind turbines' capacitors, added with those at the nearby substation. The wind farms are connected to the rest of the grid by overhead lines that are highly loaded, as wind farms produce an extensive amount of active power. Those lines are loaded at four times their surge impedance load and therefore, they drain a vast amount of reactive power. To provide this reactive power and preserve a decent voltage at the point of common coupling (PCC), capacitors are switched on. If a short circuit occurs at one wind turbine, the voltage drop causes the entire wind farm to be shut down. This quick change in line loading induces a complete change in the reactive power flows, leading to a surplus of reactive power production that raises the voltage at the PCC. If the wind farm is connected to a weak grid, the voltage deviation propagates through the entire grid, building up the voltages to unacceptable values at different places. Other wind farms could disconnect because of the excessive voltage magnitude, enlarging the amount of residual reactive power. A cascading effect can arise as wind farms are disconnected one after another. From this example, the paper details an effective voltage control system to prevent cascading issues. Each wind farm would be equipped with a voltage controller and a master system would command those

controllers.

Several key elements for voltage instabilities have been highlighted in this practical example. One can say that instabilities are likely to arise if:

- wind turbines do not have low voltage ride through capability (LVRT) or fault ride through capability (FRT),
- the voltage control of wind parks is very limited,
- only a few lines are connecting the wind parks to the rest of the grid.

The LVRT capability is enforced in modern wind turbines and therefore, it is assumed that wind turbines are now capable to operate under very low voltages. This is also a grid code requirement. This feature is relevant when dealing with short-circuits as it has been shown in [17]. With large-scale integration of wind power, the sudden disconnection of an extensive amount of wind power because of a voltage drop could jeopardize the system's stability. For this reason, wind turbine manufacturers have implemented LVRT. With a doubly-fed induction generator wind turbine, when a short-circuit takes place, a crowbar is added to reduce the rotor currents whereas the converter is disconnected. The wind turbine works as an induction generator with a large rotor resistor during the short-circuit. In full-converter wind turbines, a chopper circuit in the DC link is added to restrict the DC voltage ([23]). This ability to stay connected is important in terms of transient voltage stability and voltage stability. First, as it has been shown previously, it avoids numerous disconnections that could change the power injections. Furthermore, in the case of a short-circuit, the wind turbine could help to preserve the voltages after the fault clearance because of its reactive power capability.

The second point suggested as a key element is the voltage control of wind parks. Modern wind turbines are equipped with power electronics, allowing better controllability of the wind turbine and ensuring higher energy yield. The power electronics permit the wind parks to regulate the voltage at the PCC. If the wind parks control the voltage, they become useful after the incident occurred as they can preserve the voltages at the PCC (if the converter's limits have not been reached). But to maintain the voltages, the wind parks have to produce or consume reactive power. This reactive power injection can be at the price of the active power injection. Hence, even though wind turbines can control the voltage at the PCC, they rely a lot on external components to maintain the voltages. The wind parks have also the possibility to regulate their reactive power injections and thus, they do not control the voltages. In that case, the wind parks rely on the external components to guarantee a decent voltage at the PCC.

During and after an incident, the wind parks could provide some help to the grid but they are not designed to support constantly the network. If there is a lack of synchronous machines, specific network components can be used like SVC, STATCOM, or synchronous condensers.

Several articles covered the topic of voltage stability issues for a system with large-scale wind power integration. One tool to assess voltage stability is the PV curve, which relates the voltage magnitude regarding the active power consumption at the load side. It is of particular importance for most of the wind parks as they are connected to the rest of the grid by only a few lines. Therefore, when active power is flowing from the park to the rest of the grid, the voltages are affected as the maximum transmissible power is easily reached. In [32], an impedance modulus and a voltage stability index are used to

assess voltage stability. The aim was to find the optimal wind power capacity that can be installed to ensure voltage stability and to use fully the network. Using reactive power compensators helps for providing a stable voltage. In [22], the authors carried out the same conclusion. It is also shown that the ratio between reactive power compensation and active power production increases as wind power integration takes a larger share of the total production of active power. Researches have also been realized to minimize the amount of reactive power transfer to guarantee voltage stability. In [25], a control strategy using two SVC at two different locations permits acceptable voltage levels while limiting the reactive power transfer from wind parks to the rest of the grid. Finally, the proposed system allows for an operation as close as possible to the thermal limits of the lines without threatening voltage stability.

The wind parks are situated where the wind potential is the highest. Most of the time this means that the wind parks are far away from the load centers, where the grid is not well meshed. Therefore, important active power flows have to rush through only a few lines over long paths. That exposes the grid to instabilities ([12]). Hence, a grid reinforcement is required to prevent those instabilities.

Wind power plants replace conventional power plants with their synchronous machines. Large synchronous machines are sometimes called the workhorses of the electrical network. Indeed, with their large inertia, they ensure stable frequency under imbalances and maintain voltage levels close to their nominal values. In a grid with large integration of wind energy and therefore, a low concentration of synchronous machines, voltage levels could not be as well controlled as needed. The comparison between synchronous machines and power electronics on their impact on the grid stability is a major subject as there are more and more power electronics in modern power systems. For instance, there are major differences in terms of power system stability if grid-forming or grid-following converters are used ([26]). Indeed, grid forming converters, as the name shows, act as a source of voltage waveform, they *form* the grid. The grid following converters need a strong grid to operate as they *follow* the grid.

The voltages are analyzed in this thesis as large variations in the power flows occur because of wind events.

3.3 Rotor angle stability

3.3.1 Transient stability

The transient stability characterizes the behavior of the system and its stability under transient phenomena. One common transient phenomenon in a power grid is the short circuit. Usually, the worst short-circuit, the three-phase short-circuit, is used to investigate the transient stability of a grid component. In a power system with high integration of wind energy, the transient stability is different compared to a system dominated by conventional generator plants. The transient stability is influenced by the type of wind turbine for instance. The first type of wind turbine is the oldest and is not installed anymore nowadays. It comprises a simple squirrel cage induction generator with no power electronics interface. When a short-circuit occurs, those types of wind turbines release high reactive currents, limiting the voltage drop. But, after the short-circuit clearance, the

induction generator consumes a lot of reactive power to re-magnetize and is not helping in voltage recovery. Because of their inappropriate behavior concerning transient stability, those types of wind turbines were disconnected from the grid during large disturbances. Type 2 wind turbines are the same as type 1 except that there is a variable rotor resistance in the induction machine. This provides better controllability of the machine but in terms of transient stability, it changes nothing.

Type 3 and 4 wind turbines can help during large disturbances. As it has been revealed in [9], thanks to their reactive power capability, wind farms could enhance the critical clearing time in specific grid topologies. The critical clearing time is the maximum time allowed to get rid of the disturbance without destabilizing the power system. It has been also shown that the wind park location has a great impact on transient stability, as it changes the power flows through the lines.

The transient stability is referred to as a lack of synchronizing torque ([18]), the mechanical and electromechanical torque are not equal anymore. It thus involves large rotor angle excursions that can desynchronize the synchronous machines. For synchronous machines, a maximum angle is defined. If the rotor angle goes above this maximum angle, the machine loses its synchronism. As the total system's inertia is lowered in power systems with large integration of power electronics, the rotor angle deviation during transient events can be emphasized thus, making the loss of synchronism more likely to occur.

The grid forming converters equipped with synthetic inertia have similar dynamics that synchronous machines during transient phenomena. As the synchronous machines, they can lose synchronism because they overreach the maximum angle value, as shown in [28].

3.3.2 Small-disturbance stability

The lack of damping torque leads to small-disturbance oscillatory instabilities ([18]). Integrating converter interfaced generations affects this stability by lowering the damping torque of nearby synchronous generators or by changing the flows on important lines that could affect the damping of inter-area modes. Furthermore, the displacement of synchronous generators with power system stabilizers (PSS) caused by the increased penetration of converter interfaced generations, enhances some oscillatory instabilities. The small-signal dynamics of power converters give rise to resonance instabilities that could vary in frequency from sub-synchronous to harmonics of several kHz, depending on the grid conditions and the converter's bandwidth ([26]).

The network studied has too many components to be studied with small-signal analysis. This is not analyzed further on.

3.4 Converter-driven stability

A power electronic converter is composed of control loops and algorithms with fast response times. While the outer control loop has a relatively slow response time, the inner control loop, and the phase-locked loop (PLL), if there is one, are faster. Therefore, power electronics impact a wide timescale and it thus results in a cross-coupling with both the electromechanical dynamics of machines and the electromagnetic transients of the network, which creates instabilities over a wide range of frequencies ([18],[26]). Therefore,

two types of interactions can be studied; the fast interactions that concern the PLL and the inner control loop, and the slow interactions that involve the outer control loop.

3.4.1 Fast interactions

The fast-response of power electronics coupled with the fast-response of other components of the transmission network drives the fast interactions.

This could be several inverters close to each other that interact, as shown in [30]. In this paper, it has been concluded that, in the case of a grid with a low short circuit current, interactions between synchronization units of different inverters located nearby become stronger. Usually, the instabilities occur when the grid is weak. A grid is weak if the short-circuit ratio (SCR) is low. The SCR is specified as the ratio of the short circuit capacity of the grid to the rated power of the connected generator ([28]). The SCR can be calculated at every node of the grid and the larger it is, the stronger the grid is. A grid is announced as weak if the SCR is below 3 ([14]).

This could also be the inner control loop of one inverter interacting with passive components of the system, as shown in [31]. In this article, shunt capacitors in the inverters' filters and the cables interact with the inner control loops of inverters. In the same way, inner control loops of the inverter can trigger some resonant frequencies of the system. All those interactions would lead to high-frequency oscillations from tens to hundreds of Hz, and possibly to kHz.

The simulation tool for this thesis (RAMSES) uses the phasor approximation therefore, the fast interactions could not be detected in the results as the method does not model those dynamics. To get the full dynamics of the converters, Electromagnetic Transient Program (EMTP) software should be used. Nevertheless, the EMTP software calculations are much heavier compared to the phasor approximation method, which prohibit the simulation of a large network with EMTP software ([5]).

3.4.2 Slow interactions

The slow interactions stem from the slow dynamics of the outer control loop and the PLL of the converter with the rest of the network. The root cause of instabilities is often linked to the fact that the maximum power transfer between the converter and the weak system is reached ([18]).

Various papers show that instabilities are likely to occur if voltage source converters are installed in a weak grid, i.e a grid with low SCR ([34],[27],[2]). Those instabilities can be reduced if one chooses the proportional gains of the outer control loop and the response time of the PLL small enough. Unfortunately, there are some practical limits imposed by the filters used to restrict the harmonics and eliminate the noises ([18]). Those instabilities, and other disadvantages that the grid following converters bring, have led to other control strategies without a PLL ([29]).

In weak networks, large and fast changes in the phase angles during transients can occur. Those changes are hard to follow for the PLL that would give an incorrect angle value to the current control loops. This would lead to an improper injection into the system. That is one reason the grid following converters introduce instabilities under weak grid conditions as the angles are not correctly maintained. In a weak grid, a grid forming converter could therefore be needed ([29]). Or the grid can be strengthened by adding synchronous condensers for instance.

Some of the slow interactions can be grasped by the phasor approximation.

3.5 Resonance stability

The resonance occurs when components exchange energy periodically. It induces oscillations and when the amplitude of oscillations overreaches specific thresholds; it is said that the system meets a resonance instability. The interaction between the shaft of a turbine generator and the series compensators located nearby could provoke the resonance. If it is the case, the resonance is therefore recognized as a torsional resonance. The torsional resonances can lead to damages to the turbine shaft. The resonances could also be affected by inverters or power system stabilizers (PSS). The other type of resonance is the electrical resonance provoked by the interaction between the series compensators and the electrical characteristics of a machine. Once again, the converters placed nearby could interact with those resonances and it can bring large currents and voltages that could threaten the integrity of the power system and its components ([18]).

The resonance frequencies are not part of the dynamics modeled by the phasor approximation method. Therefore, they are not analyzed.

Chapter 4

Network description

The network studied is presented in Figure 4.1. It is composed of wind parks and HVDC links characterized by their voltage source converters (VSC). Two operation modes are implemented for those converters, the grid following and the grid forming modes. The difference between the two of them will be explained later.

For the wind parks, only the DC/AC converter (the grid side converter) is defined. The DC bus voltage is kept constant whatever the power injections of the grid side converter. In the network scheme, WP1 and WP2 represent the wind parks. WP1 and WP2 correspond to an aggregation of several wind parks. The wind parks themselves depict a group of several wind turbines that are not modeled individually.

For the HVDC links, only the DC/AC converter is considered and the DC link is not modeled. Once again, the DC bus voltage is presumed to stay constant whatever the power injections of the converter.

In the network, several synchronous machines can also be found. The machines are equipped with an automatic voltage regulator (AVR) and with over-excitation limiter (OEL). They can control their terminal voltage. The machines do not have a speed governor, therefore they do not take part in primary frequency regulation.

Some load tap changers (LTC) are implemented for the connection between the wind parks and the rest of the grid. The time between two tap changes is 10s for the wind parks WP1 whereas it is 7s for the wind parks WP2. The voltage deadband is 1%.

An equivalent node is included to represent the rest of the network. The equivalent line impedances have been tuned to match a specific short-circuit power. Two synchronous machines and one load are connected to the equivalent node. One synchronous machine has a rated size of 33 000MVA and has a primary frequency control. It simulates the response of the network if an imbalance occurs. The other synchronous machine has a rated size of 297 000MVA and simulates the inertia of the rest of the network. The load is used to consume the active power production of the two machines.

Four different control areas are considered in this network; A, B, C, and Equiv. The control area A is the studied one. Control area B is connected to control area A through the HVDC link HVDC-AB. HVDC-AB is implemented in grid following mode. The control area B represents another control area with which control area A trades active power. Control area Equiv is connected to control area A through the equivalent lines. The control area Equiv represents the rest of the network. Finally, control area C is connected to control area A through the HVDC link HVDC-AC. HVDC-AC is implemented in grid forming mode.

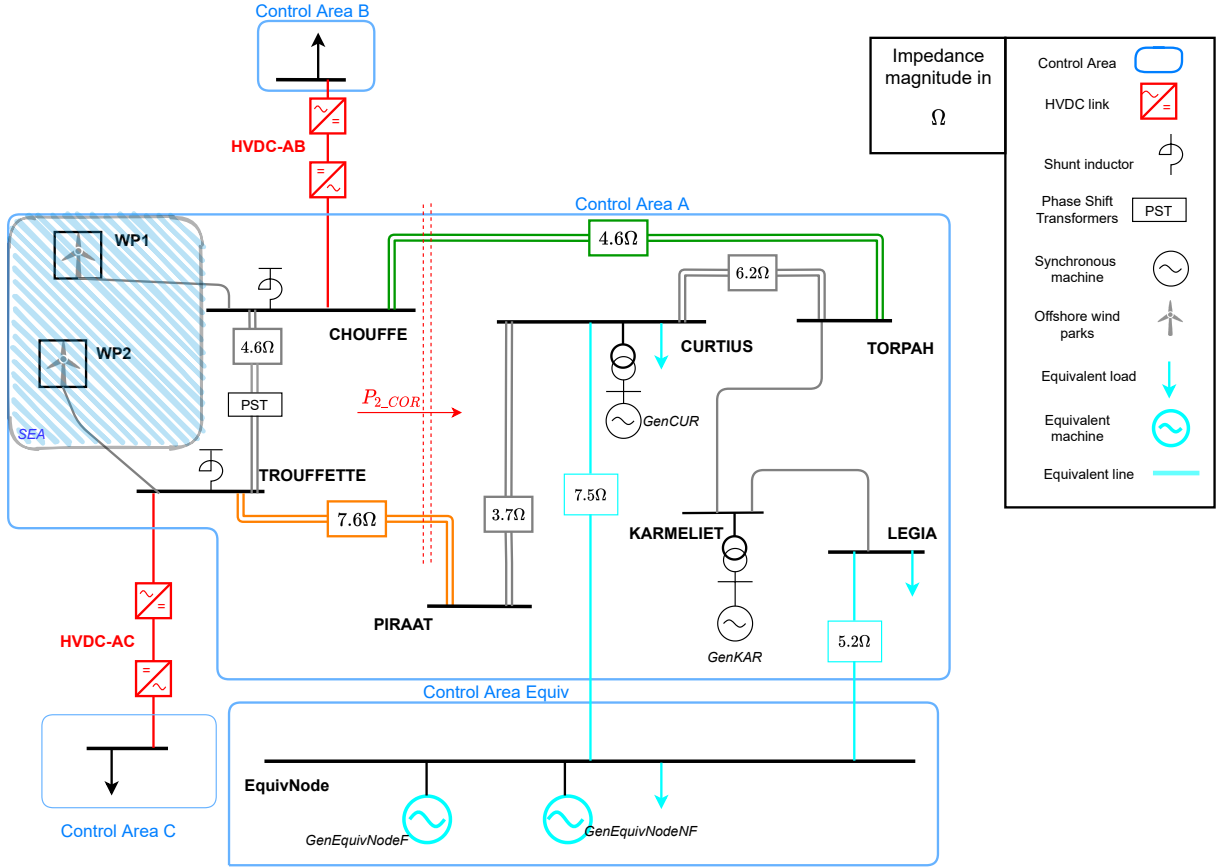


Figure 4.1: Scheme of the network studied.

4.1 Working principle of grid following and grid forming converters

4.1.1 Concept of active power control in a simple circuit

Figure 4.2 aims to describe the simple circuit that represents the connection between the grid and the converter. It helps to determine what parameters influence the transfer of power from the source \bar{V}_m to the grid \bar{V}_g .

From Figure 4.2, one way to express the reactive and active power output is shown in (4.1).

$$\begin{aligned} P_g &= V_g I_g \cos(\delta_g - \psi) = V_g I_P \\ Q_g &= V_g I_g \sin(\delta_g - \psi) = V_g I_Q \end{aligned} \quad (4.1)$$

From this simple derivation, one can observe that, for controlling the active power, one has to adjust the active current I_P . The phasor diagram showing the currents and voltages is illustrated in Figure 4.2 where the angle ψ is negative whereas the angles δ_g and δ_m are positive.

An alternative way to express the power injection can be derived. Indeed, one can write

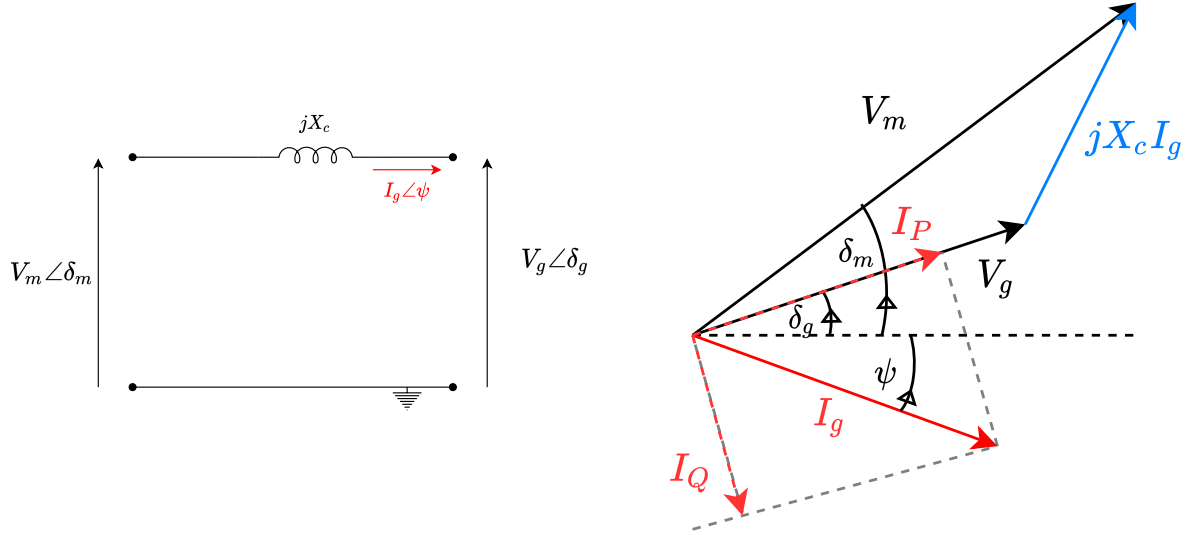


Figure 4.2: Simple representation of the circuit connecting the converter modulated voltage V_m with the grid voltage V_g . The phase reactor is represented by jX_c , the resistor is neglected. The phasor diagram of this simple circuit is shown on the right figure.

the apparent power as:

$$\begin{aligned}
 S &= \bar{V}_g \bar{I}_g^* \\
 &= \bar{V}_g \left(\frac{\bar{V}_m - \bar{V}_g}{jX_c} \right)^* \\
 &= \frac{jV_g \exp(j\delta_g) (V_m \exp(-j\delta_m) - V_g \exp(-j\delta_g))}{X_c} \\
 &= \frac{j(V_g V_m \cos(\delta_g - \delta_m) - V_g^2)}{X_c} + \frac{V_g V_m \sin(\delta_m - \delta_g)}{X_c} = jQ + P
 \end{aligned} \tag{4.2}$$

As it can be seen, the active power depends on the difference of phase angles between \bar{V}_g and \bar{V}_m .

4.1.2 Modeling of the grid following converters

For the grid following converters, the active current I_P and the reactive current I_Q are chosen to control the power output. To control the currents, the converter has to synchronize with the grid. Indeed, as seen in Figure 4.2, the active current is aligned with the grid voltage. Two reference frames are required as the converter components and the grid components have to be represented.

The grid components are displayed in a xy frame, rotating at a frequency of $2\pi\omega_{ref}$. The converter components are defined in a dq frame rotating at a frequency of $2\pi\tilde{\omega}_g\omega_N$. The grid following architecture embeds a phase-locked loop that is synchronizing the dq frame with the xy frame. The different frames are shown in Figure 4.3.

Phase-Locked Loop

The Phase-Locked Loop (PLL) adjusts the dq frame, which is the reference frame of the converter with the reference frame of the grid (the xy frame). To do so, it aligns the d

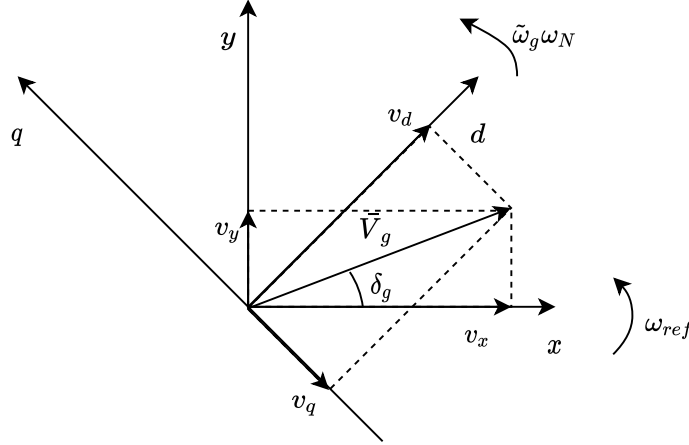


Figure 4.3: xy frame and dq frame with their respective frequency and the grid voltage V_g projected onto the different frames.

component of the voltage with the voltage phasor \bar{V}_g and thus cancels the v_q component. If the v_q component is negative, the dq reference frame has to slow down to synchronize with the xy reference frame, as seen in Figure 4.3. When both reference frames are synchronized (when the v_q component is equal to 0), the estimated speed $\tilde{\omega}_g$ coincides with the network frequency ω_{ref} . The estimated speed $\tilde{\omega}_g$ is in per unit (pu). The control logic of the PLL is shown in Figure 4.4.

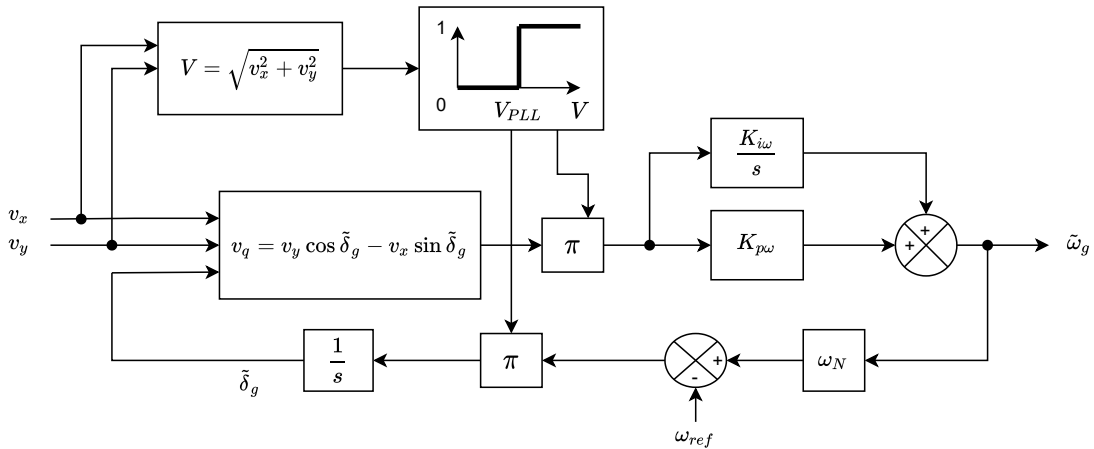


Figure 4.4: *Grid following converter*: Block diagram of the phase-locked loop.

From the block diagram, one can notice that the input of the PLL is the grid voltage components in the xy frame. The xy frame components are transformed to the dq frame components with the guess value of the grid angle $\tilde{\delta}_g$. It gives the q component of the grid voltage. The q component has to be canceled. To do so, one can use a PI controller with v_q as input. The output is the estimated xy frame speed $\tilde{\omega}_g$. The grid angle is then updated thanks to the new estimated xy frame speed.

During a large disturbance, some bus voltages can suffer from a large phase shift. To prevent the PLL from giving a wrong estimation of the grid angle, the PLL is frozen. To freeze the PLL, a voltage threshold V_{PLL} is specified. If the voltage goes below this threshold, the input and the output of the PLL are disabled.

In Figure 4.5, a short-circuit is applied at a bus close to the grid following converter, and cleared after 250ms. A 0.6Ω resistor is added to the short-circuit. As it can be seen, the voltage V drops below the threshold value V_{PLL} at $t=1s$ when the short-circuit takes place. Therefore, the multiplier $mult_{PLL}$ goes to 0 and disables the input $\tilde{\delta}_g$ and the output $\tilde{\omega}_g$ of the PLL. After the short-circuit clearance, the input and the output of the PLL are again activated.

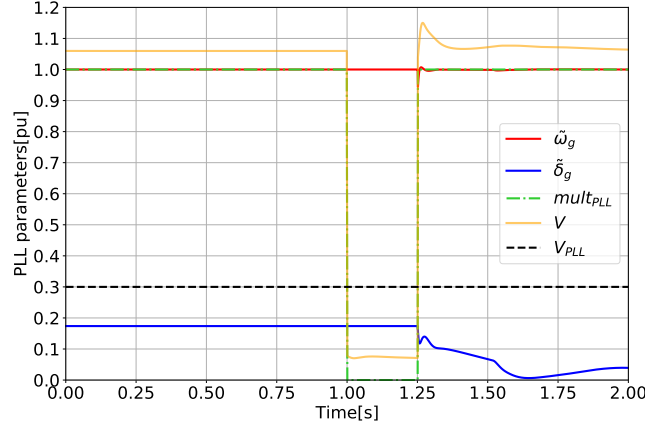


Figure 4.5: *Grid following converter*: Influence of a sudden voltage drop on the PLL dynamics.

Active power control loop

The active power control loop receives as inputs the active power setpoint P^{set} and the measured active power P . The difference between those two values feeds the integrator. The output of the integrator is then integrated to get the value of the direct current i_d . Thanks to the PLL that synchronized the converter with the grid, the direct current i_d is equal to the active current I_P as the d-axis is aligned with the grid voltage phasor \bar{V}_g . The active power control loop is shown in Figure 4.6.

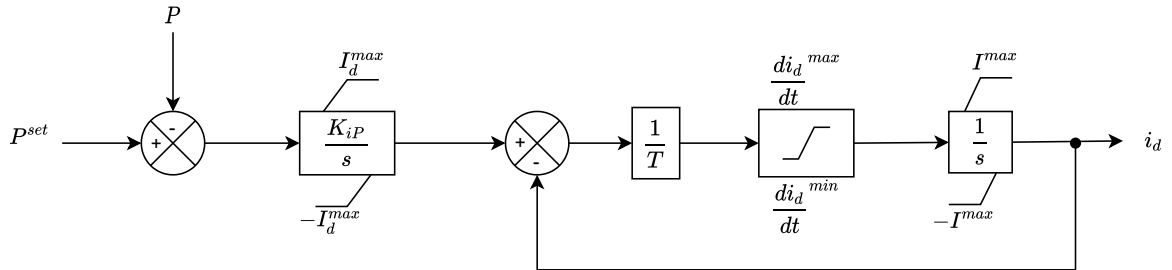


Figure 4.6: *Grid following converter*: Block diagram of the active power control loop.

In the active power control loop, the integrator presents an anti-wind-up command. This prevents the active current from overreaching the limits fixed. Those limits vary depending on the mode in which the converter is set. With a large disturbance, the quadrature current is prioritized, reducing the direct current.

In Figure 4.7, it can be seen that, during the disturbance, the direct current is limited because the quadrature current is prioritized. Then, the direct current does not recover

instantaneously as a limit on the derivative of the direct current is specified. In the example below, the limit is 0.5pu/s. The direct current and, therefore, the active power are progressively restored after the incident.

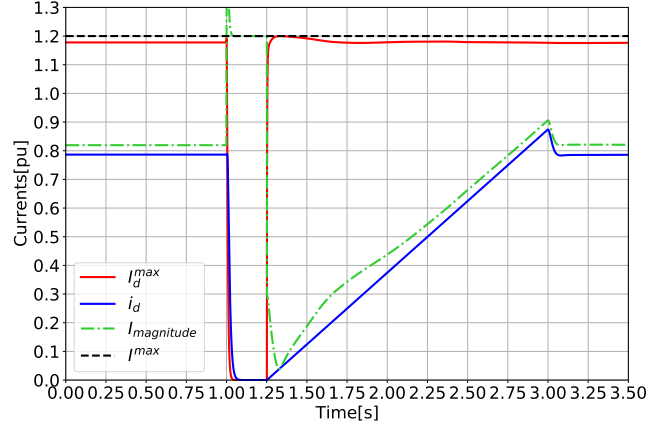


Figure 4.7: *Grid following converter*: Influence of a sudden voltage drop on the currents injection.

Reactive power control loop

The reactive power control loop can receive different inputs. The controller can either regulate the magnitude of the modulated voltage or the reactive power injection. Therefore, the inputs could be the voltage setpoint and the measured grid voltage or the reactive power setpoint and the measured reactive power injection.

If the grid voltage drops below a threshold value, the quadrature current is prioritized as the dynamic voltage support mode is engaged. As shown before, it reduces the active power. Two threshold values are specified. V_{s1} that corresponds to the voltage at which the mode is activated, and V_{s2} , the voltage at which the quadrature current is equal to the maximum current that the converter can withstand. The reactive power control loop is shown in Figure 4.8.

In Figure 4.9, the grid following converter is in voltage control mode. If the voltage remains above the threshold value V_{s1} , the quadrature current i_q takes the value of i_{q1} . A short-circuit with a 7Ω resistor is applied at a busbar close to the converter and is cleared after 250ms. Because of the short-circuit, the grid voltage V rapidly decreases and stabilizes below the threshold value V_{s1} and above the threshold value V_{s2} . The upper branch of the reactive power control loop is no longer active ($m = 0$) but, as shown in the figure, the value of i_{q1} is still changing as the inputs are still active. The value of i_{q2} depends linearly on the voltage magnitude V . Once the voltage V goes above V_{s1} , after the fault clearance, the upper branch is switched on and the quadrature current takes the value of i_{q1} . As after the short-circuit, the modulated voltage amplitude is greater than the voltage setpoint, the quadrature current increases. The quadrature current has the opposite sign of the reactive power. If the converter injects reactive power, the quadrature current is negative. This stems from the reference frame orientation seen in Figure 4.3.

In Figure 4.10, the grid following converter is in reactive power control mode. Here

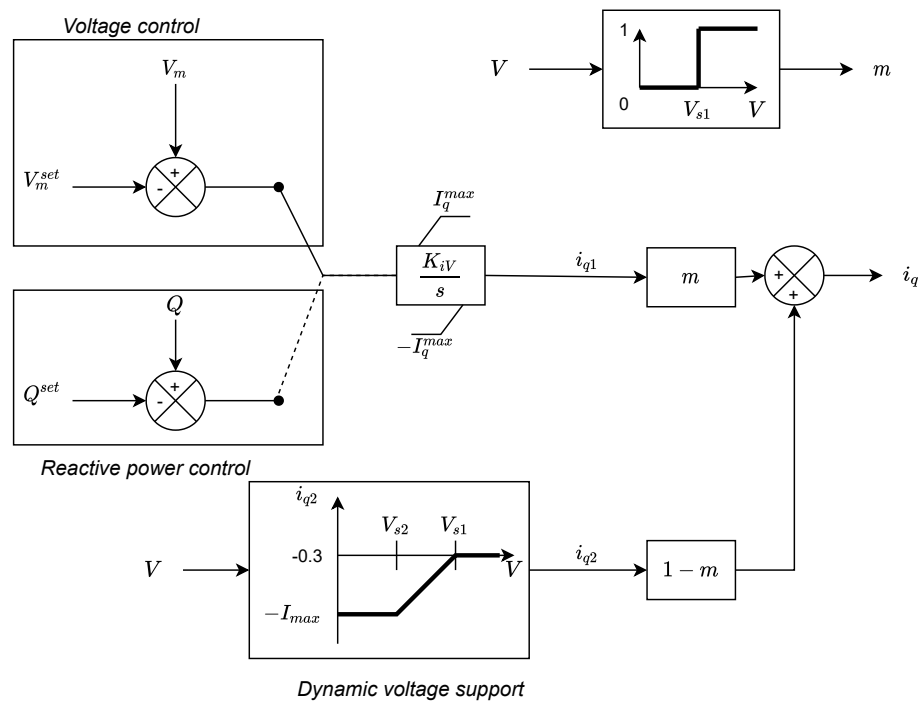


Figure 4.8: *Grid following converter*: Block diagram of the reactive power control loop.

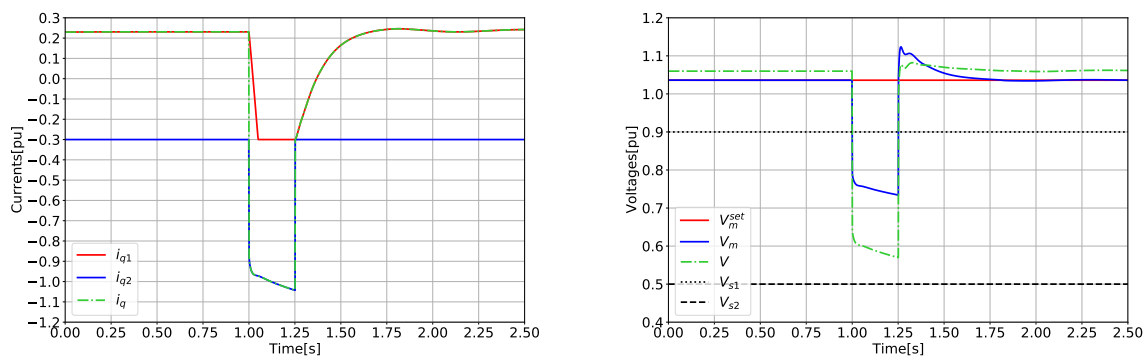


Figure 4.9: *Grid following converter*: Influence of a sudden voltage drop on the dynamics of the converter in voltage control mode.

again, the dynamic voltage support mode is switched on. As it can be seen, the reactive power injection is greater than the reactive power setpoint. Indeed, as the voltage drops, i_{q2} becomes more negative, increasing the reactive power output of the converter. The value of i_{q1} becomes positive as a positive input is given to the integrator of the upper branch of the reactive power control loop. After the short-circuit clearance, the quadrature current gets the value of i_{q1} . The steady-state values are the same for both control modes (voltage or reactive power), but the dynamics are different.

Practically, the dynamic voltage support does not work as it has been modeled here. The requirements for the dynamic support are shown in Figure 4.11 and a more detailed version is available in [7]. The activation depends on the sudden voltage change following the disturbance. If the voltage change is larger than 10%, for instance, then the dynamic support is switched on. A sudden voltage change means a voltage change that a Load

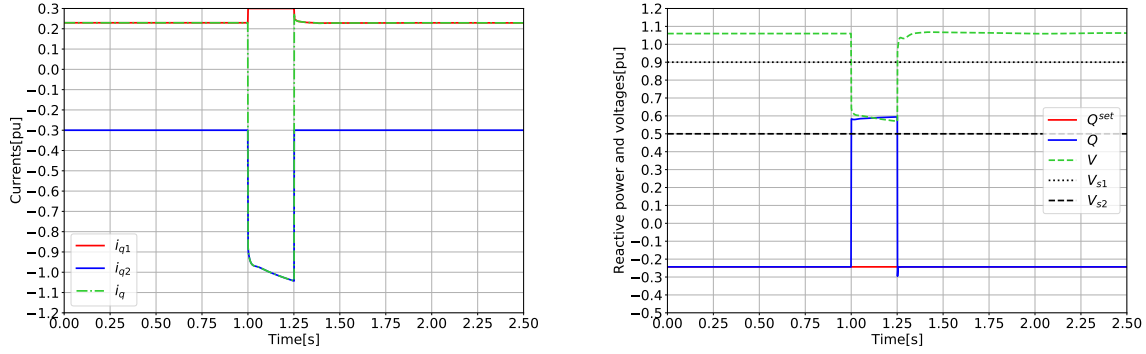


Figure 4.10: *Grid following converter*: Influence of a sudden voltage drop on the dynamics of the converter in reactive power control mode.

Tap Changer cannot follow. It means that in case of a gradual voltage deviation caused by wind events, for instance, the dynamic voltage support is deactivated as the voltage change is not considered fast enough to activate it.

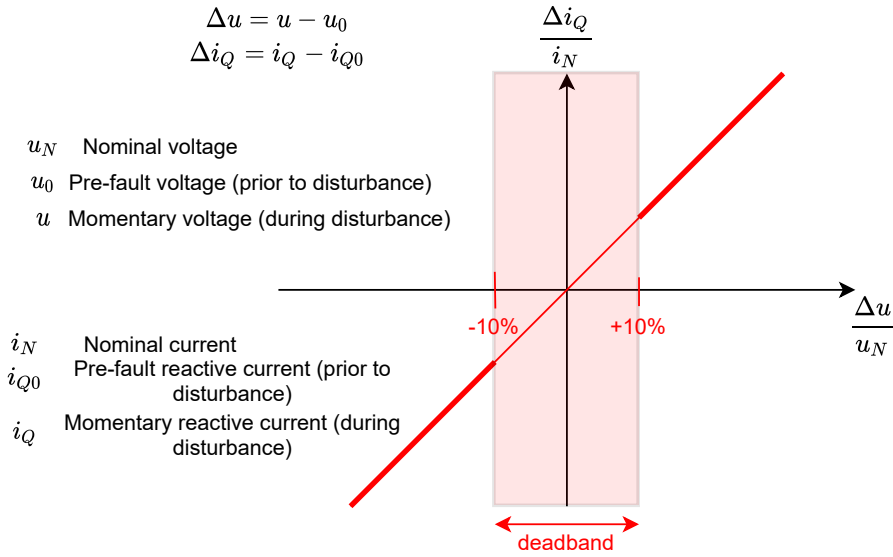
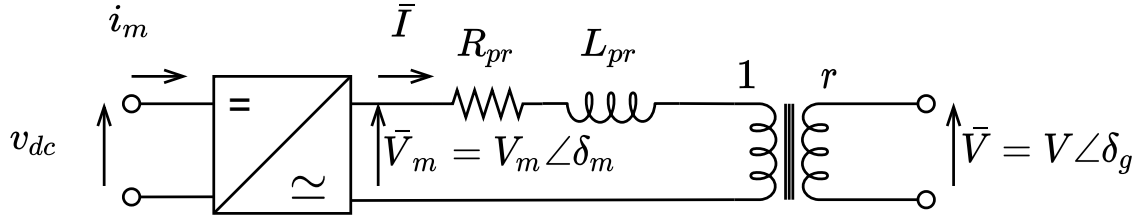


Figure 4.11: Requirements for dynamic voltage support inspired from [7].

Overall structure

The overall structure can be observed in Figure 4.12.

The AC/DC converter is a Multilevel Modular Converter (MMC). It therefore does not need a phase reactor to smooth the output signal. Instead, the phase reactor is employed to represent the transformer that connects the converter to the grid. With the proper choice of base voltages, r can be assumed equal to 1. \bar{V} represents the grid voltage at the Point of Common Coupling (PCC), whereas \bar{V}_m is the modulated voltage. \bar{I} is the current injected by the converter into the AC grid. The AC grid voltage can be decomposed into its x and y coordinates, as shown in Figure 4.3. The same can be done


 Figure 4.12: *Grid following converter: Overall structure.*

with the modulated voltage. Under the phasor approximation, one can write:

$$\begin{aligned} v_{mx} &= v_x + R_{pr}i_x - \omega_{ref}L_{pr}i_y \\ v_{my} &= v_y + R_{pr}i_y + \omega_{ref}L_{pr}i_x \end{aligned} \quad (4.3)$$

v_x and v_y are known and cannot be changed (those are the components of the grid voltage). The currents i_x and i_y result from the projection of i_d and i_q in the xy reference frame. Finally, the frames are synchronized because the PLL synchronized the converter with the grid. With this information, the value of v_{mx} and v_{my} can be found. They are the inputs of a low logic controller controlling the switching of the transistors in the MMC technology.

Typical values of the parameters

$K_{i\omega}$	$\frac{25}{T_{PLL}^2 \omega_N} [\text{s}^{-1}]$	$\frac{di_d}{dt}^{max}$	0.5 [pu s ⁻¹]
$K_{p\omega}$	$\frac{10}{T_{PLL} \omega_N} [\text{pu}]$	T	0.01 [s]
T_{PLL}	0.05 [s]	I_q^{max}	0.3 [pu]
V_{PLL}	0.3 [pu]	K_{iV}	80 [s ⁻¹]
K_{iP}	39 [s ⁻¹]	V_{s1}	0.9 [pu]
I_d^{max}	$\sqrt{(I^{max})^2 - (I_q^{max})^2} [\text{pu}]$	V_{s2}	0.5 [pu]
I^{max}	1.2 [pu]	ω_N	$2\pi f_{nom} [\text{rad s}^{-1}]$

 Table 4.1: *Grid following converter: Typical values of parameters.*

4.1.3 Modeling of the grid forming converters

The grid forming converter controls the phase angle to adjust the power output as observed in (4.2). The model adopted in this thesis does not need a PLL to synchronize with the system, but in some models, a PLL is required. The grid forming acts as a voltage source; it generates a voltage waveform with a specific magnitude V_m and an angle δ_m . On the other hand, the grid following converter does not generate a voltage source; it acts as a current injector. There is no reactive power loop in the grid forming mode as the angle is established according to the active power setpoint and the modulated voltage is kept constant. As such, the choice to have a constant reactive power injection is not possible with a grid forming converter.

Active power control loop

The control scheme is shown in Figure 4.13. A primary frequency control is implemented in this control scheme as shown in the figure. Indeed, if G_f differs from 0, the active power setpoint increases if the modulated frequency is smaller than the reference value: ω_{ref} . The primary frequency control acts the same way as a speed governor in a synchronous machine does, the change in the active power setpoint depends linearly on the difference between the reference and the measured frequency. This is called a droop speed control. This control scheme is referenced in some publications as a *virtual synchronous machine* ([29]).

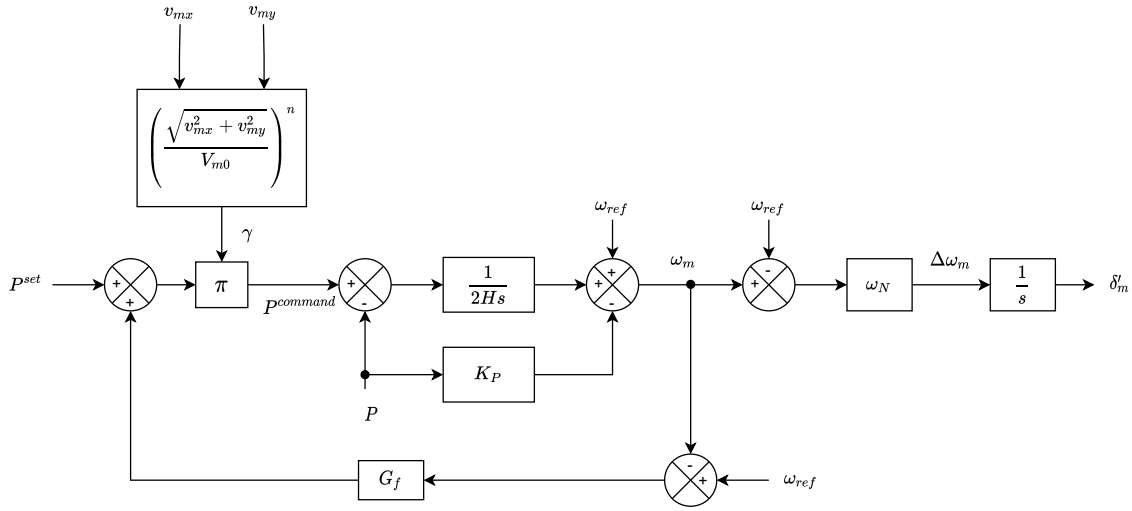


Figure 4.13: *Grid forming converter*: Bloc diagram of the active power control loop.

As it can be seen, there is no current limiter in the active power loop. The current is restricted through a virtual impedance, as shown in Figure 4.14. The voltage magnitude V_{m0} is kept constant and the active power loop returns as output the angle δ'_m . The virtual impedance is used if the current magnitude overreaches the maximum current allowed by the converter. The components of the virtual impedance are derived in (4.4).

$$\begin{aligned}
 R_{VI} &= K_{pVI} f(I) \\
 X_{VI} &= \sigma_{X/R} R_{VI} \\
 \text{with} & \\
 f(I) &= I - I_{max} \quad \text{if } I > I_{max} \\
 &= 0 \quad \text{if } I < I_{max}
 \end{aligned} \tag{4.4}$$

If the current overcomes the maximum limit, the virtual impedance is activated, and the modulated voltage magnitude V_m is reduced. This arises when the grid voltage drops because of a short-circuit, for instance, and that the converter cannot maintain its modulated voltage constant. During the short circuit, there is also a risk that the converter loses synchronism. Indeed, the power injection depends on the voltage magnitude and the current. During the short circuit, the voltage magnitude declines, and the current is restricted by the virtual impedance. Therefore, the amount of active power that can be injected is limited, whereas the active power setpoint is not adjusted. It causes an increase in the angle δ_m until it reaches the maximum angle. The transient stability for

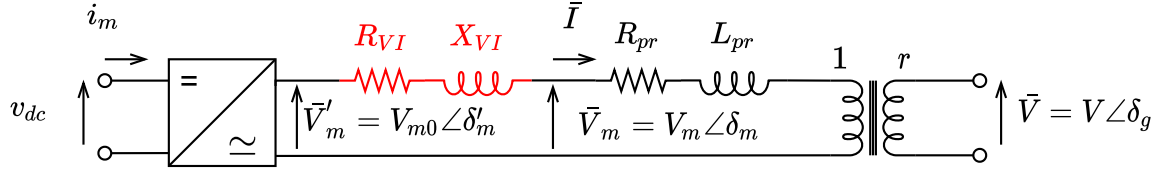
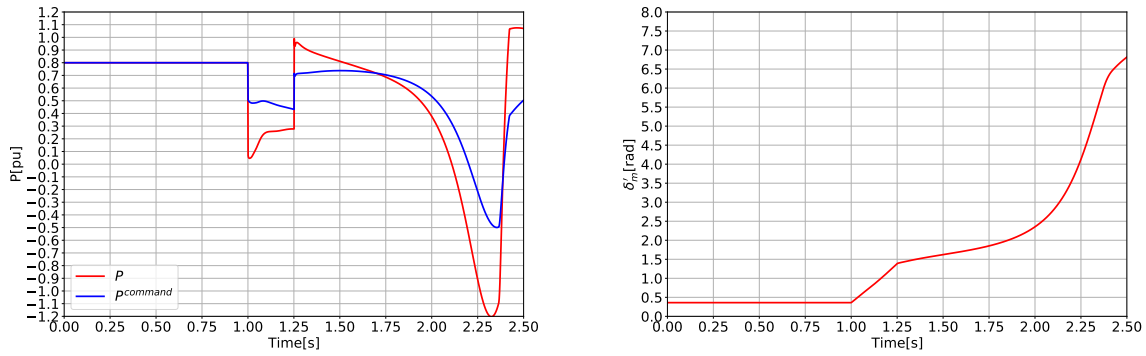


Figure 4.14: Grid forming converter: Overall structure.

grid forming converters has been explained in [28].

In Figure 4.15, one can see the results when a short-circuit is applied at $t=1s$ to a busbar close to the grid forming converter. The short-circuit lasts 250ms and is then cleared. The model of the grid forming converter used is the one presented in Figure 4.13 with the exponent $n = 0$ that always gives $\gamma = 1$. During the short-circuit, as $P^{command}$ is larger than P , the angle increases. The angle δ'_m overreaches the maximum angle, and the converter loses synchronism. Therefore, even though $P^{command}$ is smaller than P , the angle keeps increasing.


 Figure 4.15: Grid forming converter: Influence of a sudden voltage drop on the dynamic of the converter. The converter does not have a limitation of the angular deviation ($n = 0$).

For this reason, the factor γ is employed to inhibit the value of $P^{command}$ when the modulated voltage V_m differs from V_{m0} (when the virtual impedance is activated). The exponent n is equal to 2. This reduction in the active power setpoint during the short circuit prevents the converter from losing its synchronism. The results with the limitation of angular deviation γ are shown in Figure 4.16. Once the virtual impedance is deactivated, the modulated voltage V_m is equal to V_{m0} and γ is equal to 1.

The effect of the virtual impedance is shown in Figure 4.17. As one can notice, if the current overreaches the maximum current allowed by the converter, the virtual impedance is activated. Thus, the modulated voltage V_m is no longer equal to V_{m0} as R_{VI} and X_{VI} differ from 0 according to (4.4). The deactivation of the virtual impedance is a smooth process as, while the current decreases and gradually goes below the maximum current I_{max} , the modulated voltage slowly increases to reach V_{m0} . It ensures a slow and continuous restoration of the modulated voltage.

The converter synchronizes itself through its active power control loop. As the voltage phase angle and the voltage magnitude are defined, the modulated voltage can be

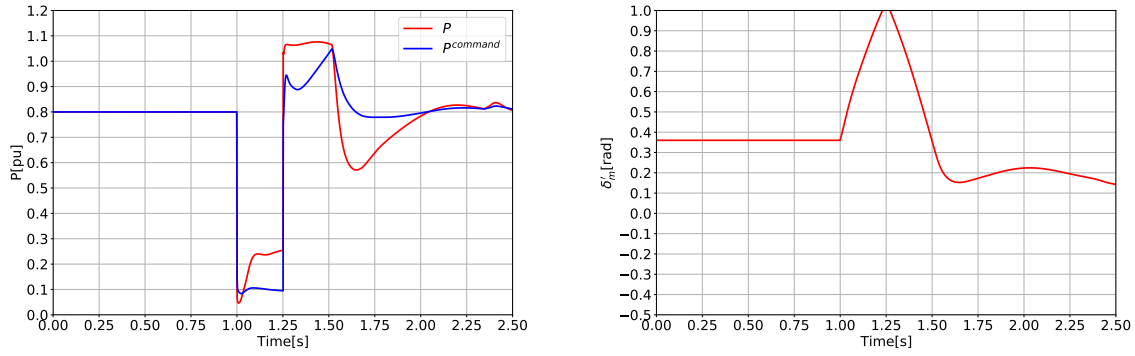


Figure 4.16: *Grid forming converter*: Influence of a sudden voltage drop on the dynamic of the converter. The converter has a limitation of the angular deviation ($n = 2$).

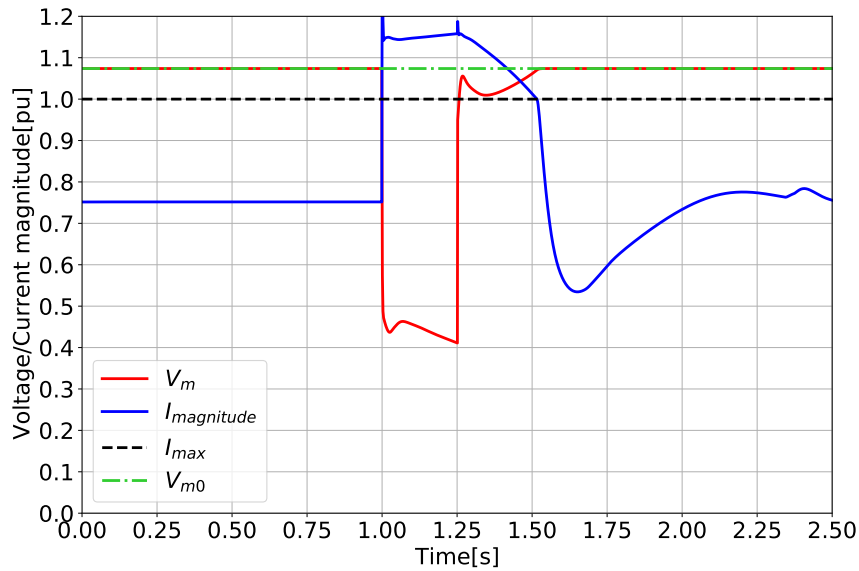


Figure 4.17: *Grid forming converter*: Effect of the virtual impedance on the modulated voltage.

projected onto the xy reference frame. With this information, the components of the modulated voltage can be given to the low logic controller that is controlling the switching of the transistors.

Typical values of the parameters

n	2 [—]	I^{max}	1 [pu]
G_f	25 [pu]	K_{pVI}	0.676 [pu]
K_P	0.01592 [pu]	$\sigma_{X/R}$	5 [pu]
H	5 [s]	ω_{ref}	1 [pu]

Table 4.2: *Grid forming converter*: Typical values of parameters.

4.2 The simulation tool

The simulation tool used for this thesis is RAMSES which stands for *RApid Multi-threaded Simulation of Electric power Systems*. The software uses the phasor approximation method for time simulation of electric power systems. The phasor approximation allows the simulation of large power systems with limited computation time. But, it does not model all the dynamics. For converters, for instance, the inner current loops are not modeled. The results shown in this thesis have to be taken with care. To be sure that the system is stable, further studies using EMTP software need to be done as some instabilities cannot be visualized with the phasor approximation method.

Chapter 5

Impact of wind events and HVDC operations on the system stability

5.1 From a lightly loaded system to a highly loaded system : The *Ramping event* scenario

As pointed out before, wind energy is an unpredictable source of energy. As the wind blows stronger, the power production of the wind turbines is rising. If the wind parks are close to each other, as it is the case in the network studied, the changes in the power flows become significant.

In this scenario, the system is first lightly loaded. The wind parks grouped as WP1 in the network produce around 1368MW whereas the wind parks grouped as WP2 produce around 1153MW. The HVDC link HVDC-AB exports 1000MW and HVDC-AC exports 1400MW.

As the system is lightly loaded, the cables generate more reactive power than the lines and transformers can draw. To compensate for this excessive amount of reactive power production in the system, the shunt inductors connected to TROUFFETTE are set to consume 900MVar under a voltage of $1pu$ (nominal reactive power). The shunt inductors connected to CHOUFFE are set to consume 300MVar under a voltage of $1pu$. The power flows in the entire system are shown in the appendix 9.2.

5.1.1 Description of the sequence of events

The sequence of events occurs on day D. Several days before day D, it has been forecasted that the wind parks installed in control area B and control area C will see their power production increase between hour H-1 and hour H on day D. This power gain results from what is called a *Ramping event*. The same *Ramping event* is forecasted for control area A but several hours later. As it has been explained previously (see 2.1), the *Ramping event* can have several definitions. In the following, the term *Ramping event* is adopted to define a rise in wind power production provoked by an increase in wind speeds.

The forecasted increase of wind power production from hour H-1 to hour H drives the prices down in control areas B and C, thus enhancing the power transfer from control areas B and C to control area A. Indeed, control area A has a limited wind power production

forecasted for hour H. The HVDC links that were set to export power from control area A to the others control areas will see their power setpoints for hour H on day D being shifted to maximize social welfare.

Therefore, a complete power shift is planned for both HVDC links, going from exporting their maximal active power to importing it. As the HVDC links do not connect the same areas, the ramping rate applied to them is not the same. The ramping rate of HVDC-AB is set to 100MW/min, therefore, it takes 20 minutes to accomplish the power shift. The power shift starts at hour H-10min and ends at hour H+10min. The ramping rate of HVDC-AC is set to 280MW/min, therefore, it takes 10 minutes to complete the power shift. The power shift starts at hour H-5min and ends at hour H+5min.

The day D, the *Ramping event* in control area A occurs earlier than expected. From hour H-10min to hour H+20min, the wind parks produce more active power because of the increase in wind speeds. At hour H+20min, the wind parks are injecting their full active power output, this means that wind parks WP1 are producing 2626MW whereas wind parks WP2 are producing 2100MW.

The sequence of events takes 30 minutes in total. To keep the network balanced and to avoid any frequency issue as it is out of the scope of this thesis, the excess of power is consumed in the control area Equiv. The active power setpoint of the 300 000MVA machine *GenEquivNodeNF* is progressively reduced by 6890MW in 30 minutes. This power decrease could be depicted as if the control area Equiv was buying power from control area A because of the lower prices resulting from the unexpected large production of wind power.

The sequence of events is illustrated in Figure 5.1.

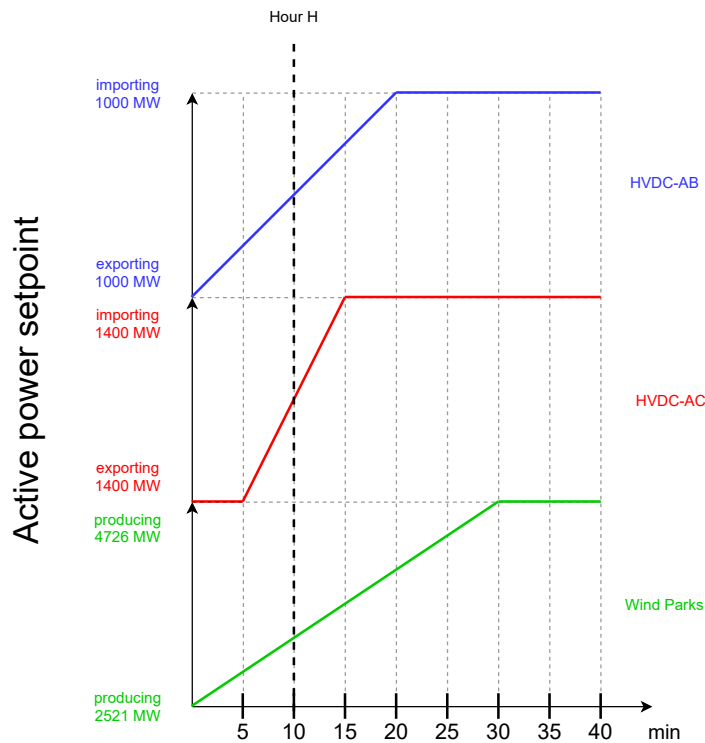


Figure 5.1: *Ramping event*: Illustration of the sequence of events.

5.1.2 Influence of the sequence of events on the power flows and on the network frequency after the network balancing

In Figure 5.2, the influence of the sequence of events on the active power flows through the green (CHOUFFE-TORPAH) and (TROUFFETTE-PIRAAT) orange circuits of Figure 4.1 is shown. The power injected by the different injectors is distributed among the green and orange circuits depending on the impedance magnitude of those circuits. The lower impedance circuit sees the larger power flow. The phase shift transformers have almost no effect in this case.

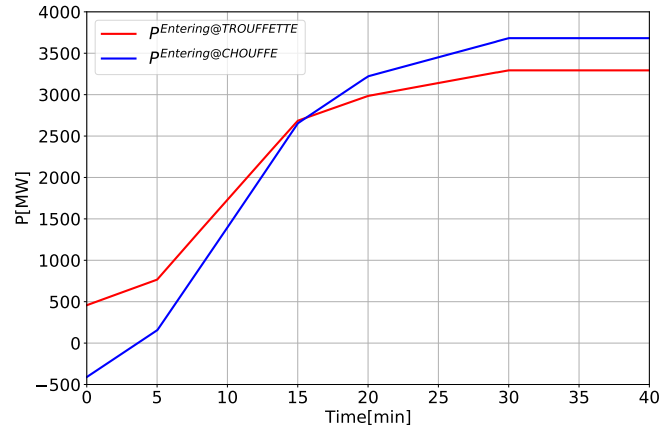


Figure 5.2: *Ramping event*: Active power flowing through the green and orange circuits. The addition of the two curves gives the evolution of $P_{2,COR}$ with time.

Figure 5.3 shows that the system is correctly balanced as the frequency returns to the nominal frequency (50Hz) after the sequence of events.

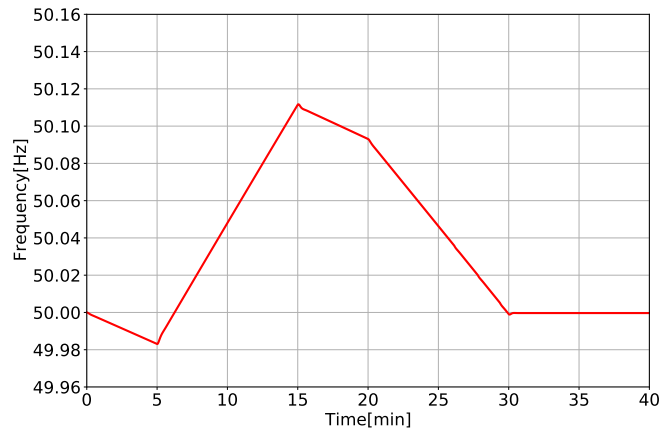


Figure 5.3: *Ramping event*: Network frequency evolution.

5.1.3 The different types of control available for the reactive power loop of the wind parks

As shown in the grid following converter model in Figure 4.10, the converter could either follow a voltage setpoint or a reactive power setpoint. For the wind parks, several control modes are available. To control the converter of each wind turbine, a wind park controller is employed. A wind park controller allows an overall control of the wind park. The wind park controller can communicate with each wind turbine and can set their power setpoint according to specific control modes ([21]).

If one controls the voltage, two schemes can be used: decentralized or centralized. In a decentralized scheme, each wind turbine controls its voltage through an automatic voltage regulator. The voltage setpoints are assigned by the wind park controller according to the measurements realized at the point of common coupling (PCC). In the centralized scheme, the wind turbines receive a reactive power setpoint sent by the wind park controller based on voltage measurements. The wind park controller generates the reactive power setpoints. The centralized, and the decentralized schemes have similar performances if the communication delay between the wind park controller and the wind turbines of the centralized scheme is around 10ms. If the communication delay is not negligible (150ms), the centralized scheme is less effective than the decentralized scheme ([21]).

The wind park can also be operated in reactive power control mode. The wind park controller assigns a reactive power setpoint to each wind turbine to control the reactive power injection at the PCC.

One can also operate wind turbines to control the power factor.

In the model used for this thesis, the voltage control mode corresponds to a decentralized voltage control scheme whereas the reactive power control mode corresponds to a control of the reactive power injection at the PCC. For the issues investigated in this thesis, the voltage control mode has a powerful advantage as it provides some voltage support whereas the reactive power control mode injects always the same reactive power output whatever the voltages. Nevertheless, it would be unrealistic to consider that every wind park controls their voltage and none of them are in reactive power control mode. Therefore, three configurations are studied:

- The wind parks WP1 and WP2 are in voltage control mode (*configuration V*),
- The wind parks WP1 and WP2 are in reactive power control mode (*configuration Q*),
- The wind parks WP1 are in reactive power control mode and the wind parks WP2 are in voltage control mode (*configuration VQ*).

5.1.4 Wind parks WP1 and WP2 are in voltage control mode: *configuration V*

Voltages at various 380kV buses

The voltage levels of different busbars of the network are shown in Figure 5.4.

The loading of the system causes the voltage levels to decline. Indeed, as the system

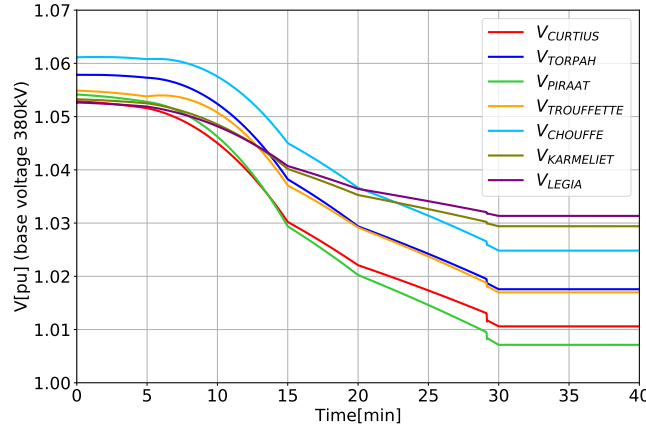


Figure 5.4: *Configuration V*: Voltages at various 380kV buses.

gets more loaded, the currents running through the lines and the cables become more important. For a larger current, a line consumes more reactive power, and a cable produces less reactive power. A line or a cable can be characterized by its π -equivalent, as depicted in Figure 5.5. The reactive power consumption of the π -equivalent is equal to XI^2 . Therefore, the larger the current, the greater the reactive power consumption is. On the other hand, the π -equivalent produces reactive power through the half shunt susceptances. The reactive power production of a half shunt susceptance depends on the voltage across the capacitor and is equal to $\frac{\omega C}{2}V^2$ where V is the voltage across the capacitor.

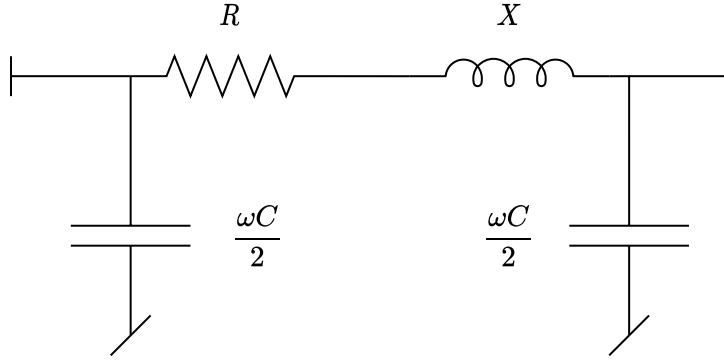


Figure 5.5: π -equivalent of a line or a cable (the modeling in RAMSES).

The half shunt susceptance is larger in a cable than in a line therefore the cable produces more reactive power than a line. As the line becomes more loaded, the currents circulating through the lines are larger, leading to larger consumption of reactive power through the reactance. This reactive power absorbed by the lines has to be produced somewhere and then transferred to the place where it is consumed. It induces voltage deviations as a voltage drop is required to transfer reactive power. Indeed, starting from (4.2) and Figure 4.2, one can derive the reactive power injected at terminal g (5.1).

$$-Q_{gm} = \frac{V_g V_m \cos(\delta_g - \delta_m) - V_g^2}{X_c} \quad (5.1)$$

The same derivation as the one shown in (4.2) can be done for the power injected at

terminal m . Finally, the reactive power transfer from terminal m to terminal g can be expressed as shown in (5.2). It shows that to transfer reactive power, the magnitude of the sending end voltage has to be greater than the magnitude of the receiving end voltage. For larger reactive power transfer, the voltage gradient is greater.

$$\begin{aligned} -Q_{gm} + Q_{mg} &= \frac{V_g V_m \cos(\delta_g - \delta_m) - V_g^2}{X_c} + \frac{V_m^2 - V_g V_m \cos(\delta_m - \delta_g)}{X_c} \\ &= \frac{V_m^2 - V_g^2}{X_c} \end{aligned} \quad (5.2)$$

All in all, while the system gets more loaded, the components of the network consume more reactive power, larger reactive power transfers occur in the system which leads to voltage discrepancies.

From the network description shown in Figure 4.1, most of the power is injected at busbars CHOUFFE and TROUFFETTE. The active power is flowing to where the power is absorbed, meaning the busbar EquivNode. Two different paths exist. The lower impedance path, which is the green one, sees the largest active power flow, as it can be seen in Figure 5.2. The lines and transformers consume reactive power that is produced by the injectors at CHOUFFE and TROUFFETTE. This leads to lower voltages at busbars TORPAH and CURTIUS. The same can be noticed through the other path, the orange one.

The more affected busbar is PIRAAT. As it is between CURTIUS and TROUFFETTE, which are both connected to equipment that controls their terminal voltages and injects reactive power, PIRAAT, with no equipment installed, has the lower voltage. The less affected busbars are KARMELIET and LEGIA as the active power flowing through those lines is limited, therefore the amount of reactive power consumed remains small.

For a 400kV operated network, the lower voltage that can be tolerated for long-term operation is 370kV according to ELIA. The voltage levels are above this lower limit, which means that the voltages are acceptable.

Voltages of wind parks

The voltages of the wind parks WP1 and WP2 are shown in Figure 5.6. The voltages are correctly held as the wind parks are in voltage control mode.

Power injections of HVDC links and synchronous machines

In Figure 5.7, one can notice the power injections of the main injectors. On the left, the active and reactive power injections of the HVDC links can be seen. As stated in the sequence of events, the active power setpoints of the HVDC links are shifted during the simulation. Indeed, both start from a negative power output (HVDC links export power) and change to positive power output (they import power at the end of the simulation). For HVDC-AC, the active power output is not completely stabilized at $t=15\text{min}$ as it should be, according to the sequence of events. Whereas the sequence of events shows the shifting in the active power setpoint, Figure 5.7 displays the active power injected into the network. As the frequency is not equal to the reference frequency during the simulation, the active power setpoint does not correspond to the power injected because of the primary frequency control of the grid forming converter. Indeed, as the frequency is slightly above 50Hz, as shown in Figure 5.3, the active power setpoint of the grid forming

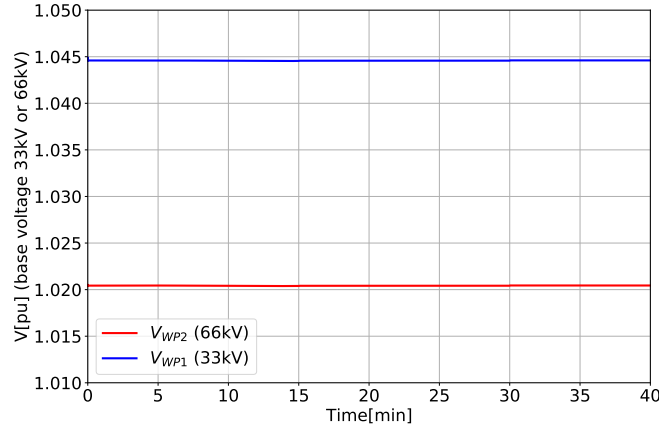


Figure 5.6: *Configuration V*: Voltages at the PCC of one wind park of WP1 and of one wind park of WP2.

converter is slightly reduced. At the end of the simulation, the active power output of HVDC-AC reaches 1400MW as the frequency reaches 50Hz.

On the left figure, one can also see the reactive power production of the HVDC links. Both are controlling their modulated voltage to keep it constant. Therefore, they inject reactive power. The injection of reactive power increases all along the simulation as the system gets more loaded and consumes more reactive power.

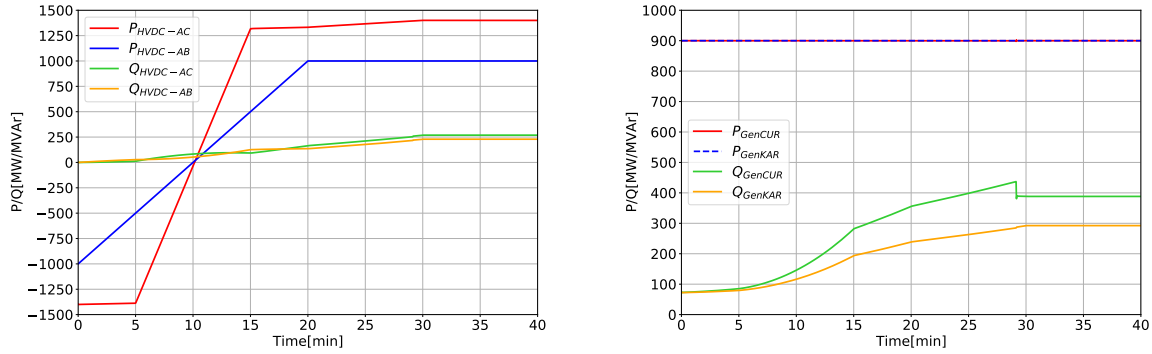


Figure 5.7: *Configuration V*: Power injections of HVDC links (left figure) and synchronous machines (right figure).

On the right figure, one can see the power injections of the two synchronous machines. The active power output remains constant as it has not been changed during the sequence of events and as the synchronous machines are not equipped with a primary frequency control. The reactive power production does not stay constant as the synchronous machines preserve the voltage at their terminals. As it can be seen, the reactive power output of the synchronous machine *GenCUR* drops around $t=28\text{min}$. The over-excitation limiter implemented in the synchronous machine leads to this drop. The excitation system of the synchronous machines is described in Figure 5.8. The value of i_{f2}^{lim} is settled at $1pu$ for every synchronous machine. The value of i_{f1}^{lim} has been calculated for the machine to remain within its capability. For the synchronous machine *GenCUR*, i_{f1}^{lim} is equal to

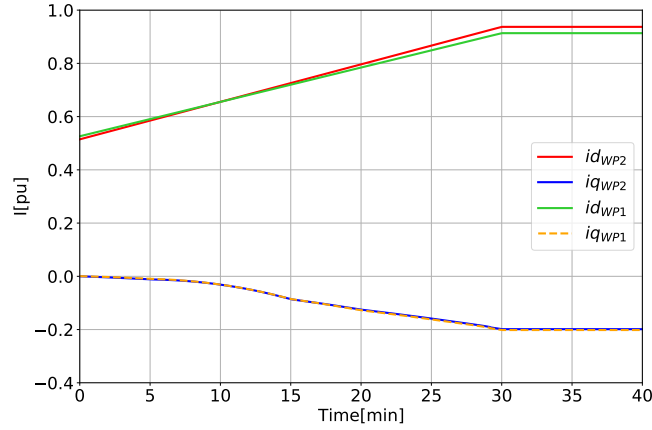


Figure 5.10: *Configuration V*: Direct and quadrature currents of wind parks.

5.1.5 Wind parks WP1 and WP2 are in reactive power control mode: *Configuration Q*

The system is now investigated with wind parks in reactive power control mode. As explained before, the dynamic voltage support is not activated as the system does not suffer from a sudden voltage drop. Indeed, the dynamic voltage support reacts with a large incident, for instance, a short-circuit. Here, the voltage drop is provoked by the progressive loading of the system.

The voltage levels are shown in Figure 5.11. The voltages go below the lower limit. As the wind parks are in reactive power control mode, there is a lack of reactive power production. The other injectors compensate for this lack and quickly reach their limit. An extra source of reactive power has to be added to keep decent voltage levels.

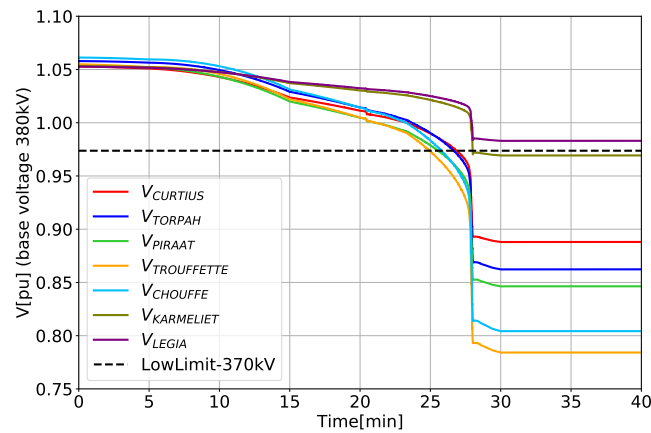


Figure 5.11: *Configuration Q*: Voltages at various 380kV buses.

5.1.5.1 Using an automaton to disconnect shunt inductors based on TROUFFETTE voltage: *Configuration Q+Automaton version 1*

As shown in Figure 4.1, which describes the network, there is one shunt inductor placed at TROUFFETTE busbar. This shunt inductor has a size of 900MVar nominal. When the simulation begins, the shunt inductor is switched on as the system is lightly loaded. It compensates for the excess of reactive power produced by the network components. As the system is progressively loaded, the shunt inductor becomes pointless. To restrain the voltage drop, one can disconnect it. Practically, a shunt inductor of 900MVar is unrealistic thus it is divided into five smaller shunt inductors, four of 200MVar and one of 100MVar.

The system can be provided with an automaton that manages the connection and disconnection of the shunt inductors. If the voltage goes below 375kV during more than 25s, the automaton disconnects one shunt inductor (it starts first with the 200MVar ones). This response time is used because the automaton should not disconnect the shunt if a short-circuit occurs. Furthermore, during wind events, the dynamic is pretty slow, and rapid actions are not required to save the system.

The automaton helps the operator in his task. The operator may not be prepared for such events, or the sequence of events happens too quickly and prevents the operator from reacting.

This automaton can also work for over-voltages. If the voltage goes above the maximum limit of 415kV for 25s, the automaton can connect a shunt inductor.

Voltages at various 380kV buses

Figure 5.12 shows the voltage levels when the automaton is implemented. Four shunt inductors out of five have been activated. There is still a 100MVar shunt inductor connected to TROUFFETTE. The voltage profiles are acceptable.

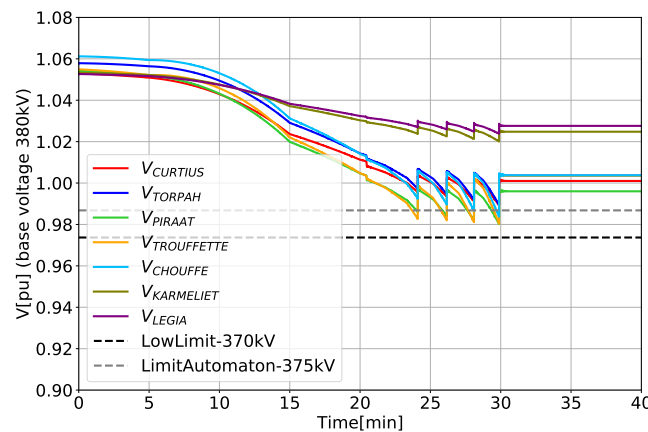


Figure 5.12: *Configuration Q+Automaton version 1*: Voltages at various 380kV buses.

Dynamic reserves of HVDC links

Even though the voltage levels are acceptable, Figure 5.13 shows that both HVDC links have reached their limit. For HVDC-AC, while the current magnitude overreaches $1pu$,

the virtual impedance is activated, and the modulated voltage drops. During those moments, in case of contingency, the HVDC-AC cannot react as it is already close to its limit. Furthermore, the converter does not maintain its voltage as the virtual impedance is switched on.

When a shunt inductor is disconnected, the current magnitude of the converter decreases as its reactive power output also declines. Indeed, the disconnection of the shunt inductor reduces the amount of reactive power needed in the system. Therefore, the current goes below $1pu$ and the modulated voltage rises back to its initial value. At the end of the simulation, it can be seen that the virtual impedance is not activated anymore. Nevertheless, the current amplitude is still high and very close to $1pu$. Operating the converter close to its limit for a long time is not acceptable.

The quadrature current reaches $-0.3pu$ for HVDC-AB at the end of the simulation. The dynamic voltage support can be activated if an incident occurs. It prioritizes the reactive current and permits a larger reactive power production. Nevertheless, the HVDC-AB converter operation is not comfortable. If the virtual impedance is activated and the limit of $-0.3pu$ for HVDC-AB is reached, there is nothing left to control the voltage in the system except the synchronous machines. The synchronous machine *GenCUR* has also reached its limit, therefore even this synchronous machine is not controlling the voltage. As the wind parks are in reactive power control mode, they do not control their voltage either. It left the system with no control over the voltages, which is not acceptable. If an incident occurs, the efforts to save the system will be noticeably large as the network components cannot fully react. It can be concluded that some dynamic reserves should be preserved in the case of a contingency.

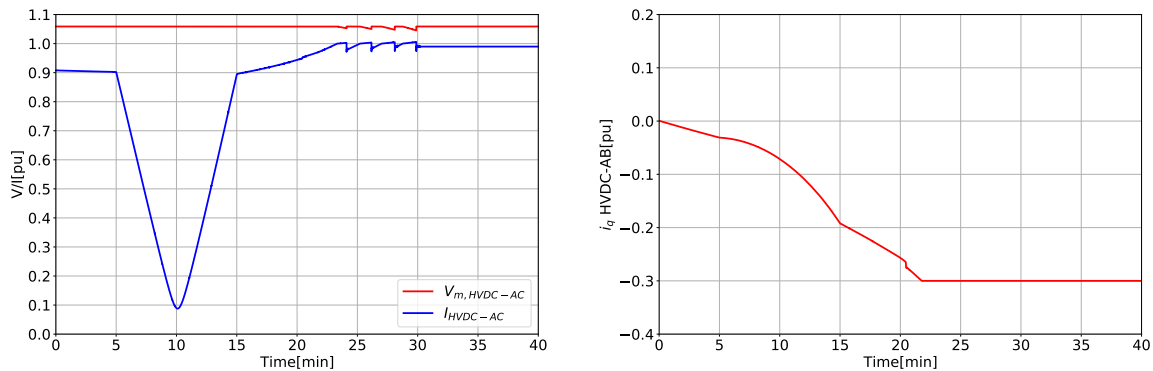


Figure 5.13: *Configuration Q+Automaton version 1*: Modulated voltage and current amplitude of HVDC-AC on the left. Quadrature current of HVDC-AB on the right.

5.1.5.2 Using a master controller that manages the dynamic reserves of the network components: *Configuration Q+Automaton version 2*

As it has been shown before, an automaton that disconnects the shunt inductors based on the voltage is enough to get acceptable voltage levels. But, how to maintain sufficient dynamic reserves to guarantee a safe operation of the system? To secure the system operation, the converters should not be at their limit after or during the wind event. Furthermore, there is still a shunt inductor of 100MVar connected to TROUFFETTE, which

consumes the reactive power produced by the converters. It involves extra efforts for the converters to provide useless reactive power (as the shunt inductor can be disconnected).

To keep sufficient dynamic reserves, one can use a master controller to notify the operator or command an automaton if the limits of the converters are reached. In the latter case, the master controller can command the automaton to trip a shunt inductor if the current amplitude of HVDC-AC overreaches $0.95pu$ during 25s. This control logic is pretty simple. A better control logic would look at the major injectors and alert the operator if one converter is close to its limit or if one converter is taking more part in the voltage support than others. As there is no need for rapid response during wind events, there is no need for an automatic control. If the operator is aware of the issue, he could make a better decision than what an automaton would do. For simplicity, the automaton solution was tested, as it would be difficult to simulate the operator's decisions.

Voltages at various 380kV buses

The voltage levels are acceptable, as it is shown in Figure 5.14. The shunt inductors connected to TROUFFETTE have been disconnected by the automaton.

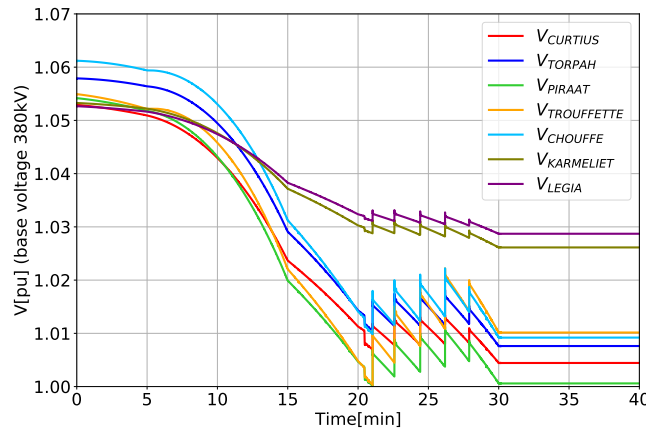


Figure 5.14: *Configuration Q+Automaton version 2*: Voltages at various 380kV buses.

Voltages of wind parks

Because the wind parks are in reactive power control mode, they do not control their voltage. Therefore, some Load Tap Changers (LTCs) have been installed. As the voltage diminishes or rises and extends beyond the deadband of the LTC, the tap position is changed to maintain the voltage within the deadband. The LTCs have a reaction time of 7s (for WP2) or 10s (for WP1). Because the wind events and the HVDC power shifts cause slow changes compared to other incidents (as a short-circuit, for instance), the LTCs are very useful. The deadband is equal to $\pm 1\%$. It can be seen in Figure 5.15 that the voltages remain within the deadband.

Dynamic reserves of HVDC links

As shown in Figure 5.16, the shunt inductors are tripped when the current magnitude of HVDC-AC overreaches $0.95pu$ for 25s. Both HVDC-AC and HVDC-AB have never attained their limit during the simulation. It means that some dynamic reserves were

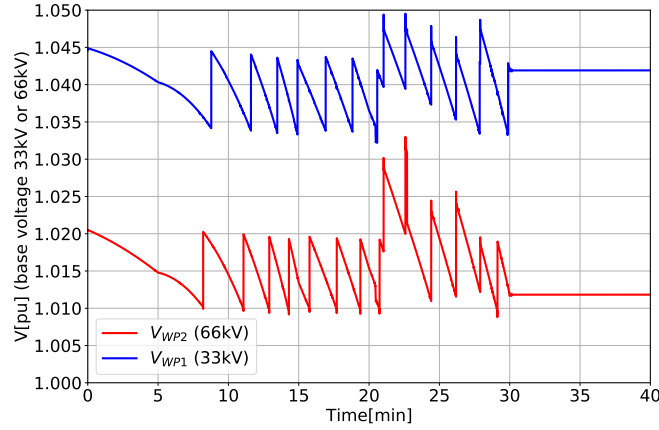


Figure 5.15: *Configuration Q+Automaton version 2*: Voltages at the PCC of one wind park of WP1 and of one wind park of WP2.

available during the wind events, and the voltages were correctly held.

The choice has been made to only command the shunt inductors at TROUFFETTE during the wind events. If the choice is left to the operator, other shunt inductors could be tripped. For instance, there is still a shunt inductor of 300MVar at CHOUFFE that the operator can disconnect.

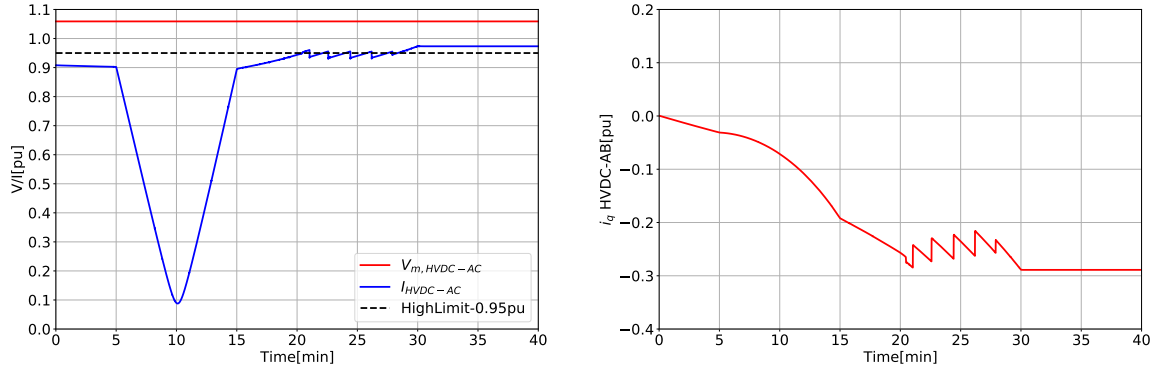


Figure 5.16: *Configuration Q+Automaton version 2*: Modulated voltage and current amplitude of HVDC-AC on the left. Quadrature current of HVDC-AB on the right.

Power injections of HVDC links and synchronous machines

As it can be seen in Figure 5.17, the reactive power productions of HVDC links and the synchronous machine *GenKAR* are greater than with wind parks in voltage control (see Figure 5.7). Indeed, as the wind parks do not take part in the voltage control, the reactive power is supplied by the converters and the synchronous machines.

Once again, the figure on the right shows that the synchronous machine *GenCUR* is over-excited.

Direct and quadrature currents of wind turbines

In Figure 5.18, one can see that the quadrature current of both wind parks remains con-

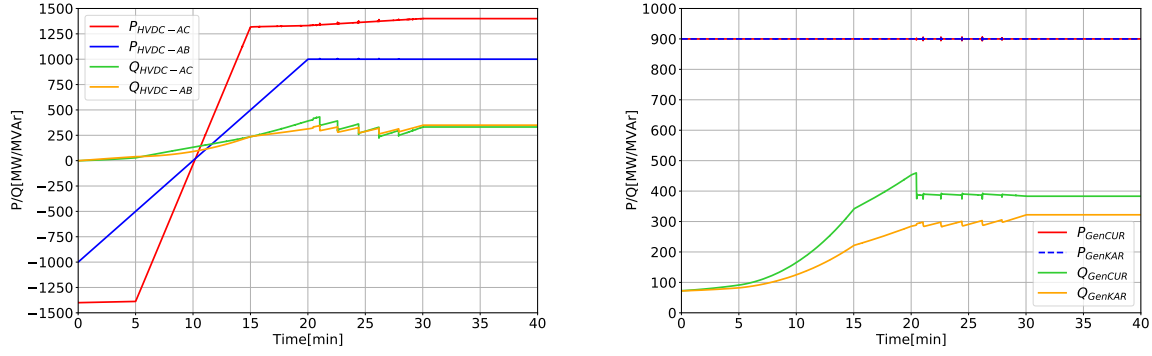


Figure 5.17: *Configuration Q+Automaton version 2*: Power injections of HVDC links (left figure) and synchronous machines (right figure).

stant. They control their reactive power output. Even though the voltages deviate, the converters do not change their reactive power production.

One can also observe that the direct current presents a staircase effect. It does not increase linearly as it has been the case for wind parks in voltage control (see Figure 5.10). As the voltages of the wind parks vary, to keep the same active power output, the direct current has to change. If the voltage declines, the direct current rises. Thus, the current increases because of the wind event, and because of the variation in the voltage magnitude. As the LTC changes the tap position, the voltage is pulled up, and the direct current drops to inject the same active power. Without the LTC, the direct current would have increased much faster as it would have to compensate for the voltage drop. Finally, the current would have overreached the maximum current of $1pu$ which would have led to an unacceptable operation of the wind parks.

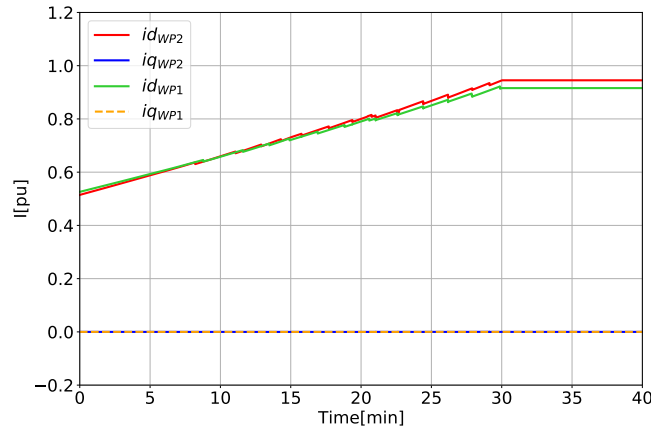


Figure 5.18: *Configuration Q+Automaton version 2*: Direct and quadrature currents of wind parks.

Remark about the control logic

The automaton that disconnects the shunt inductors when the current magnitude of HVDC-AC overcomes $0.95pu$ works properly in this case. But it works well because

HVDC-AC is at its full active power output. Indeed, if HVDC-AC exports 1000MW instead of 1400MW, the current magnitude is much smaller. Under a voltage of $1pu$ and with a nominal apparent power of 1462MVA for HVDC-AC, a current of $0.95pu$ corresponds to a reactive power output of :

$$Q = \sqrt{(0.95S_{nom})^2 - P^2} = 963.87\text{MVar}.$$

The test with HVDC-AC changing its active power setpoint from -1400MW to 1000MW has been realized (see appendix 9.4). The results show the automaton does not disconnect the shunt inductors as the current magnitude never overreaches $0.95pu$. Practically, as the injected power is smaller, it can be supposed that the voltage drop is smaller. It is the case but anyway, the voltage levels go below the voltage limit of 370kV which is unacceptable.

In brief, the control logic here is too simple. The test shows that, while the current of HVDC-AC has never overreached the limit, the quadrature current of HVDC-AB has reached its limit of $-0.3pu$. With that information, an operator would have disconnected the shunt inductors at CHOUFFE, for instance, whereas the automaton did not disconnect any shunt inductors.

The disconnection of the shunt inductors based on the HVDC-AC current magnitude could also be joined with an automaton that disconnects the shunt inductors based on the voltage. It would prevent the system from reaching unacceptable voltage levels if the dynamic reserves are still considered sufficient.

5.1.6 Wind parks WP1 are in reactive power control mode and wind parks WP2 are in voltage control mode: *Configuration VQ*

Voltages at various 380kV buses

As it can be seen in Figure 5.19, the voltage levels are acceptable. Even though no shunt inductors have been disconnected, the voltages stay above the lower limit imposed by the TSO.

Dynamic reserves of HVDC links

In Figure 5.20, one can see that the HVDC link converters are close to their limit. Indeed, the converter HVDC-AC has a current magnitude almost equal to $1pu$. If the voltage drops further on, it will activate the virtual impedance. If it is the case and the voltage of TROUFFETTE is still above the lower limit under which the automaton reacts, the automaton based on the voltage of TROUFFETTE will not disconnect any shunt inductors. The virtual impedance will therefore stay active for a long time which is not acceptable. Furthermore, one can see that the converter HVDC-AB also reached the limit for its quadrature current.

The system needs a master controller managing the dynamic reserves to ensure a safe operation of the system.

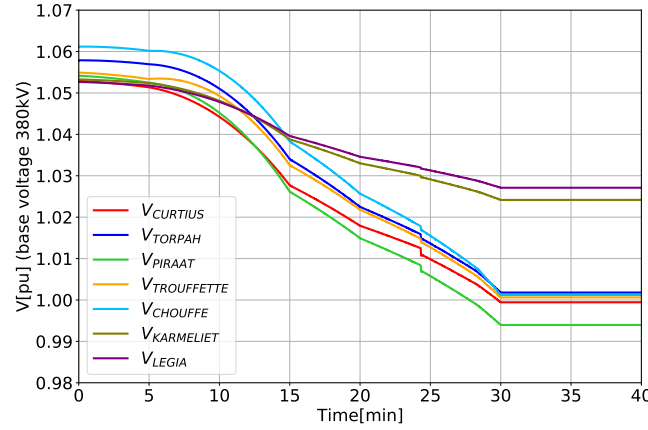


Figure 5.19: *Configuration VQ*: Voltages at various 380kV buses.

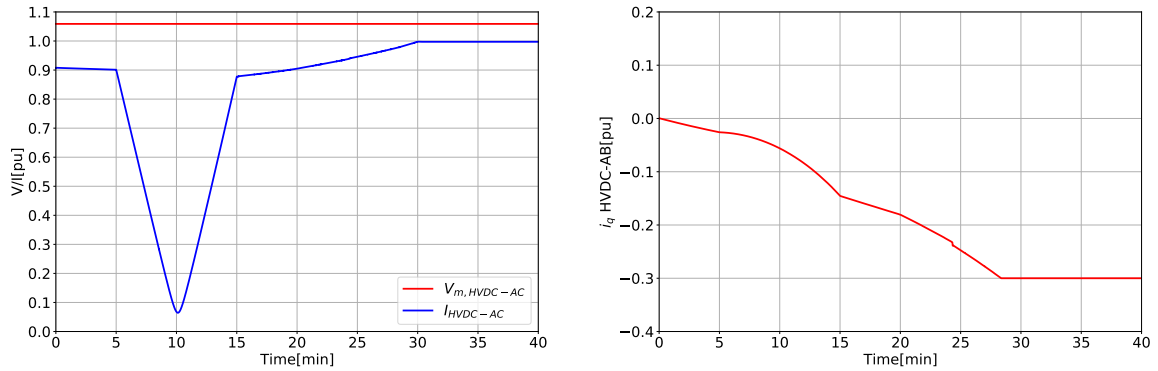


Figure 5.20: *Configuration VQ*: Modulated voltage and current amplitude of HVDC-AC on the left. Quadrature current of HVDC-AB on the right.

5.1.6.1 Using a master controller that manages the dynamic reserves of the network components: *Configuration VQ+Automaton version 2*

As pointed out, the control logic implemented here is pretty simple. The controller looks at the current magnitude of HVDC-AC. If it overcomes $0.95pu$ during more than 25s, it disconnects a shunt inductor connected to TROUFFETTE. It would be better to oversee every converter (not only HVDC-AC) and notify the operator if the limits are close to being reached.

As HVDC-AC is importing its nominal active power, the current magnitude is already high. The current amplitude easily reaches $0.95pu$ if the converter injects reactive power to control its modulated voltage. Thus, this control logic works properly in this scenario.

Voltages at various 380kV buses

The voltage levels shown in Figure 5.21 are acceptable. Three shunt inductors out of five were disconnected. It means there is still 300MVar of shunt inductors connected to TROUFFETTE.

Voltages of wind parks

The voltages of the wind parks are correctly held, as seen in Figure 5.22. As the wind

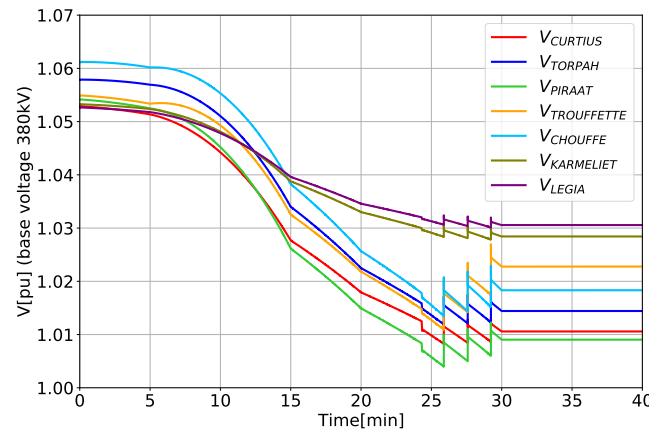


Figure 5.21: *Configuration VQ+Automaton version 2*: Voltages at various 380kV buses.

parks WP1 are in reactive power control mode, the voltages remain within the limits thanks to the Load Tap Changer. The wind parks WP2 control the voltages as they are in voltage control mode. The spikes stem from the disconnection of the shunt inductors that is affecting all voltages.

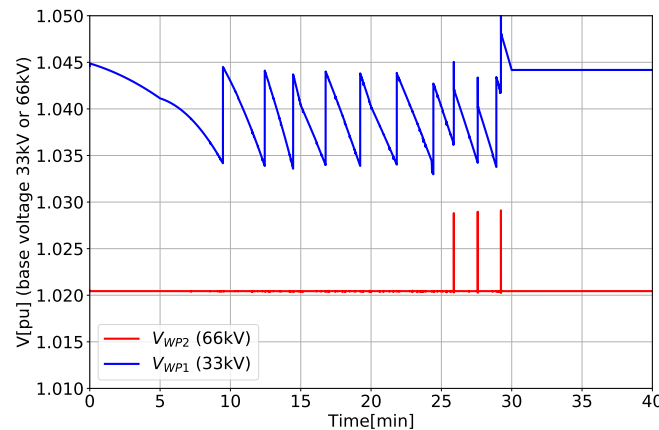


Figure 5.22: *Configuration VQ+Automaton version 2*: Voltages at the PCC of one wind park of WP1 and of one wind park of WP2.

Dynamic reserves of HVDC links

In Figure 5.23 one can see that at the end of the simulation, some reserves are available in case of contingency. The figure on the right shows that the quadrature current of HVDC-AB did not reach its limit of $-0.3pu$.

Power injections of HVDC links and synchronous machines

The power injections of the HVDC links and the synchronous machines are shown in Figure 5.24. Once again, the synchronous machine *GenCUR* activates the over-excitation limiter. It reduces the voltage setpoint of the machine and the machine becomes less excited. In the three wind park configurations, this synchronous machine has always been overexcited.

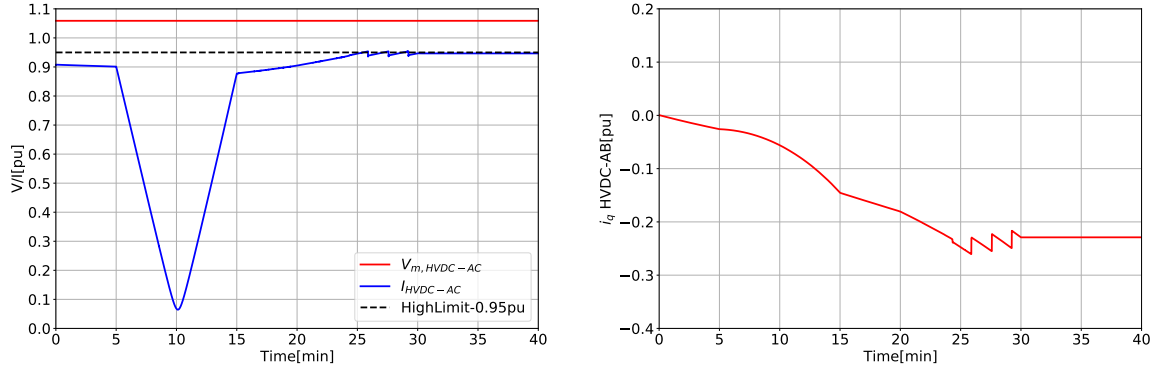


Figure 5.23: *Configuration VQ+Automaton version 2*: Modulated voltage and current amplitude of HVDC-AC on the left. Quadrature current of HVDC-AB on the right.

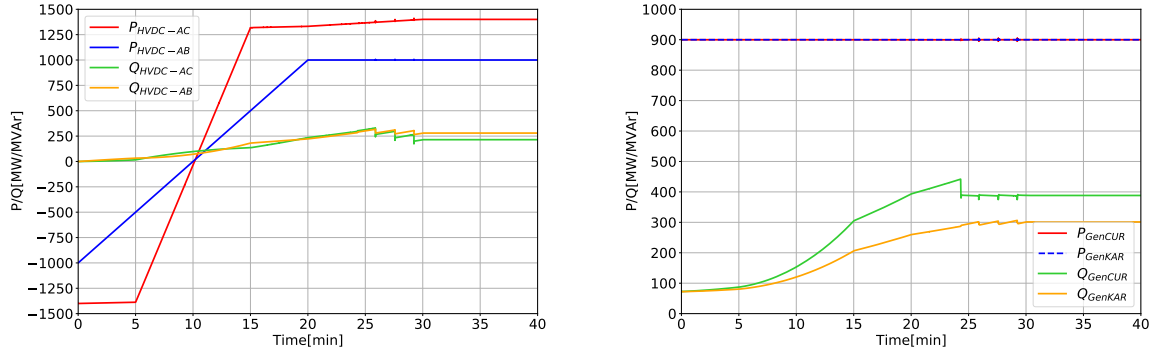


Figure 5.24: *Configuration VQ+Automaton version 2*: Power injections of HVDC links (left figure) and synchronous machines (right figure).

Direct and quadrature currents of wind turbines

The direct and quadrature currents observed in Figure 5.25 illustrate that the wind parks WP1 are in reactive power control mode as the quadrature current remains constant during the simulation. On the other hand, the quadrature current of wind parks WP2 varies with time as the converter is in voltage control mode.

5.2 From a highly loaded system to a lightly loaded system : The *Storm event* scenario

If the system is unloaded, the voltages rise as the cables and the lines produce more reactive power or consume less reactive power. The loaded system is very similar to the system after the *Ramping event*. The wind parks are injecting their full active power output, wind parks WP1 produce 2626MW, and wind parks WP2 produce 2100MW. The HVDC links import 1400MW for HVDC-AC and 1000MW for HVDC-AB. It can be assumed that, at the end of the *Ramping event*, some operations were realized, restoring the voltages to their nominal values. The sequence of events described here happens some hours after the *Ramping event*. The shunt inductors at TROUFFETTE have been tripped, and there are still 300MVar of shunt inductors connected to CHOUFFE.

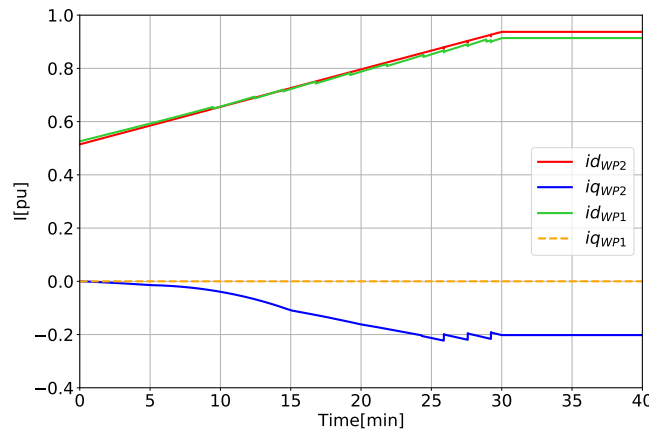


Figure 5.25: *Configuration VQ+Automaton version 2*: Direct and quadrature currents of wind parks.

The power flows in the entire system are shown in the appendix 9.3.

5.2.1 Description of the sequence of events

In this scenario, two types of wind turbine are considered. The wind turbines represented by WP1 do not have *high wind ride trough capability* (HWRT). Thus, their *P-v curve* looks like the left side of Figure 2.1. The wind turbines represented by WP2 have the HWRT. Their *P-v curve* looks like the right side of Figure 2.1.

It is supposed that a storm passes through the wind parks. The wind parks WP1 are the first affected by the storm. The wind parks WP1 are composed of only wind turbines without HWRT. When the wind speeds overreach the cut-out wind speed, the wind turbines see their active power production falls to 0MW. Every minute, starting from minute 0, the storm hits a wind park of WP1.

At $t=17\text{min}$, the storm reaches the wind parks WP2. As they have HWRT, the turbines do not stop immediately after the wind speeds overreach the cut-out wind speed. Their power output declines as the wind speeds rise. After 12 minutes, the power output of the turbine is decreased to 0MW because the wind speeds reach the maximum wind speed that the turbine can withstand. Every minute a wind park of WP2 is affected by the storm. For instance, at $t=17\text{min}$, one of the wind park in WP2, that can be named *WPnum1*, is hit by the storm. At $t=18\text{min}$, a wind park named *WPnum2*, is impacted. It continues until every wind park that is composing WP2 has been impacted. In the meantime, *WPnum1* has seen its power output reduced. At $t=29\text{min}$, the wind park *WPnum1* has a power output of 0MW while the power output of *WPnum2* is still decreasing. At $t=30\text{min}$, the wind park *WPnum2* has a power output of 0MW.

At $t=40\text{min}$, wind parks WP1 and WP2 are producing 0MW. The lack of active power caused by the decreased power output of the wind turbines is compensated by the synchronous machine of 300 000MVA at the equivalent node *EquivNode*. The power setpoint of this machine increases by 4780MW in 40 minutes. It leads the frequency to stabilize at 1pu after the sequence of events.

The scenario is illustrated in Figure 5.26.

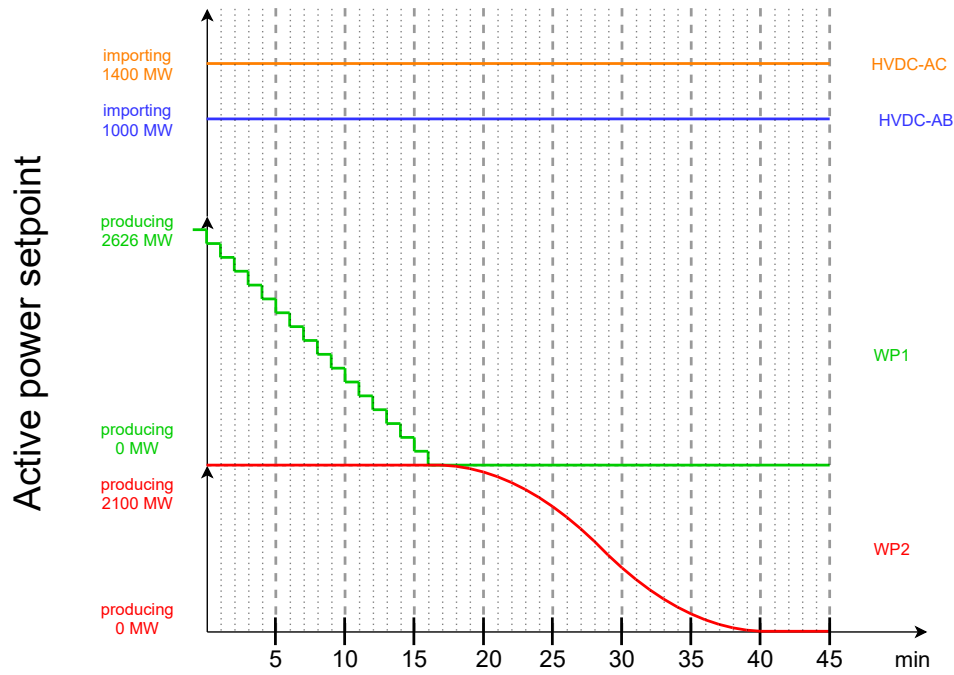


Figure 5.26: *Storm event*: Illustration of the sequence of events.

5.2.2 Influence of the sequence of events on the power flows and on the network frequency after balancing

In Figure 5.27 one can see the influence of the sequence of events on the active power flows through the green and orange circuits (see Figure 4.1). The system starts from a highly loaded situation and is progressively unloaded.

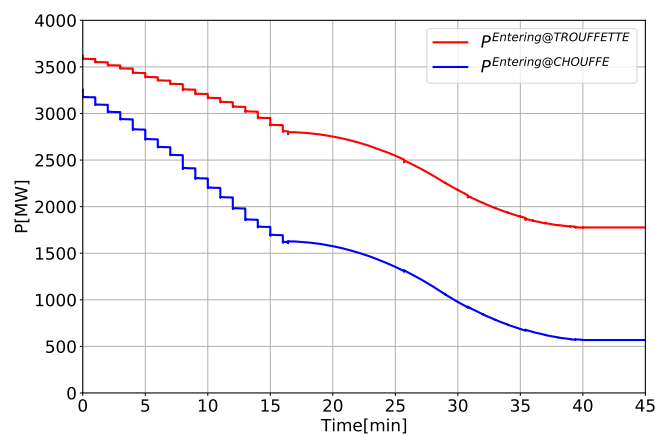


Figure 5.27: *Storm event*: Active power flowing through the green and orange circuits. The addition of the two curves gives the evolution of $P_{2,COR}$ with time.

Figure 5.28 shows that the system is correctly balanced as the frequency returns to the nominal frequency (50Hz) after the sequence of events.

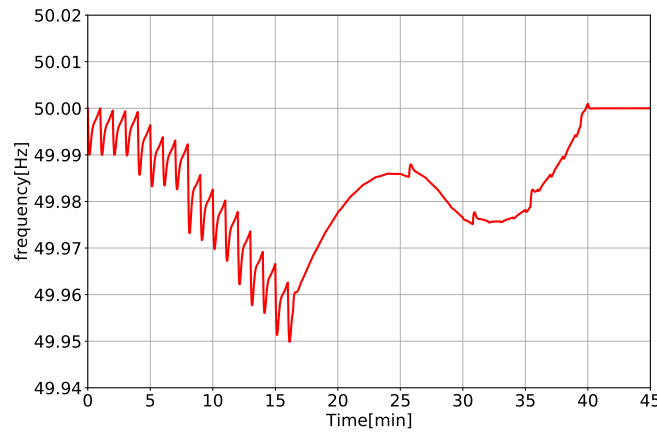


Figure 5.28: *Storm event*: Network frequency evolution.

5.2.3 The different options available for wind parks after being impacted by the storm.

The wind park progressively or suddenly reduces its power output after being impacted by the storm. Two choices were made available for the wind park when its active power production drops to 0MW. It can stay connected, injecting no active power, or it can be disconnected from the grid. If it disconnects, the system loses the voltage support brought by the wind park (if the latter was in voltage control mode). Thus, two cases are studied. The first is that all wind parks are disconnected from the grid. Therefore, it does not matter whether they are in voltage control mode or in reactive power control mode as, in the end, they inject nothing into the grid. The second option is that only the wind parks WP2 stay connected with an active power production of 0MW. For this option to make sense, the wind parks WP2 are in voltage control mode to provide voltage support during the event. The wind parks WP1 are disconnected from the grid for both options. The two configurations studied are:

- The wind parks WP1 and WP2 are in voltage control mode and are disconnected from the grid when the active power setpoint is decreased to 0MW (*Configuration AllTripped*),
- The wind parks WP1 and WP2 are in voltage control mode but the wind parks WP2 stay connected to the grid even though the active power setpoint is decreased to 0MW (*Configuration WP1Tripped*).

5.2.4 Wind parks WP1 and WP2 are disconnected from the grid: *Configuration AllTripped*

Voltages at various 380kV buses

Figure 5.29 shows the voltage levels of the network. The voltages increase because the system is progressively unloaded.

In the first part of the *Storm event*, between $t=0\text{min}$ and $t=17\text{min}$, the wind parks WP1 are progressively disconnected. The wind parks WP1 are connected to CHOUFFE,

and as seen, the busbar CHOUFFE suffers from the largest voltage rise compared to the other busbars. Two things cause the step increase in voltage levels. First, the rapid active power reduction increases the voltage level. Secondly, as the wind park is disconnected, the system loses its voltage support. As the simulation runs, the wind park's participation in the voltage support becomes more prominent. Thus, the disconnection of a wind park induces a larger voltage rise (given the same active power reduction).

In the second part of the *Storm event*, between $t=17\text{min}$ and $t=29\text{min}$, the wind parks WP2 see their active power injection progressively decreased. More and more wind parks are affected by the storm, thus the total active power of WP2 reduces with time. The voltages gradually increase, as the active power reduction is not a sudden reduction like for wind parks WP1. The busbar TROUFFETTE is the more impacted because the wind parks WP2 are connected to it.

In the last part of the *Storm event*, between $t=29\text{min}$ and $t=40\text{min}$, the wind parks WP2 start being disconnected. The step increase in the voltages is caused by the sudden disconnection of the wind parks, and so, the sudden loss of reactive power they were consuming.

The voltage levels shown in the figure are not acceptable as they overreached the maximum limit of 420kV allowed by the TSO.

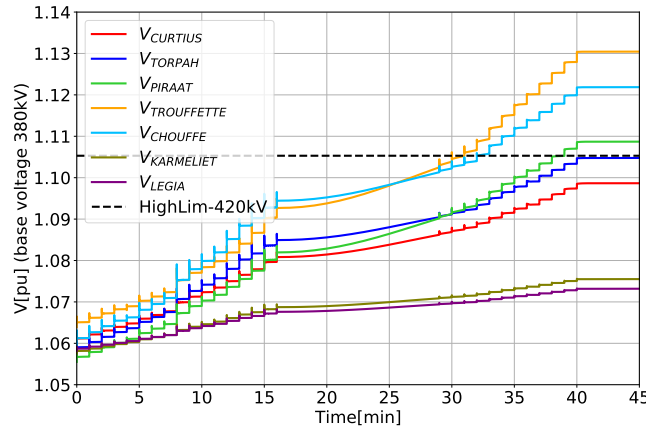


Figure 5.29: *Configuration AllTripped*: Voltages at various 380kV buses.

5.2.4.1 Using an automaton to connect the shunt inductors based on TROUFFETTE voltage: *Configuration AllTripped+Automaton version 1*

At the beginning of the *Storm event*, the 900MVar of shunt inductors placed at TROUFFETTE are disconnected. To prevent the voltage rise, one can progressively connect these 900MVar as the voltage increases. The use of an automaton, as in the *Ramping event* scenario, works well. Indeed, in this case, the automaton connects the shunt inductors when the voltage of TROUFFETTE goes above 415kV for 25s. The 900MVar are split into five different shunt inductors, four of 200MVar and one of 100MVar.

Voltages at various 380kV buses

With the automaton, the voltage levels stay under the upper limit as shown in Figure 5.30. At the end of the simulation, the five shunt inductors have been connected.

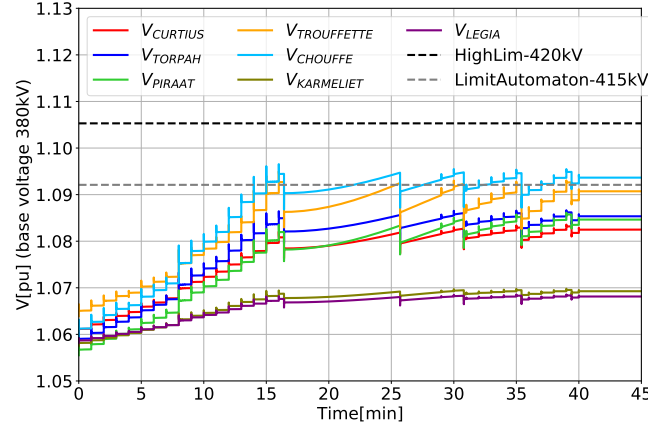


Figure 5.30: *Configuration AllTripped+Automaton version 1*: Voltages at various 380kV buses.

Power injections of HVDC links and synchronous machines

In Figure 5.31, one can see the power injections of the HVDC links and the synchronous machines. As observed, the synchronous machines and the HVDC links consume reactive power to limit the voltage rise. For the synchronous machines, an under-excitation limit is imposed. The limit is fixed following the requirement imposed by the TSO. The machine should be able to absorb 25% of its nominal apparent power. Therefore, the synchronous machines *GenCUR* and *GenKAR* can absorb 250MVar under a voltage of 1pu. The figure shows the limit has not been reached.

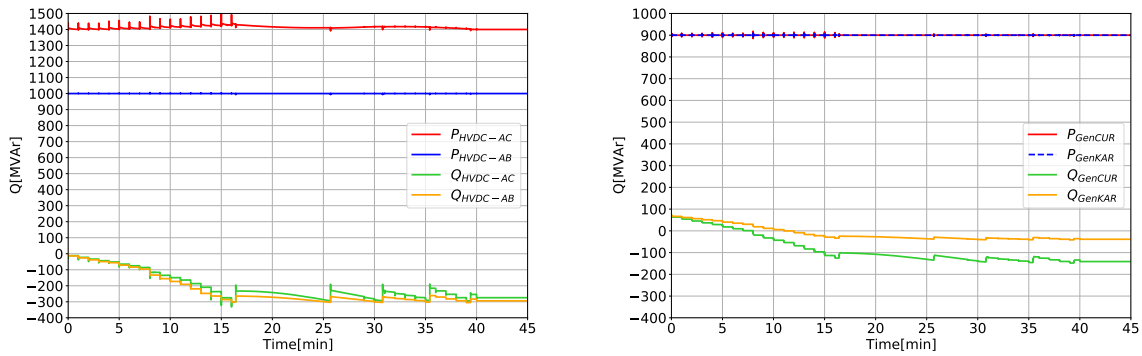


Figure 5.31: *Configuration AllTripped+Automaton version 1*: Power injections of HVDC links (left figure) and synchronous machines (right figure).

5.2.5 Wind parks WP1 are disconnected from the grid and wind parks WP2 stay connected: *Configuration WP1Tripped*

Voltages at various 380kV buses

As seen in Figure 5.32, the voltage levels remain in the limits except for the busbar TROUFFETTE. Compared to the initial case where all wind parks were disconnected (Figure 5.29), the voltage increase between $t=29\text{min}$ and $t=40\text{min}$ does not appear here. This part was mostly due to the loss of voltage support caused by the disconnection of wind parks WP2.

Nevertheless, the voltage of TROUFFETTE is not kept within the acceptable range. As it can also be seen, in this case, the voltage of TROUFFETTE is greater than the one of CHOUFFE. In *Configuration AllTripped + Automaton version 1* (Figure 5.30), the largest voltage magnitude was found at CHOUFFE busbar. The difference stems from the shunt inductors' activation at TROUFFETTE that inhibits the voltage rise at that busbar. In this scenario, the shunt inductors stay connected, thus the busbar TROUFFETTE presents the largest voltage magnitude.

Even though the voltage of TROUFFETTE is not acceptable, the option of keeping the wind parks connected after the *Storm event* is still interesting. With the use of an automaton to connect shunt inductors, this solution can become acceptable.

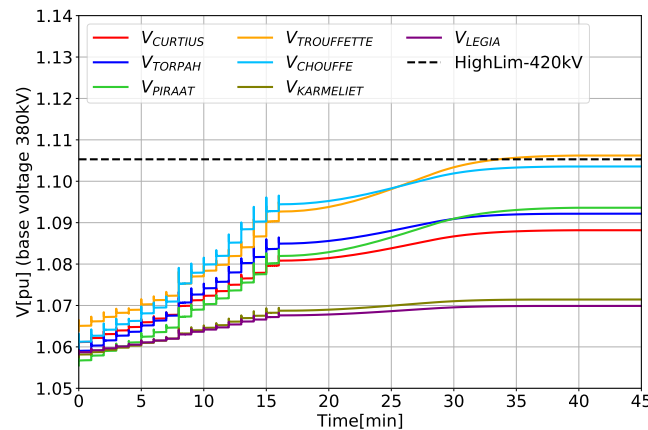


Figure 5.32: *Configuration WP1Tripped*: Voltages at various 380kV buses.

Direct and quadrature currents of one wind park in WP2

As shown in Figure 5.33, the direct current is reduced as the storm passes through the wind park. But the reactive power consumption of the wind park, represented by the quadrature current, increases as the wind parks are progressively disconnected (WP1) or as the wind parks see their active power decreased to 0MW (WP2). This reactive power consumption is lost if the wind park is disconnected. It leads to a sudden voltage rise, as it was seen in Figure 5.29 and Figure 5.30.

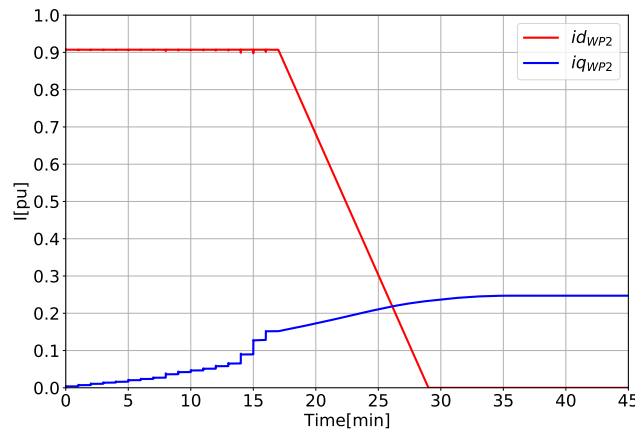


Figure 5.33: *Configuration WP1Tripped*: Direct and quadrature current of one wind park in WP2.

5.3 Conclusion

In this first part, the impact of wind events and HVDC power shifts has been analyzed.

About the sequence of events. In modern power systems, the HVDC links are used to enhance the power transfer between different zones. It increases the market liquidity. As such, the HVDC links' operation is correlated with wind energy production. In the *Ramping event* scenario, the worst-case scenario has been investigated. The *Ramping event* hits different control areas close to each other, and the HVDC links are used to ensure optimal social welfare. The operation on the HVDC links brought an increase in power flows added to the wind power production. It thus results in significant changes in power flows in a short amount of time.

In the *Storm event*, the HVDC links' operation has been neglected. The worst-case scenario would have been to reduce the active power setpoint of both HVDC links to 0MW. Nevertheless, this scenario has been considered as not conceivable. Indeed, if the HVDC links were set to 0MW, this would mean that the electricity prices were the same in the different control areas. Furthermore, even though it is not always forecasted accurately, the storm is at least predicted to occur during the day. The HVDC links are therefore set to import power to mitigate the loss of the wind parks.

The wind events presented in this section correspond to extreme and rare phenomena. Nevertheless, both *Ramping event* and *Storm event* stay realistic compared to the wind events introduced in section 2.1. Furthermore, as the wind parks are very close to each other in this network, changes in wind speeds are of greater importance and lead to larger variations in power productions.

About the problem of wind events. Because of the high variability in wind power production, such events can be hard to forecast, or the forecast is not accurate enough to define when the wind event occurs. Therefore, the operator may not react in time, and as shown, the system could reach unacceptable voltage levels under 40minutes. For this reason, solutions have been tested. They help the operator reacting in time or disconnect the shunt inductors.

About the solutions found. An automaton that disconnects shunt inductors based on the voltage of a busbar works well, as seen in the *Ramping event* scenario. But, the dynamic reserves of some converters are drastically reduced at the end of the wind event. At some point, the system is left with almost nothing to control the voltages. Another control logic has been proposed to prevent any further issues in case of an incident. It consists in managing the dynamic reserves of the principal injectors to ensure at least a margin before reaching the limits of the converters. This control logic does not need an automaton to be applied. The fact that the wind event is pretty slow compared to other incidents leaves the possibility of a control logic that interacts with the operator. The operator can be notified that the dynamic reserves are consumed, and he can have some time to react and to activate, for instance, shunt inductors.

In the case of the *Storm event* scenario, the only issue that has been faced is the excessive voltage levels. An automaton activating shunt inductors based on a voltage is enough to ensure a safe grid operation. Indeed, the consumption of the dynamic reserves does not threaten the system in this case. One can also see that significant results can be achieved if the wind parks stay connected to the network after the *Storm event*. The reactive power that they consume permits to limit the voltage rise if they are in voltage control mode. Anyway, the connection of shunt inductors is needed to keep the voltage levels within acceptable values.

What next? In both scenarios, the voltage levels have stabilized around low or high but acceptable values. Nevertheless, it is interesting to see how the system behaves when an incident occurs. Some dynamic reserves have been preserved, but the injectors are close to their limit and have a limited reaction capability. The solutions found work well for slow dynamics like wind events. In case of an incident, the reaction time is more restricted, and the use of an automaton, or the operator's actions, cannot guarantee a safe operation of the system. Other solutions have to be found.

Chapter 6

Impact of a transmission outage on the network post wind event

As shown in Chapter 5, the network, for both wind events, has reached an acceptable operating point in terms of voltage levels and dynamic reserves. Nevertheless, the voltages deviate from the nominal values, and the dynamic reserves are close to being completely consumed.

If an incident occurs, the system could collapse or reach an unacceptable operating point. Those cases are analyzed in this chapter.

6.1 Incident in the network post *Ramping event*: Loss of the green circuits

6.1.1 Description of the incident

As the network post *Ramping event* is highly loaded, the loss of one or several circuits could lead to a significant voltage drop. Indeed, the power flowing through the circuits deviates to other circuits already highly loaded. From the network scheme shown in Figure 4.1, the loss of the green circuits is more severe than the loss of the orange circuits as the green circuits represent a lower impedance path.

It has been decided to test two incidents on this network. The first one is the loss of the green circuits. The second one is a short-circuit applied at TORPAH, lasting 100ms and then cleared by opening the green circuits.

6.1.2 The different scenarios analysed

Table 6.1 describes the scenarios analyzed. The post-fault corrective controls are explained later on when the scenario is investigated. The three wind park configurations studied in Chapter 5 are included. At the end of the *Ramping event*, three configurations were considered as acceptable:

- The wind parks WP1 and WP2 are in voltage control mode. There are 900MVar of shunt inductors connected to TROUFFETTE (scenarios 1 and 2).

- The wind parks WP1 and WP2 are in reactive power control mode. There is 0MVar of shunt inductor connected to TROUFFETTE (scenario 3).
- The wind parks WP1 are in reactive power control mode, and wind parks WP2 are in voltage control mode. There are 300MVar of shunt inductors connected to TROUFFETTE (scenarios 4,5,6).

	Scenario					
	1	2	3	4	5	6
Pre-fault configuration						
Control of WP1	V	V	Q	Q	Q	Q
Control of WP2	V	V	Q	V	V	V
Synchronous Condenser (nominal MVar @TROUFFETTE)	0	0	300	0	0	0
Synchronous Condenser (nominal MVar @CHOUFFE)	0	0	200	0	200	200
Shunt inductors (nominal MVar @TROUFFETTE)	900	900	0	300	300	300
Shunt inductors (nominal MVar @CHOUFFE)	300	300	300	300	300	300
Post-fault corrective controls						
Reactor tripping @TROUFFETTE	yes	yes	yes	yes	yes	yes
Reactor tripping @CHOUFFE	no	no	yes	no	yes	no
$P_{HVDC-AC}^{setpoint}$ decreased to 0 MW	yes	no	yes	yes	no	no
$P_{HVDC-AB}^{setpoint}$ decreased to 0 MW	no	yes	no	no	yes	yes
Full Q capability of HVDC-AB released	no	no	no	no	no	yes

Table 6.1: Configuration of the different scenarios analysed. Q means reactive power control mode. V means voltage control mode.

6.1.3 Scenario 1

First, an incident occurs in the system, and no post-fault corrective controls are performed. It aims to show the new operating point reached by the system if nothing is done. Then, the post-fault corrective controls are described. Finally, the results are shown.

6.1.3.1 Without the post-fault corrective controls

As seen in Figure 6.1, the voltage levels are unacceptable.

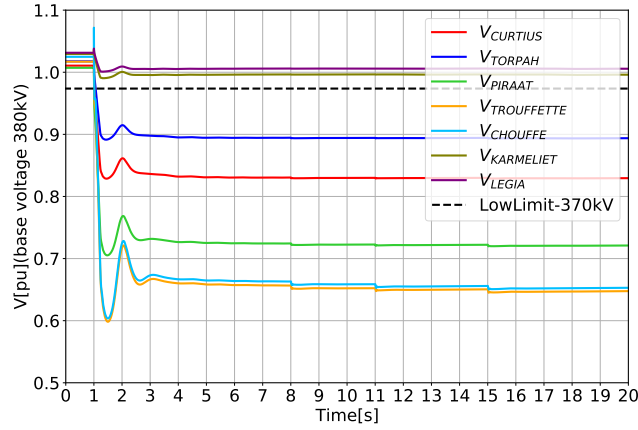


Figure 6.1: *Scenario 1 without post-fault corrective controls*: Voltages at various 380kV buses

6.1.3.2 Description of the post-fault corrective controls

The system stabilizes around a low voltage operating point. It results from multiple dynamics. While the green circuits are tripped, the grid forming converter HVDC-AC activates its virtual impedance and does not control the voltage anymore. Furthermore, the grid following converters, with the dynamic voltage support available, switch to the dynamic voltage support mode when the voltage suddenly drops. It is difficult to understand what makes the system stabilize around an acceptable or unacceptable operating point. Nevertheless, it has been tested that a crucial point is to let the grid forming converter controls the voltage again (see appendix 9.5).

As the orange circuits become suddenly highly loaded, the voltage drop is consequent. The converters quickly reach their limit to meet the reactive power demand. It causes the grid forming converter HVDC-AC to not control the voltage as its current overreaches the maximum current allowed. It has been decided to reduce the active power injections of the HVDC links and to trip the shunt inductors still connected to TROUFFETTE to help the injectors.

The central goal is to prevent wind turbines from being disconnected from the grid. The recovering time accepted for the voltages has been selected based on that criteria. To know for which voltage the wind turbine is disconnected, one can use its fault ride-through capability (FRT) as shown in Figure 6.2. If the voltage drop stays within the FRT, the wind turbine is not disconnected as required by the TSO. From Figure 6.1, the voltage nadir reaches $0.6pu$. Therefore, if one looks at the FRT, the voltage levels should recover in about 1s to prevent any unintended disconnections.

As explained, the idea is to reduce the active power injections. In scenario 1, the active power setpoint of HVDC-AC is lowered from 1400MW to 0MW. As it is an emergency, the active power reduction has not been optimized. A less significant active power reduction may also perform well. The 900MVar of shunt inductors connected to TROUFFETTE are tripped. The post-fault corrective controls are *event-based*, once the tripping of the green circuits has been detected, a message is sent to the HVDC links and the breakers at

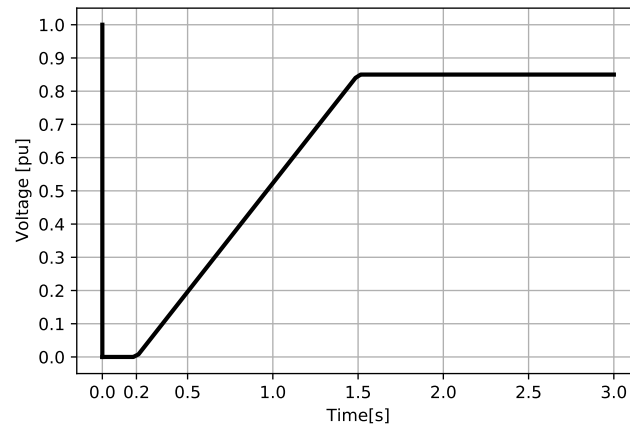


Figure 6.2: Wind turbines fault ride-through capability ([7]).

TROUFFETTE. The communication delay is 100ms. After 100ms, the shunt inductors at TROUFFETTE are disconnected. The active power reduction of HVDC-AC can start. It takes 700ms to reduce the active power setpoint of HVDC-AC from 1400MW to 0MW. The timeline of the post-fault corrective controls is shown in Figure 6.3.

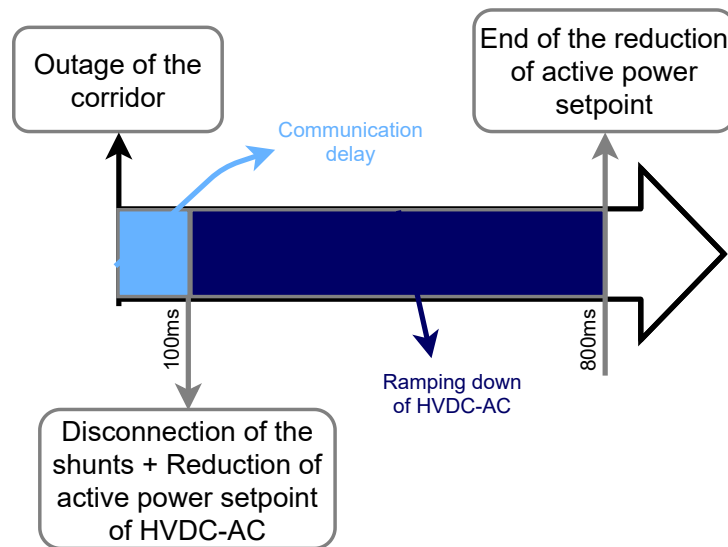


Figure 6.3: *Scenario 1*: Timeline of the post-fault corrective controls.

6.1.3.3 Results

Voltages at various 380kV buses

In Figure 6.4, one can see the voltages of the different buses of the network. The post-fault corrective controls brought the system back to an acceptable operating point.

Voltages of wind parks

As shown in Figure 6.5, the voltage drop can be withstood by the wind parks. Following their FRT, they have to stay connected to the grid. At the end of the simulation, the voltages are correctly held by the wind parks.

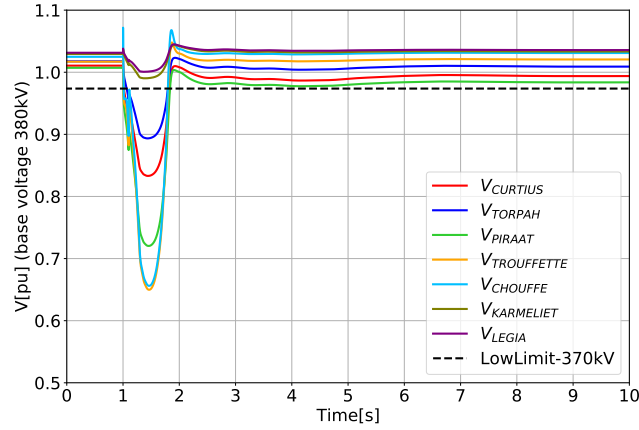


Figure 6.4: *Scenario 1*: Voltages at various 380kV buses.

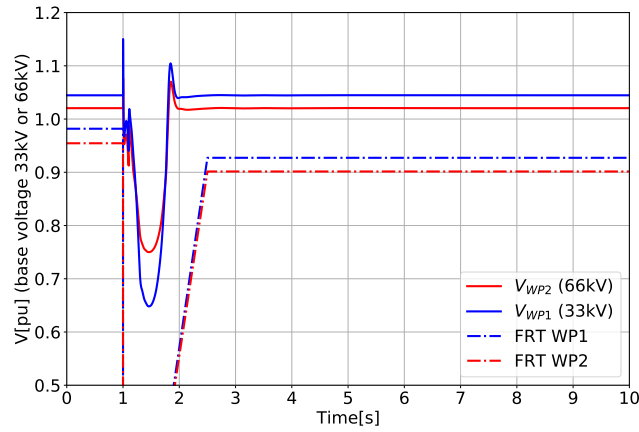


Figure 6.5: *Scenario 1*: Voltages at the PCC of one wind park of WP1 and of one wind park of WP2.

Power injections of HVDC links

The dynamics of the different HVDC links are shown in Figure 6.6. For HVDC-AC, which is in grid forming mode, the active power production drops, and the reactive power rises steeply after the incident occurred. When the incident takes place, the phase angles are shifted upward. The active power produced by the grid forming converter is quickly reduced as its angle has not changed yet. The reactive power is quickly increased as the modulated voltage stays constant. The HVDC-AC acts as a perfect voltage source for the very first moments after the incident. When the current overreaches $1pu$, the modulated voltage is no longer controlled.

The synthetic inertia also plays a role in the dynamics of HVDC-AC. The active power production is not decreased to 0MW within 800ms. It is the case for the active power setpoint. Tests have shown that with a limited synthetic inertia, the active power production reaches 0MW under 800ms (see appendix 9.6).

One can also see that the HVDC-AB activates its dynamic voltage support as the voltage of CHOUFFE goes below the limit of $0.9pu$, and because of the sudden voltage

drop. The reactive power is prioritized, and the active power is reduced.

Finally, the power injections stabilize around acceptable values. The reactive power production could rise towards the nominal apparent power if needed as the active power production of HVDC-AC has been reduced to 0MW. The reactive power production of HVDC-AB is smaller than before the contingency.

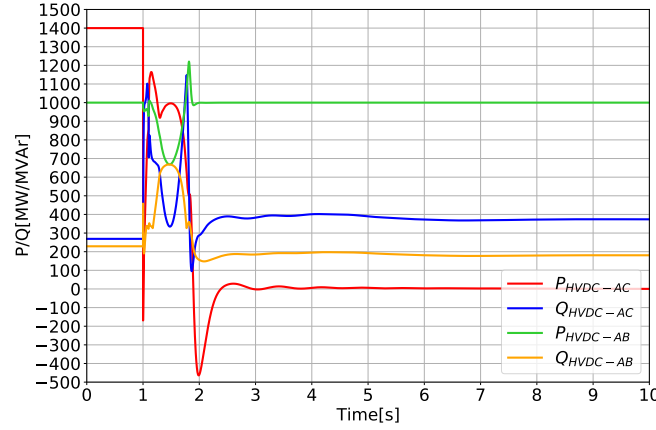


Figure 6.6: *Scenario 1*: Power injections of HVDC links.

HVDC-AC modulated voltage and current magnitude

During the incident, the virtual impedance of HVDC-AC has been activated. It is due to the current magnitude overreaching the maximum limit of $1pu$. As seen in Figure 6.7, the modulated voltage is reduced to restrict the current magnitude. While the virtual impedance is activated, the grid forming converter does not act as a voltage source. As the active power is reduced and the voltages rise, the current slowly decreases. The virtual impedance is gradually deactivated.

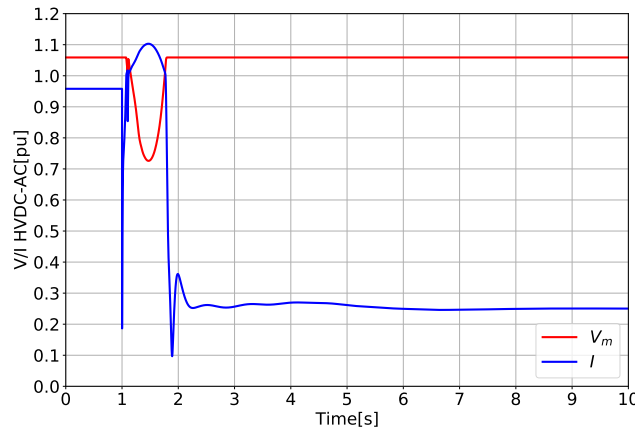


Figure 6.7: *Scenario 1*: HVDC-AC modulated voltage and current magnitude

Direct and quadrature currents of wind parks

Figure 6.8 shows the direct and quadrature currents of the wind parks WP1 and WP2. The wind parks WP1 do not have the dynamic voltage support activated. Therefore, the quadrature current is limited to $-0.3pu$. On the other hand, the wind parks WP2, with their dynamic voltage support activated, inject more reactive power during the incident.

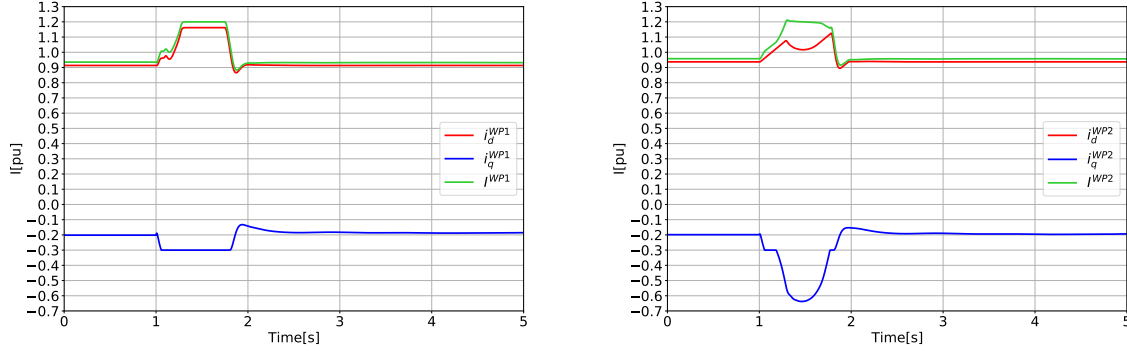


Figure 6.8: *Scenario 1*: Direct and quadrature currents of one wind park of WP1 (left) and of one wind park of WP2 (right).

6.1.4 Scenario 2

6.1.4.1 Description of the post-fault corrective controls

In this scenario, instead of diminishing the active power setpoint of HVDC-AC, one decreases the setpoint of HVDC-AB. It leads to a smaller active power reduction as HVDC-AB is injecting 1000MW compared to 1400MW for HVDC-AC.

Then, reducing the active power setpoint of HVDC-AC leaves more room for reactive power production. Indeed, HVDC-AC is constrained by the current magnitude. If the active power is reduced, so the current magnitude is, and the margin before reaching the limit is enlarged.

For HVDC-AB in grid following mode, even though the active power is reduced, the reactive power is limited. If the dynamic voltage support is no longer activated, the reactive power is limited by the threshold value of $-0.3pu$ applied to the quadrature current. If the dynamic voltage support is activated, the reactive power is already prioritized. Therefore, diminishing the active power of HVDC-AB is less helpful than reducing the active power of HVDC-AC.

Only 500ms are needed to curtail the active power setpoint of HVDC-AB as the active power reduction is smaller than in scenario 1. The timeline of the post-fault corrective controls is shown in Figure 6.9.

6.1.4.2 Results

Voltages at various 380kV buses

In Figure 6.10, one can see the voltages at various 380kV buses for scenario 2. The voltage drop is smaller than in scenario 1 (see Figure 6.4). One can also see that the voltage of PIRAAT is below the lower limit. A long time operation under the limit is unacceptable, but in this case, the point is to save the system. The voltage levels stabilized around

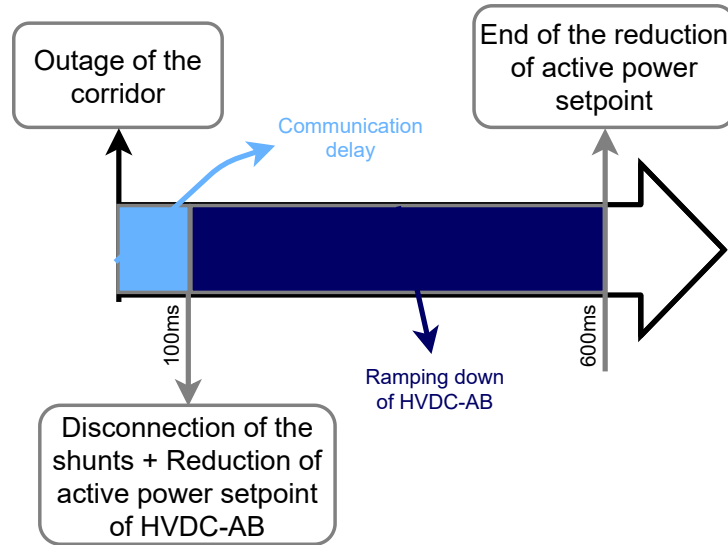


Figure 6.9: *Scenario 2*: Timeline of the post-fault corrective controls.

acceptable values even though one voltage is below 370kV. The grid operator can solve this issue with additional post-fault corrective controls that do not need a fast reaction time.

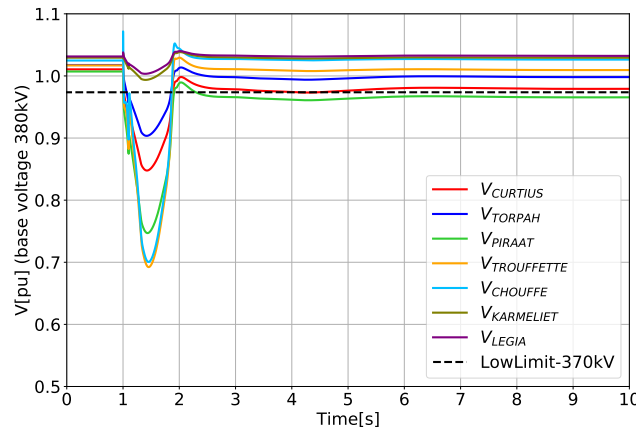


Figure 6.10: *Scenario 2*: Voltages at various 380kV buses.

Voltages of wind parks

In Figure 6.11, one can see that the wind parks stay connected to the grid. The voltages lie inside the FRT capability of the wind parks.

Power injections of HVDC links

In this scenario, the active power reduction is applied on HVDC-AB. As shown in Figure 6.12, the active power is brought to 0MW in 500ms, as expected. Here, the active power reduction corresponds to the active power setpoint reduction. The power reduction is faster and can explain the smaller voltage drop seen in Figure 6.10 compared to scenario 1 (see Figure 6.4). Appendix 9.6 confirms that the voltage drop is smaller for a faster active power reduction.

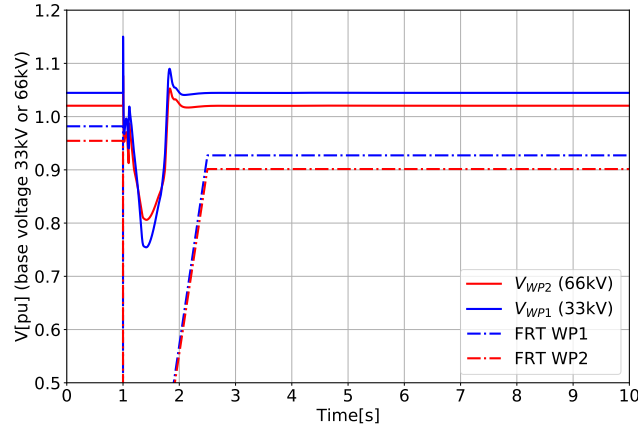


Figure 6.11: *Scenario 2*: Voltages at the PCC of one wind park of WP1 and of one wind park of WP2.

The active power injected by HVDC-AC is greater post-contingency. It is because of its primary frequency control. Imbalances occur because of the loss of HVDC-AB active power and are compensated by the increased production of HVDC-AC. HVDC-AC becomes very close to its limit and cannot produce more reactive power. Compared to scenario 1, the reactive power production is shared among the two converters, each of them injects around 300MVar.

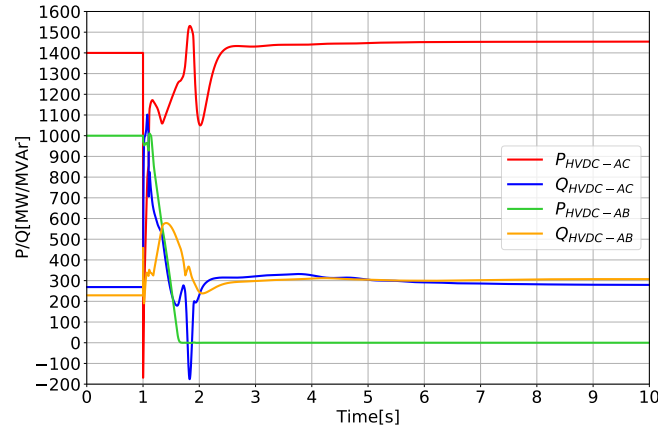


Figure 6.12: *Scenario 2*: Power injections of HVDC links.

6.1.5 Global Results

6.1.5.1 Explanation of the table of results

Table 6.2 shows the results of multiple tests performed on the network. The table quantifies the needs for ensuring a stable and operational system if the N-2 incident occurs (loss of the green circuits). It includes the post-fault corrective controls and the support provided by the different injectors.

Under the pre-fault tab, one can see the different network configurations before the fault takes place. Those pre-fault configurations derive from wind events. The color code illustrates the wind parks' control modes. For instance, the line *Pre-1* shows that, for wind parks in voltage control mode, the pre-fault configuration corresponds to 900MVar of shunt inductors connected to TROUFFETTE and all injectors producing their maximum power output. It corresponds to the configuration at the end of the wind event for wind parks in voltage control mode (*Configuration V*). The line *Pre-1* also gives the reactive power production of the different injectors, as well as the value of P_{2COR} . In Figure 4.1, the value P_{2COR} represents the sum of the active power flowing through the green and orange circuits.

Under the post-fault tab, one can see the post-fault corrective controls and the response of the different converters. The scenario 1 corresponds to line *Post-2*. The first column shows that, as corrective control, 900MVar nominal are injected. It corresponds to the disconnection of the 900MVar of shunt inductors that were connected before the fault. The second column indicates the active power setpoint of HVDC-AC is reduced by 1400MW. Indeed, the active power setpoint was brought to 0MW in scenario 1. The active power setpoint remains unchanged for HVDC-AB. The values underlined correspond to the post-fault corrective controls.

The responses of the different converters correspond to the values found below ΔQ . The new value of P_{2COR} is also shown. As the green circuits have been tripped, the value of P_{2COR} corresponds to the active power flowing through the orange circuits. One can also see a column that determines if extra equipment is needed. Installing extra equipment has to be considered if the disconnection of the shunt inductors at TROUFFETTE does not ensure a stable system. For instance, the line *Post-1* shows that 1500MVar are needed. Unfortunately, only 900MVar of shunt inductors can be disconnected. Therefore, 600MVar of shunt capacitors can be added. The last column indicates if the solution is analyzed in one of the scenarios shown in Table 6.1. Finally, the minimum value acceptable to ensure a safe system is framed in red. In this table, all the results represent solutions that guarantee a secure system. But, for instance, instead of injecting 1500MVar in line *Post-1*, one injects 1400MVar, the voltage levels would collapse, and the system would not be operable. On the other hand, in line *Post-2*, it can be seen that if only 800MVar are injected, this would be enough to guarantee a safe system as the value is not framed in red.

line n°	Pre-fault											Checked for further analysis (scenario n°)
	Q ^{nom} [MVar] injected at TROUF-FETTE	P[MW]				Q[MVar]				P _{2COR} [MW]		
		HVDC-AC	HVDC-AB	WP1	WP2	HVDC-AC	HVDC-AB	WP1	WP2			
Pre-1	-900	1400	1000	2626	2100	270	230	385	444	6902		
Pre-2	0	1400	1000	2626	2100	332	350	-60	0	6889		
Pre-3	-300	1400	1000	2626	2100	215	280	-60	456	6894		
Post-fault (the corrective controls are <u>underlined</u>)												
	ΔQ ^{nom} [MVar] injected at TROUF-FETTE	ΔP[MW] = P ^{setpoint} _{post-fault} - P ^{setpoint} _{pre-fault}				ΔQ[MVar] = Q _{post-fault} - Q _{pre-fault}				P _{2COR} [MW]	Needs for extra equipments	
		HVDC-AC	HVDC-AB	WP1	WP2	HVDC-AC	HVDC-AB	WP1	WP2			
Post-1	1500	0	0	0	0	164	107	88	174	6736	✓	/
Post-2	900	-1400	0	0	0	103	-50	-37	-24	5440	×	1 (6.1.3)
Post-3	300	-1400	0	0	0	300	70	59	126	5436	×	/
Post-4	0	-1400	0	0	0	392	128	99	202	5430	×	/
Post-5	-900	-1400	0	0	0	953	108	272	198	5400	✓	/
Post-6	900	0	-1000	0	0	10	77	-17	36	5866	×	2 (6.1.4)
Post-7	300	0	-1000	0	0	130	130	163	216	5796	×	/
Post-8	100	0	-1000	0	0	190	120	229	219	5740	×	/
Post-9	900	-1400	0	0	0	138	5	0	0	5454	✓	3 (6.1.6)
Post-10	1400	0	-1000	0	0	-242	-107	0	0	5860	✓	/
Post-11	0	-1400	-1000	0	0	433	0	0	0	4460	×	/
Post-12	300	-1400	0	0	0	445	74	0	204	5420	×	4 (6.1.7)
Post-13	800	0	-1000	0	0	109	82	0	120	5850	✓	5& 6 (6.1.8)

Table 6.2: Wind park configurations are defined as following : **Voltage control**, **Reactive power control**, **WP1 in reactive power control**, **WP2 in voltage control**. Values in value correspond to the minimum injection for the system to be saved. The symbol Δ expresses the difference between the steady-state value after the incident minus the pre-fault value (under the pre-fault tab). The symbol \checkmark indicates that the configuration needs extra equipment as a synchronous condenser for instance. The symbol \times indicates that the configuration does not need extra equipment.

6.1.5.2 Analysis of the table of results

Wind parks in voltage control mode

As shown in the table, the system can be saved without acting on the active power injection of the HVDC links (line *Post-1*). But one has to inject 1500MVar. For instance, one can install 600MVar of shunt capacitors at TROUFFETTE and activate them as well as tripping the 900MVar of shunt inductors after 100ms. Nevertheless, this scenario has not been investigated as investing 600MVar of capacitor banks makes little sense in a part of the grid mostly composed of cables. Furthermore, this solution would work only for wind parks in voltage control mode, which is the best configuration. One has to invest in more capacitor banks to make all power go through the only circuits left if only some of the wind parks are in voltage control mode.

The two scenarios analyzed are way above the limit for ensuring a stable system. Indeed, in scenario 1, 900MVar were disconnected while HVDC-AC active power setpoint was brought to 0MW. The table shows that, for this active power reduction, the minimum injection needed at TROUFFETTE is -900MVar. It corresponds to an activation of 900MVar of shunt inductors. For scenario 2, the minimum is the deactivation of 100MVar of shunt inductors whereas 900MVar have been tripped.

Finally, the reduction in reactive power injection at TROUFFETTE is compensated by the converters. For instance, in line *Post-2*, 900MVar are injected at TROUFFETTE. In line *Post-3*, only 300MVar are injected. This difference of 600MVar is taken by the converters that produce about 563MVar more in line *Post-3* than in line *Post-2*.

Wind parks in reactive power control mode

With the wind parks in reactive power control mode, the system loses some voltage support. Therefore, it becomes more difficult to survive the incident, and the efforts that have to be realized are greater. Furthermore, the dynamic voltage support is deactivated for every wind park. Indeed, the dynamic voltage support was bringing numerical issues. If one does not want to install any extra equipment, one needs to reduce the active power production of both HVDC links. The costs associated with these corrective controls may become important. The most credible scenario is the active power setpoint reduction of HVDC-AC. For instance, 900MVar of capacitor banks have to be installed to make this solution works. For the sake of simplicity, and because this table aims at simply quantifying the needs, only the injection at TROUFFETTE was considered. In the scenarios proposed in the following, those 900MVar at TROUFFETTE are split among other buses. It may thus result in smaller injections because the injection of reactive power depends on the injection place. The amount of nominal reactive power installed also depends on the equipment used as the dynamics differ. For instance, instead of installing capacitor banks, one can set up synchronous condensers. They can provide more reactive power than their nominal value during very few moments because they can be overexcited. Capacitor banks provide less reactive power if the voltages are low. The scenario 3 shown in Table 6.1 corresponds to line *Post-9*. As explained, 900MVar nominal have to be injected at TROUFFETTE to guarantee a stable system in this configuration. In scenario 3, those 900MVar become 500MVar nominal of synchronous condensers and the disconnection of 300MVar of shunt inductors. The values shown in the table are base values. Then, fine-tuning is done on the configurations that have been checked for further analysis.

One can see that in line *Post-10*, 1400MVar are needed to ensure a stable system. The converters consume a part of this injection as the ΔQ of HVDC-AC and HVDC-AB are negative. It seems counter-intuitive as the converters partly consume the effort produced.

Then, why do we have to produce this extra effort? The system of governing equations is highly non-linear. Several solutions are feasible. Here, to reach an acceptable operating point, a significant effort has been done. It pushed the voltage levels above the voltage levels before the disturbance. Thus the ΔQ becomes negative. It has been tested that one major thing to stabilize around a viable operating point is to let the grid forming converter HVDC-AC control its voltage again (see appendix 9.6). Indeed, during the incident, the virtual impedance is activated. Therefore, the grid forming converter is no longer controlling its voltage. The grid forming converter can control its voltage again if the voltage levels become good enough thanks to the corrective controls.

Wind parks WP2 in voltage control mode and wind parks WP1 in reactive power control mode

In this wind park configuration, the wind parks WP2 provide some support, and the efforts to be done are smaller than if the wind parks control their reactive power injection. In line *Post-12*, the disconnection of the 300MVar of shunt inductors cumulated with the reduction in the active power setpoint of HVDC-AC is enough to make the system survives to the incident. The line *Post-13* illustrates what is needed to guarantee a stable system if the active power production of HVDC-AB is brought to 0MW. Both configurations are studied in the following.

6.1.6 Scenario 3

6.1.6.1 Description of the post-fault corrective controls

In Table 6.2, this scenario is associated with line *Post-9*. One needs 900MVar with the active power setpoint reduction of HVDC-AC to save the system. As the 900MVar are not available, equipment has to be installed. Two synchronous condensers are included in the system, one at TROUFFETTE, the other one at CHOUFFE. Furthermore, the 300MVar of shunt inductors at CHOUFFE are tripped.

The synchronous condensers bring inertia to the system compared to other compensation devices. But, the effect of the additional inertia was not studied in this thesis.

The synchronous condenser at TROUFFETTE has a rated size of 300MVar. Like the synchronous machines, it is equipped with an OEL that sets the over-excitation of the machine. The synchronous condenser is installed on an 18kV bus connected to TROUFFETTE through a 300MVA transformer.

The synchronous condenser at CHOUFFE has a rated size of 200MVar. It is also installed on an 18kV bus connected to CHOUFFE through a 200MVA transformer.

Both synchronous condensers have a lower limit for the field voltage fixed at $0.2pu$ and an upper limit of $5pu$. Their inertia is equal to $H = 7s$ as they are supposed to be equipped with a fly-wheel.

6.1.6.2 Results

Voltages at various 380kV buses

The voltages are shown in Figure 6.13. The voltage drop is greater compared to scenarios 1 and 2. Furthermore, the voltages take more time to stabilize, and almost all end values are below the lower limit.

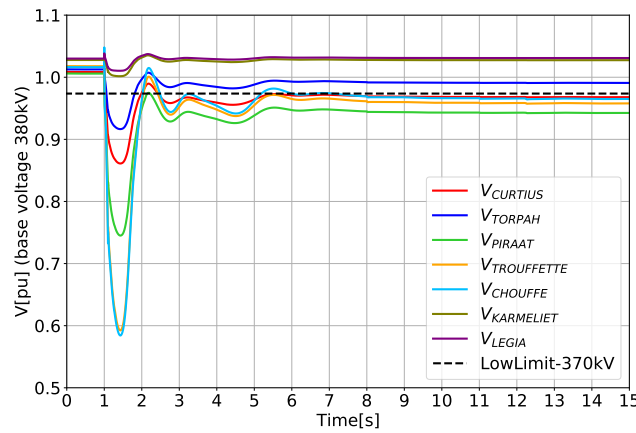


Figure 6.13: *Scenario 3*: Voltages at various 380kV buses.

Voltages of wind parks

In Figure 6.14 one can observe the voltages of the wind parks. The wind parks should not disconnect, as they remain within the limit of the FRT. One can notice a second smaller voltage drop starting at $t=2s$ and ending at $t=6s$. This second voltage drop did not appear in the other scenarios. It occurs because the wind parks are not in voltage control mode. Therefore, they do not take part when the voltage drops. If this second voltage drop is too large, the voltages can fall outside the FRT, and the wind parks may disconnect.

To prevent this voltage drop, one can limit the maximum ramping rate of the HVDC-AB direct current. The maximum ramping rate shown in the model scheme of the grid following converter (see Figure 4.6) is applied when the dynamic voltage support is deactivated. The direct current is reduced, as the dynamic voltage support prioritizes the quadrature current. When the voltages increase, the converter switches to its pre-fault control, and the direct current recovers its initial value at a specific rate. In our case, with a smaller ramping rate, the increase of HVDC-AB active power is slower, and the other injectors have the time to adapt their reactive power production.

The other way to prevent this voltage drop is to increase the gain of the synchronous condensers' AVR. With an increased gain, for the same voltage drop, the reactive power produced instantaneously by the synchronous condenser is larger. The effect of the synchronous condenser gain and the ramping rate of HVDC-AB direct current are introduced in appendix 9.7.

Power injections of HVDC links and reactive power production of synchronous condensers

On the left of Figure 6.15, one can see the power injections of the HVDC links. The dynamics during the first instants are similar to scenario 1 (see Figure 6.6). The reactive power production of HVDC-AC at the end of the simulation is about 900MVar. It wouldn't be possible without its active power setpoint reduction. On the right, one can see the reactive power produced by the synchronous condensers. Their power production stabilizes below their limit.

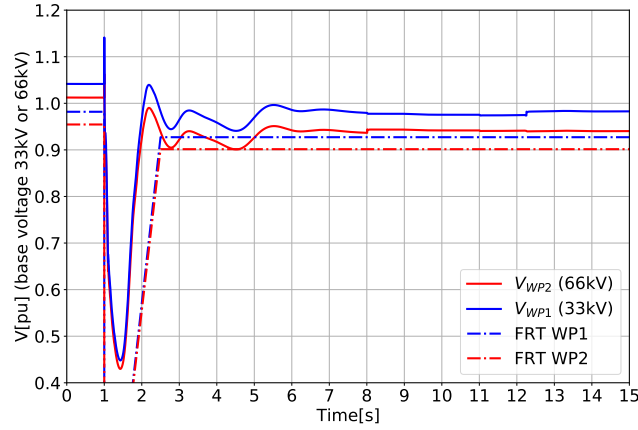


Figure 6.14: *Scenario 3*: Voltages at the PCC of one wind park of WP1 and of one wind park of WP2.

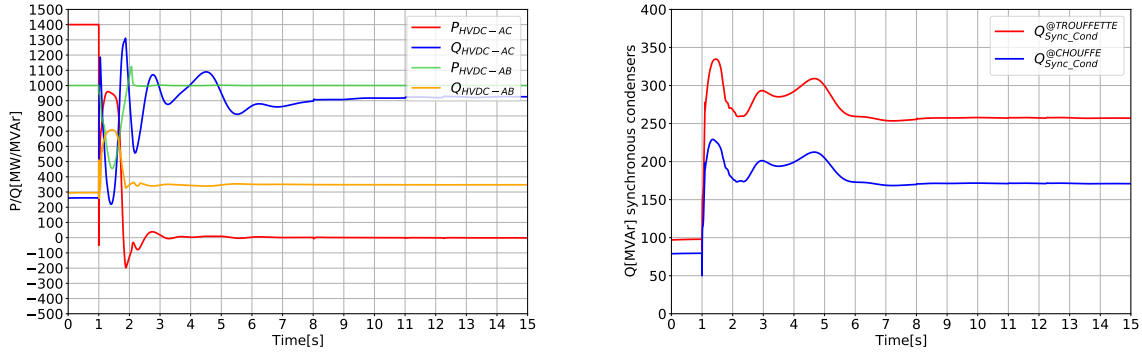


Figure 6.15: *Scenario 3*: Power injections of HVDC links (left) and reactive power of synchronous condensers (right).

6.1.7 Scenario 4

6.1.7.1 Description of the post-fault corrective controls

For this scenario, the wind parks WP1 are in reactive power control mode, whereas the wind parks WP2 are in voltage control mode. The active power setpoint of HVDC-AC is brought to 0MW within 700ms. As seen in Table 6.2, for this scenario, there is no need for extra equipment. Indeed, the shunt inductors' disconnection at TROUFFETTE is enough to guarantee a stable system. The timeline is the same as the one shown in Figure 6.3.

6.1.7.2 Results

Voltages at various 380kV buses

The voltage drop seen in Figure 6.16 is similar to the one seen in scenario 1 (see Figure 6.4). In this case, the voltage nadir of CHOUFFE is lower than the voltage nadir of TROUFFETTE. It stems from the fact that the wind parks WP2, close to TROUFFETTE, are in voltage control mode. On the other hand, the wind parks WP1, close to CHOUFFE, are in reactive power control mode.

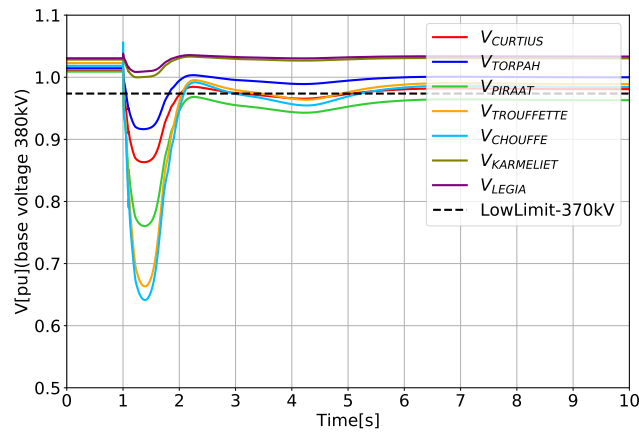


Figure 6.16: *Scenario 4*: Voltages at various 380kV buses.

Voltages of wind parks

In Figure 6.17, one can observe that the voltage drop is smaller if the wind parks are in voltage control mode. The voltages of wind parks WP2 reach back their pre-fault values, whereas it is not the case for the voltages of wind parks WP1.

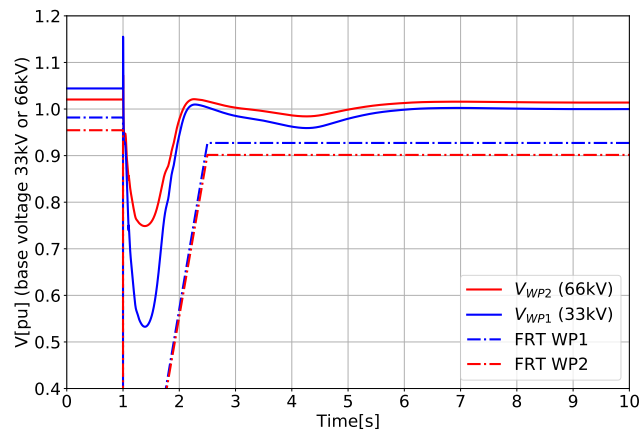


Figure 6.17: *Scenario 4*: Voltages at the PCC of one wind park of WP1 and of one wind park of WP2.

6.1.8 Scenario 5 & Scenario 6

6.1.8.1 Description of the post-fault corrective controls

The scenario 5 corresponds to line *Post-13* in Table 6.2. One has to inject 800MVar to ensure a stable system. Therefore, extra equipment has to be installed. One has installed a synchronous condenser of 200MVar at CHOUFFE. The 300MVar of shunt inductors at CHOUFFE are tripped, as well as the 300MVar at TROUFFETTE. The fact that the shunt inductors at CHOUFFE are part of the solution can bring an issue. What happens if the shunt inductors were tripped before the wind event?

To tackle this issue, scenario 6 proposes an alternative approach. As it has been explained,

reducing the active power setpoint of HVDC-AC is more helpful than reducing the active power setpoint of HVDC-AB. Because of the amount of active power reduced, but also because of the extended reactive power capability. HVDC-AC can increase its reactive power production if the active power is brought to 0MW, while HVDC-AB cannot. In scenario 6, an *emergency configuration* for HVDC-AB has been defined. This *emergency configuration* is theoretical as it is not implemented in the current version of the grid following converter. The limit of $-0.3pu$ fixed on the quadrature current is canceled and allows the converter to inject as much reactive power as it can when its active power is reduced. In this scenario, the tripping of the shunt inductors at CHOUFFE is not needed. Both scenarios are compared, and the results of scenario 6 are analyzed to check if any instabilities can occur when the *emergency configuration* is activated.

6.1.8.2 Results

Voltages at various 380kV buses

Figure 6.18 compares the voltages for scenarios 5 and 6. The voltage levels for scenario 6 are lower than those of scenario 5. Nevertheless, for both scenarios, the voltage levels remain acceptable. The voltage nadir is similar for both scenarios. But, it can be noticed that the voltages for scenario 6 fluctuate more than those of scenario 5. Even though the fluctuations are damped, this does not mean that the system is stable. Indeed, the solver is using the phasor approximation method. As explained, some dynamics are not modeled under the phasor approximation. In phasor approximation, the *emergency configuration* does not introduce instabilities and gives excellent results, but it should be checked with more detailed solvers.

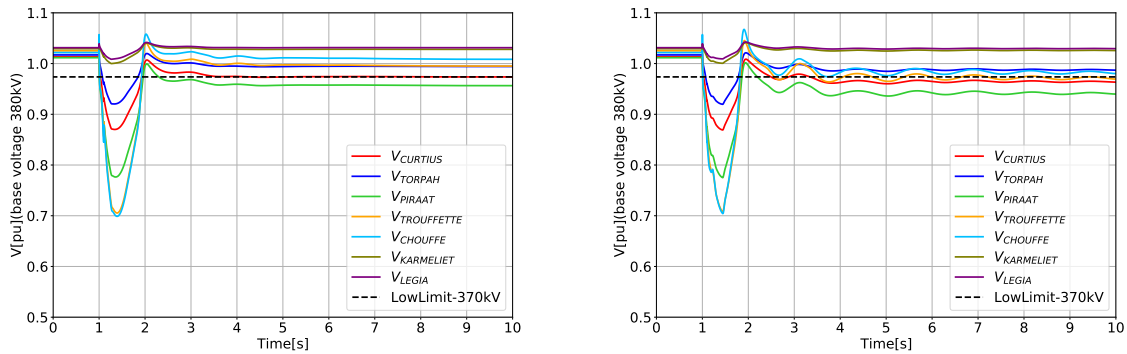


Figure 6.18: *Scenario 5&6*: Voltages at various 380kV buses. The scenario 5 is on the left, the scenario 6 is on the right.

Voltages of wind parks

In Figure 6.19, it can be seen that the voltages stay within the FRT for both scenarios. The voltages of scenario 6 show oscillations that are not present in scenario 5. Furthermore, whereas the voltages of WP2 return to their pre-fault value in scenario 5, this is not the case in scenario 6.

Power injections of HVDC links

In Figure 6.20, the injections of both HVDC links are shown. The main difference lies in the reactive power production of HVDC-AB. In scenario 5, the HVDC-AB is saturated,

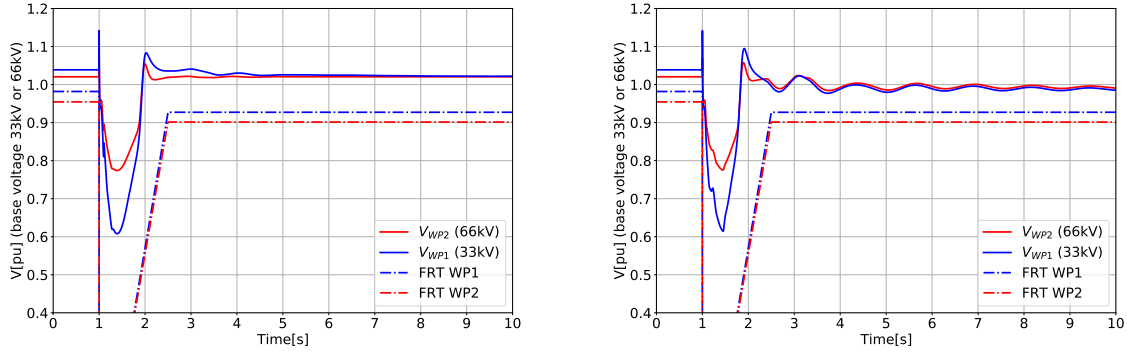


Figure 6.19: *Scenario 5&6*: Voltages at the PCC of one wind park of WP1 and of one wind park of WP2. The scenario 5 is on the left, the scenario 6 is on the right.

and it cannot produce more reactive power. In scenario 6, the full reactive power capability of HVDC-AB is released. It gives a larger reactive power production.

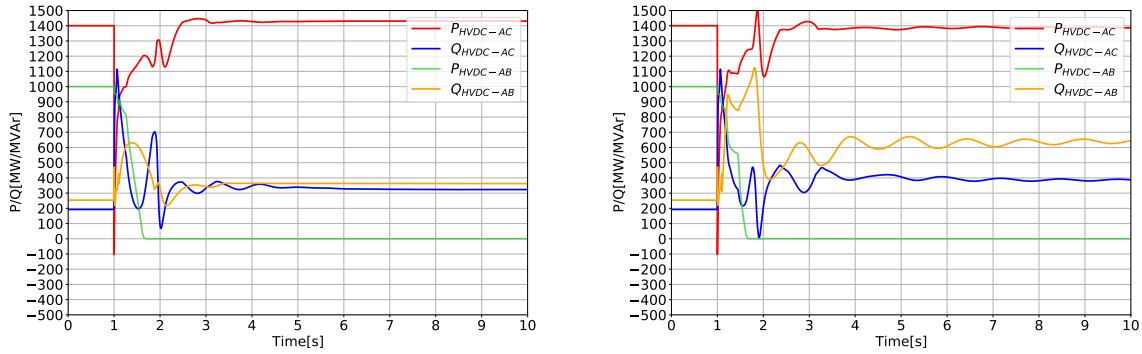


Figure 6.20: *Scenario 5&6*: Power injections of HVDC links. The scenario 5 is on the left, the scenario 6 is on the right.

Conclusion about the *emergency configuration*

Even though the results show good voltage levels, the oscillations show that the system is more prone to instabilities. Further tests with EMTP software should be realized to validate this *emergency configuration*.

Because of the uncertainties of possible instability issues, scenario 6 shouldn't be considered as an acceptable solution. Extra equipment should be added if one does not want to count on the shunt inductors' availability at CHOUFFE for designing post-fault corrective controls. One can add another synchronous condenser at TROUFFETTE to ensure a safe system.

6.2 Incident in the network post *Ramping event*: Three-phase short-circuit at TORPAH cleared by the tripping of the green circuits

6.2.1 Description of the incident

In this section, the three-phase short-circuit is supposed to be the initiating event for the tripping of the green circuits. One can wonder if the system could survive to the succession of the short-circuit and the loss of circuits. The tests realized show if the system stabilizes around an unacceptable operating point if a short-circuit arises before the tripping of the circuits. The tests also aim at verifying if the wind parks can withstand the short-circuit followed by the loss of the green circuits.

The short-circuit occurs at TORPAH at $t=0.9s$ and lasts 100ms. A 5Ω resistor is added because numerical difficulties have been met. The short-circuit is a three-phase short-circuit and is cleared by the tripping of the green circuits at $t=1s$. For this incident, only scenarios 1,2, and 5 are analyzed. It shows the impact of the short-circuit for scenarios with various wind park configurations and an active power reduction applied on different HVDC links. The configuration: *wind parks WP1 and WP2 in reactive power control mode* has not been studied here because convergence issues were encountered. A greater resistance should have been considered to get rid of the numerical difficulties, and the impact of the short-circuit is not correctly illustrated with a larger resistance.

6.2.2 Scenario 1

Voltages of wind parks

Figure 6.21 compares the wind park voltages with and without the short-circuit. The voltage nadir is lower if a short-circuit occurs. But the voltage nadir does not appear at the same time. One can see that the loss of the circuits after the short-circuit does not affect significantly the voltages. The figure on the left shows that the voltage nadir is higher, but the voltage drop lasts longer.

For both cases, the voltage of WP2 suffers from a smaller voltage drop than the voltage of WP1. It is due to the dynamic voltage support of wind parks WP2.

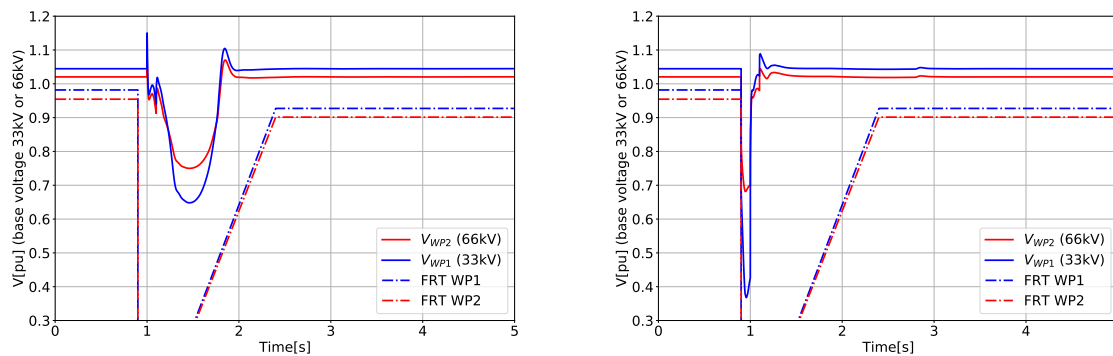


Figure 6.21: *Scenario 1 without (left figure) and with (right figure) a short-circuit*: Voltages at the PCC of one wind park of WP1 and of one wind park of WP2.

Power injections of HVDC links

Figure 6.22 shows the dynamics of the converters during the incident. The active power of HVDC-AB is suddenly reduced as the short-circuit occurs. Indeed, the dynamic voltage support of HVDC-AB is activated, and the quadrature current is prioritized when the voltage drops. There is no more room for active power, which is reduced to 0MW. After the short-circuit clearance, the active power of HVDC-AB slowly reaches its pre-fault value. A maximum ramping rate is fixed on the active power recovery. Therefore, when the green circuits are tripped, the active power flow is already curtailed because of the short-circuit.

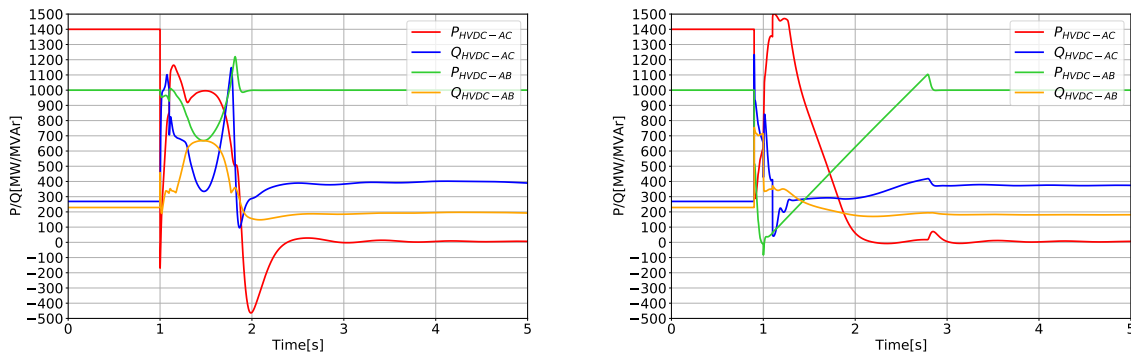


Figure 6.22: *Scenario 1 without (left figure) and with (right figure) a short-circuit: Power injections of HVDC links.*

6.2.3 Comparison between scenarios 1 and 2

The comparison aims at assessing the impact on the results of active power reductions applied on different HVDC links. In scenario 1, the active power reduction is applied on HVDC-AC. Whereas in scenario 2, it is applied on HVDC-AB.

Voltages of wind parks

Figure 6.23 compares the wind park voltages for the two scenarios. The differences are barely visible between the two figures. The voltage levels during the short-circuit are the same because the wind park configurations are identical for both scenarios. The evolution of the voltages are also similar after the short-circuit clearance.

Power injections of HVDC links

Figure 6.24 compares the dynamics of the converters for the two scenarios. In scenario 2, the active power reduction is applied on HVDC-AB. One can see that the active power of HVDC-AB is brought to 0MW during the short-circuit. It increases after the short-circuit clearance. Then, the post-fault corrective controls act on the active power setpoint of HVDC-AB. As in scenario 1, the active power flow has already been reduced when the green circuits are tripped. In scenario 1, the effect of the progressive recovery of the active power of HVDC-AB, added with the progressive reduction of the active power of HVDC-AC, was limiting the active power flow. In scenario 2, only the active power production of HVDC-AB is affected. Nevertheless, it does not have an impact on the voltages.

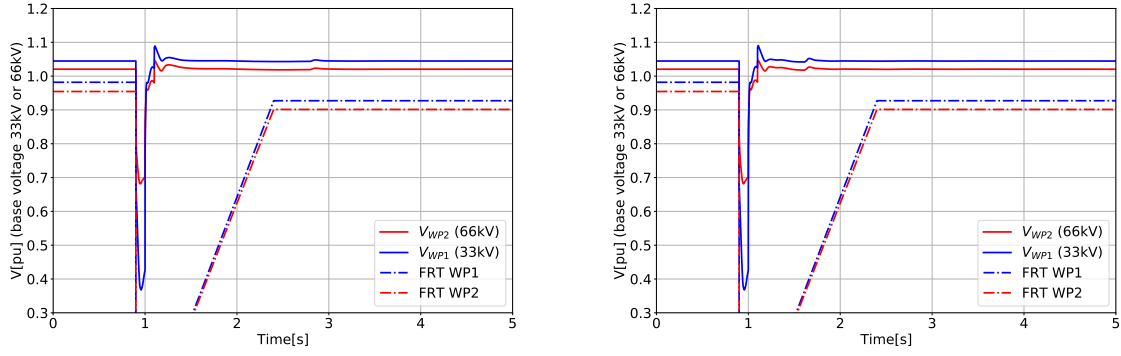


Figure 6.23: *Scenario 1 (left figure) and scenario 2 (right figure) with a short-circuit: Voltages at the PCC of one wind park of WP1 and of one wind park of WP2.*

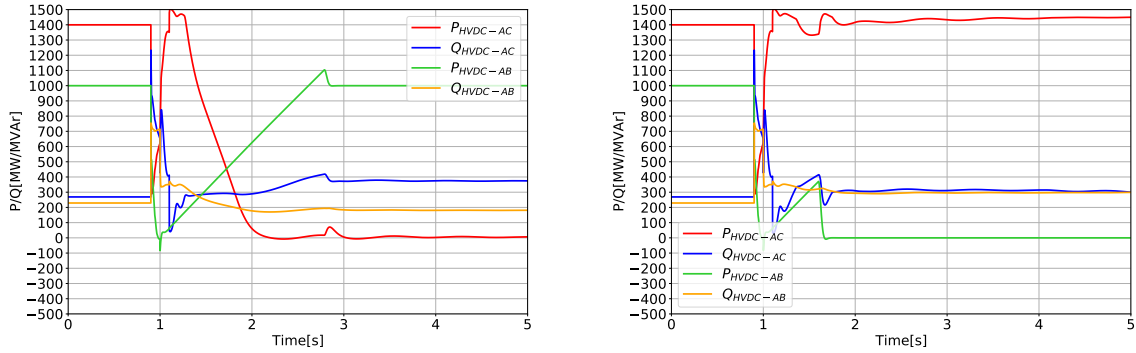


Figure 6.24: *Scenario 1 (left figure) and scenario 2 (right figure) with a short-circuit: Power injections of HVDC links.*

6.2.4 Scenario 5

Voltages of wind parks

As seen in Figure 6.25, the voltage nadir is lower with a short-circuit. The voltage of wind parks WP1 reaches $0.3pu$ because the wind parks are in reactive power control mode, and their dynamic support is not activated. Compared to scenario 1, the loss of the circuits impacts the voltages even though a short-circuit occurred before. It can be explained by the wind park configuration. The wind parks WP1 are in reactive power control mode and do not participate in voltage support. The wind park configuration of WP1 also impacts the voltages of wind parks WP2.

Power injections of HVDC links

Figure 6.26 compares the power injections for scenario 5 with and without the short-circuit. It is similar to the results of scenario 2.

6.2.5 Conclusion

The results showed that the voltages are less impacted by the tripping of the circuits if a short-circuit initiates it. The short-circuit affects the active power production of the grid following converter, reducing the active power flow through the green and orange circuits.

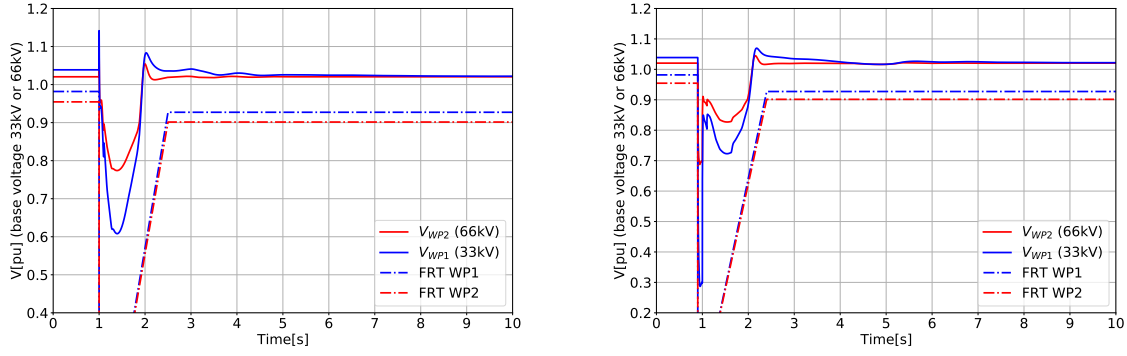


Figure 6.25: *Scenario 5 without (left figure) and with (right figure) a short-circuit: Voltages at the PCC of one wind park of WP1 and of one wind park of WP2.*

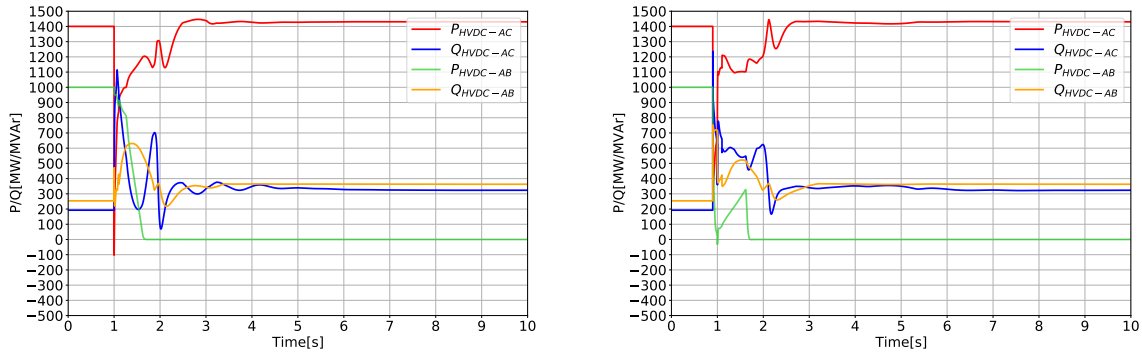


Figure 6.26: *Scenario 5 without (left figure) and with (right figure) a short-circuit: Power injections of HVDC links.*

The excessive amount of power flowing through the orange circuits after the loss of the green circuits was found to be problematic as it drives the voltages down. The scenarios presented in this thesis always include the active power reduction of an HVDC link to ensure a safe system. The effect of the short-circuit is therefore beneficial as it naturally decreases the active power production of HVDC-AB. When the green circuits are tripped, the amount of power flowing through the system is already decreased.

The main issue then becomes the short-circuit. For very low voltages, the converters' PLL are frozen and do not synchronize with the grid. Instabilities may appear. Further studies with EMTP software should be done to ensure the stability of the system when a short-circuit occurs.

6.3 Incident in the network during *Storm event*: Loss of HVDC-AB before the automaton connects a shunt inductor

6.3.1 Description of the incident

The voltage levels are very high at the end of the *Storm event* as the system is lightly loaded. To make it worse, one can study the impact of the loss of an injector. As it is

shown in Figure 5.30, the voltage of CHOUFFE is the highest. One has chosen to break HVDC-AB, as it is the closest to the bus CHOUFFE, which already presents the highest voltage. With the loss of HVDC-AB, the system sees the active power flows further reduced. It also loses the reactive power consumed by the converter.

The more critical timing for the loss of HVDC-AB is before the connection of a shunt inductor. It is between the moment the voltage is above the limit of the automaton and the moment the shunt inductor is connected. Indeed, the automaton takes 25s to engage the shunt inductor after the voltage of TROUFFETTE has crossed 415kV. The voltage rise could trigger some overvoltage protections. For instance, the wind parks could be disconnected, and an extensive amount of active power can be quickly lost.

For this incident, the wind parks are in voltage control mode. The incident occurs after the disconnection of wind parks WP1, and when the storm is passing through the wind parks WP2.

6.3.2 Results

Voltages at various 380kV buses

Figure 6.27 shows the voltages at various 380kV buses during the *Storm event*. The loss of HVDC-AB occurs around $t=25\text{min}$. The active power flows are further reduced by the loss of 1000MW, and the voltage support brought by the converter is also lost. The voltages suddenly rise. The voltage of CHOUFFE is the more impacted as HVDC-AB is connected next to it. The voltage of CHOUFFE overrides the limit of 420kV during 25s. The overvoltage is small enough and lasts for a sufficiently short time to be considered as acceptable.

The voltages are then brought back to acceptable values as a 200MVar shunt inductor is connected. The end values for the voltages are considered as acceptable.

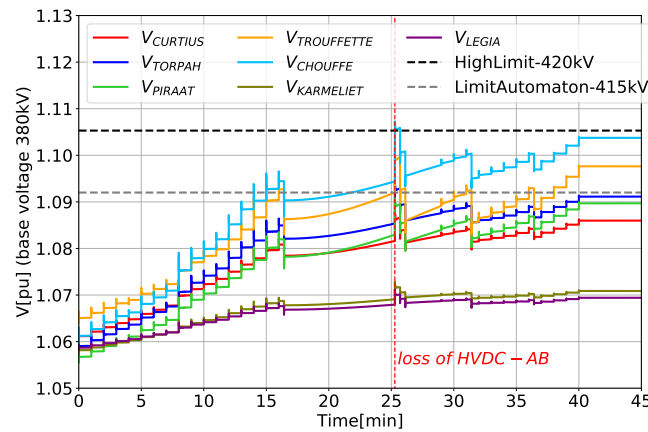


Figure 6.27: *Storm event-Loss of HVDC-AB: Voltages at various 380kV buses.*

In Figure 6.28, one can see a zoom of Figure 6.27. It shows that the voltage rise is more significant at CHOUFFE and that the overvoltage is small enough to guarantee a safe operation of the network.

Voltages of wind parks

In Figure 6.29, one can see the voltage of wind parks WP2. The wind parks WP1 have

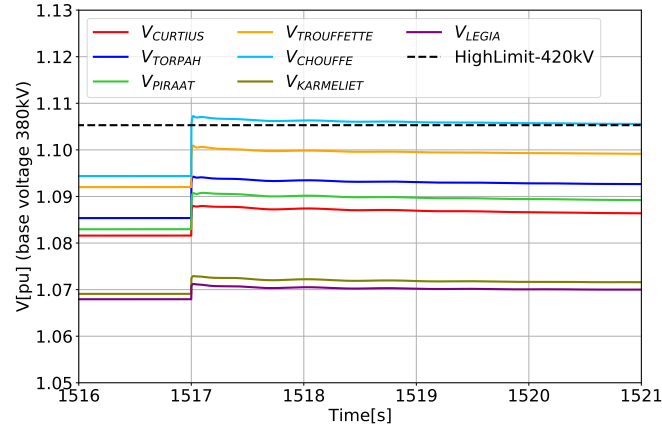


Figure 6.28: *Storm event-Loss of HVDC-AB*: Voltages at various 380kV buses. Zoom on the time frame when the incident occurs.

been disconnected, thus the voltage is equal to 0. The overvoltage of wind parks WP2 can be withstood by the wind turbines. Indeed, the wind parks must be able to withstand overvoltages as specified by the TSO. The voltage levels required by the TSO ([7]) are greater than the peak voltage seen in the figure. Because the wind parks WP2 are in voltage control mode, the voltage quickly returns to its pre-fault value.

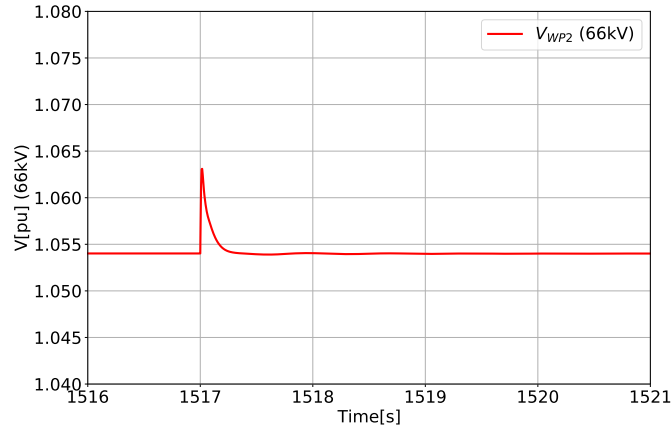


Figure 6.29: *Storm event-Loss of HVDC-AB*: Voltages at the PCC of one wind park of WP2. Zoom on the time frame when the incident occurs.

6.4 Conclusion

In this second part, the impact of an incident on the network post wind event has been analysed.

About the incidents. The incidents described in this section are the most severe incidents that could occur in this network. They are also very unlikely to realize. Nevertheless, even though those are rare incidents, the consequences could be costly if no solution has been planned.

For the incident post *Ramping event*, the voltage collapse observed if there is no solution applied, can propagate through other control areas, and many injectors can be tripped because of under-voltages. Preventive actions could be taken to avoid this scenario. One can see in the appendix (9.8) the power reductions that are to be applied to secure the system before the incident takes place. The conclusion is that the preventive actions are not worthy as the cost associated with those actions would probably be too large. One should do a cost-benefit analysis to verify this affirmation. Solutions that affect the network post-incident are assumed to be better.

For the incident during the *Storm event*, it has been shown that the network is safe. The use of an automaton shows good results for the *Storm event*. No further actions should be taken to ensure a safe system.

About the solutions found. Table 6.1 summarizes the solutions. They comprise actions taken on the reactive and active power injections. One has to limit the active power flow as it cannot go through the remaining lines. Indeed, the system is highly loaded, and the impedance of the network is suddenly increased because lines are lost. One also has to inject more reactive power to increase the voltage levels. The timing for those actions has been defined to ensure that the wind parks remain connected to the network. One can see that the amount of actions depends on the wind park configuration. If they are in reactive power control mode, extra efforts are needed to guarantee an acceptable operating point after the incident. It is unrealistic to oblige every wind park to be operated in voltage control mode. But, it has been shown that a mix, with some wind parks in voltage control mode and others in reactive power control mode, can be viable with a smaller volume of actions.

In some scenarios, a synchronous condenser does not need to be added. Nevertheless, the addition of an extra source of reactive power is useful to allow a security margin. For instance, scenario 4 only needs the tripping of the shunt inductors at TROUFFETTE and the active power reduction of HVDC-AC. But, as shown in Table 6.2, this solution is right at the limit. If the shunt inductors were disconnected before the wind event, the network would collapse.

The source of reactive power can also be a STATCOM, for instance. The type of compensation device has not been analyzed. On the other hand, if a synchronous condenser is installed, it could be installed in various places. The placement of the synchronous condenser has not been optimized.

In terms of active power reduction, it has been observed that it is helpful to limit the active power production of HVDC-AC instead of HVDC-AB. First, it allows a greater active power reduction as HVDC-AC is injecting 1400MW whereas HVDC-AB injects 1000MW. Second, while the active power injection is limited, there is more room for HVDC-AC to inject reactive power without reaching its limit. It is not the case for HVDC-AB as the

reactive power is limited or prioritized if the dynamic voltage support is activated. The solutions presented show that fewer efforts are needed to guarantee a secure system if the active power reduction is realized on HVDC-AC.

What next ? As explained, that HVDC-AC is in grid forming mode offers some advantages for the system. But, as an HVDC link is supposed to connect control areas, and as a grid forming converter cannot be implemented in both ends of the HVDC link, there is a possibility of having a grid following converter instead of a grid forming converter for HVDC-AC. The next of this thesis addresses the issues of having only grid following converters.

Chapter 7

HVDC-AC in grid following mode

7.1 The different scenarios analyzed

The chapter aims at evaluating the stability of some scenarios if HVDC-AC is in grid following mode. Four scenarios are investigated. Some of them are taken from Table 6.1. Others are different as the post-fault corrective controls change when HVDC-AC is in grid following mode. Therefore, additional scenarios have been implemented for this chapter. The scenarios are summarized in Table 7.1.

Scenarios α and β correspond to scenarios 1 and 2 previously studied. Scenarios α and β have large enough post-fault corrective controls to guarantee a great security margin, as it was observed in Table 6.2. Scenario δ does not have this security margin, but the addition of a synchronous condenser brings inertia to the system. Scenario γ does not have the additional inertia or a security margin. The impact of changing the grid forming converter to a grid following converter is thus the greatest. Scenario γ shows interesting results, but the addition of 700MVar of shunt capacitors is not realistic.

In the following sections, one can observe the results. As they have been already explained, the post fault corrective controls are not further detailed. The tripping of the shunt inductors, or the connection of the shunt capacitors, happens 100ms after the fault occurs, like the active power reduction of the HVDC links. The power reduction can last between 500ms or 700ms depending on the HVDC link on which it is applied.

	Scenario				
	α	β	γ	γ'	δ
Pre-fault configuration					
Control of WP1	V	V	V	V	Q
Control of WP2	V	V	V	V	V
Synchronous Condenser (nominal MVar @CHOUFFE)	0	0	0	300	300
Shunt inductors (nominal MVar @TROUFFETTE)	900	900	900	900	300
Shunt capacitors installed (nominal MVar @TROUFFETTE)	0	0	700	500	0
Shunt inductors (nominal MVar @CHOUFFE)	300	300	300	300	300
Post-fault corrective controls					
Reactor tripping @TROUFFETTE	yes	yes	yes	yes	yes
Reactor tripping @CHOUFFE	no	no	yes	yes	yes
Capacitors connection @TROUFFETTE	no	no	yes	yes	no
$P_{HVDC-AC}^{setpoint}$ decreased to 0 MW	yes	no	no	no	yes
$P_{HVDC-AB}^{setpoint}$ decreased to 0 MW	no	yes	no	no	no

Table 7.1: Configuration of the different scenarios analysed. Q means reactive power control mode. V means voltage control mode.

7.2 Scenario α

The voltage magnitudes and phase angles are shown in Figure 7.1. Let first examine the voltage magnitudes. The voltages decrease faster when HVDC-AC is in grid following mode, but the voltage nadir is higher. The spike at $t=1.1s$ coincides with the tripping of the reactors and can be seen if HVDC-AC is in grid following mode or grid forming mode. The phase angles are shown on the right. When HVDC-AC is in grid forming mode, the angle increases at a slower rate. It is because of the grid forming model. The grid forming acts as a voltage source and keeps its angle constant for the first moment after the tripping of the circuits. The rate of change of the angle depends on the synthetic inertia of the grid forming converter (see appendix 9.6). The larger the inertia is, the slower the rate of change will be. In both configurations, the angle zenith is almost the same.

When HVDC-AC is in grid following mode, one can see some fluctuations in the voltage magnitudes and angles around $t=2s$. Nevertheless, the network stabilizes at the end of the simulation for both configurations.

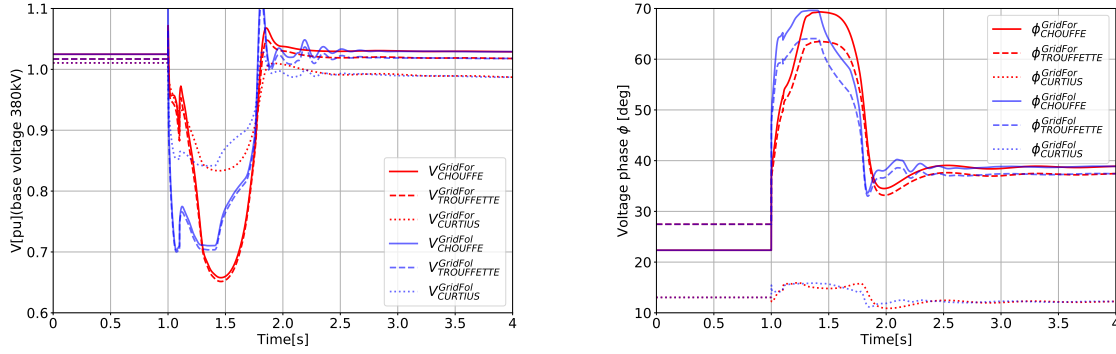


Figure 7.1: *Scenario α -Comparison between HVDC-AC in grid following mode (GridFol) and grid forming mode (GridFor): Voltage phasors at various buses. On the left, the voltage magnitudes. On the right, the phase angles.*

7.3 Scenario β

Figure 7.2 shows the results for scenario β . Similar conclusions as in scenario α can be drawn here. The voltage angles increase at a slower rate if HVDC-AC is in grid forming mode, whereas the voltage magnitudes decrease at a slower rate. One can also see some oscillations around $t=2s$ when HVDC-AC is in grid following mode. The voltage nadir is higher if HVDC-AC is in grid forming mode and the voltage angle zenith is lower. But, the voltage magnitudes and angles take more time to stabilize when HVDC-AC is in grid forming mode.

For HVDC-AC in grid following mode, the results for scenario α and scenario β are very similar. The only difference stems from the time needed for the voltage magnitudes and angles to reach acceptable values. While in scenario α , around 800ms are needed to see the voltage magnitude rises, about 600ms are necessary for scenario β . The active power reduction can explain this. The power reduction is not the same for scenario α and scenario β . In scenario α , it lasts 700ms and is applied on HVDC-AC. In scenario β , it lasts 500ms and is applied on HVDC-AB. Additional tests show that the voltage drop lasts longer if the active power reduction takes more time. It also lasts longer if the active power reduction is applied on HVDC-AC. The following test confirms the last affirmation. The HVDC-AB and HVDC-AC locations have been swapped. In this new configuration, it appears that the voltage drop lasts longer for HVDC-AB, which was connected to TROUFFETTE. Therefore, both the duration of the active power reduction and the HVDC link location are significant parameters for the evolution of the voltages when both HVDC links are in grid following mode.

7.4 Scenarios γ and γ'

As seen in Figure 7.3, the system becomes unstable for HVDC-AC in grid following mode. The sustained oscillations have a frequency of around 5Hz. This type of instability can be considered as a converter-driven instability and can be caused by the PLL which cannot synchronize with the grid. The system has nothing to hold the voltages as there are no synchronous condensers or grid forming converters. The network is weak and more

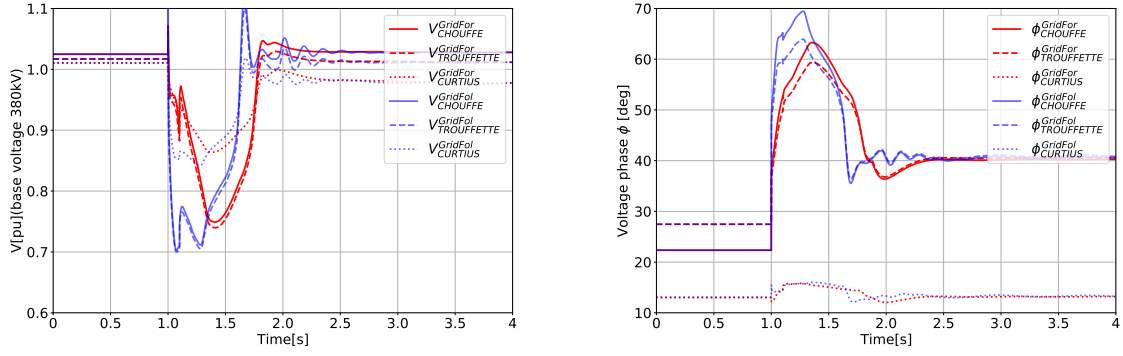


Figure 7.2: *Scenario β -Comparison between HVDC-AC in grid following mode (GridFol) and grid forming mode (GridFor): Voltage phasors at various buses. On the left, the voltage magnitudes. On the right, the phase angles.*

prone to stability issues. This scenario shows that the use of a grid forming converter can prevent those instabilities.

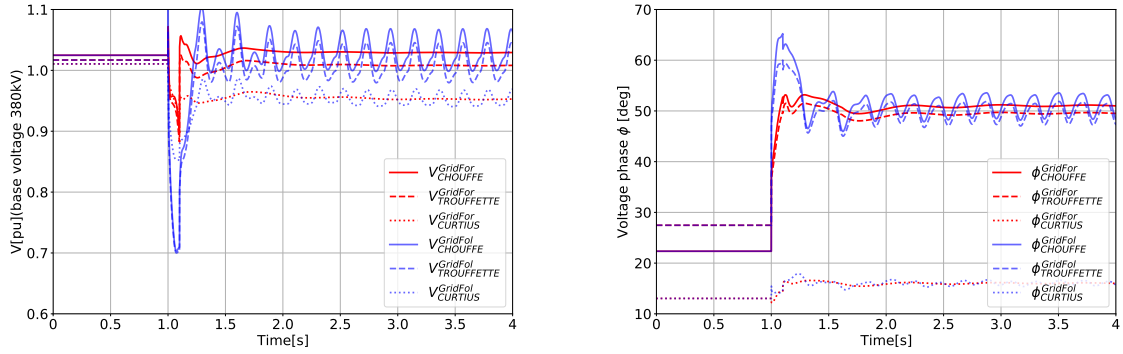


Figure 7.3: *Scenario γ -Comparison between HVDC-AC in grid following mode (GridFol) and grid forming mode (GridFor): Voltage phasors at various buses. On the left, the voltage magnitudes. On the right, the phase angles.*

The same scenario is realized with a synchronous condenser. The scenario is named γ' . A synchronous condenser of 300MVAR is installed at CHOUFFE. 500MVAR of shunt capacitors are installed and are activated to prevent the system from collapsing. The results are shown in Figure 7.4. One can see that the oscillations are damped and progressively disappear. Compared to scenario γ , the voltage magnitudes decrease at a slower pace. Furthermore, the voltage angles increase more slowly. The results with HVDC-AC in grid forming show fewer oscillations and stabilizes faster. But, the synchronous condenser solution works well if HVDC-AC has to be in grid following mode.

7.5 Scenario δ

The results are shown in Figure 7.5. In this scenario, a synchronous condenser has been added. Thus, the voltage magnitudes and phase angles vary more slowly when HVDC-AC is in grid following mode, compared to scenarios α and β . Indeed, the synchronous

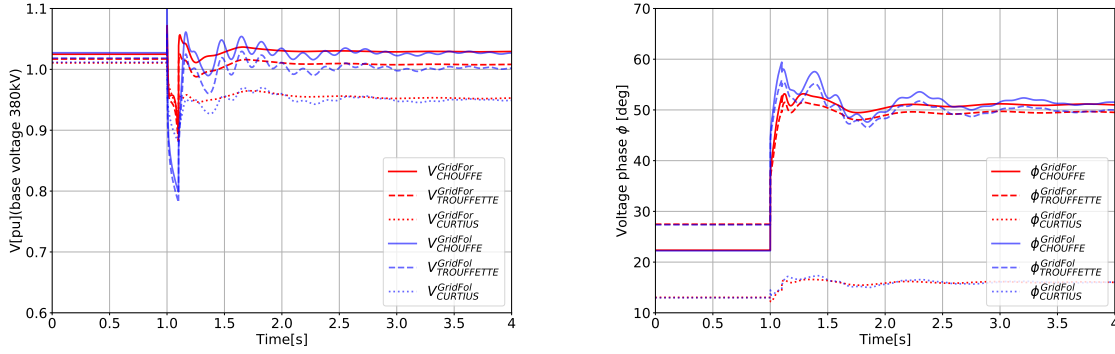


Figure 7.4: *Scenario γ' - Comparison between HVDC-AC in grid following mode (GridFol) and grid forming mode (GridFor): Voltage phasors at various buses. On the left, the voltage magnitudes. On the right, the phase angles.*

condenser prevents the voltage angles from changing steeply and injects a large amount of reactive power during the incident.

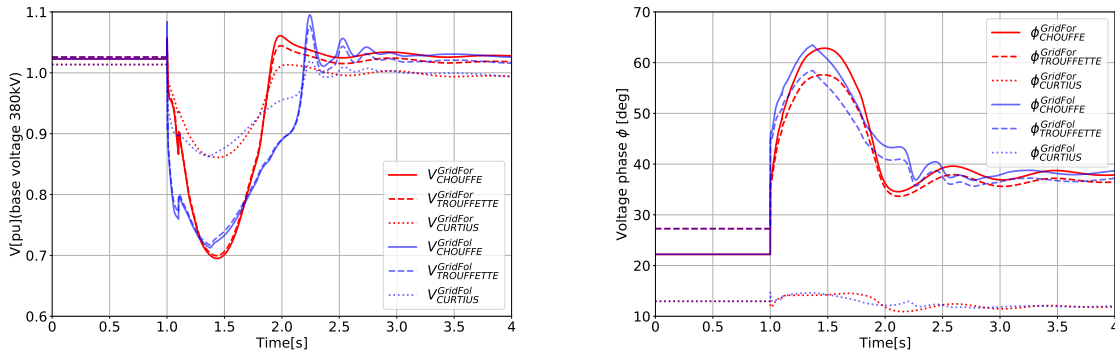


Figure 7.5: *Scenario δ - Comparison between HVDC-AC in grid following mode (GridFol) and grid forming mode (GridFor): Voltage phasors at various buses. On the left, the voltage magnitudes. On the right, the phase angles.*

7.6 Conclusion

The last chapter aims at assessing the stability of the system if HVDC-AC was in grid following mode. The results show that, in the presence of a grid forming converter, the voltage magnitudes and phase angles vary more slowly. Furthermore, the instant after the incident, the voltages are better held. Similar results can be achieved with a synchronous condenser as shown in scenario δ . The scenario γ shows that sustained oscillations can appear if only grid following converters are installed. On the other hand, the scenario γ' has shown that this issue can be troubleshot by adding a synchronous condenser. Nevertheless, fewer oscillations are seen if one uses a grid forming converter.

Chapter 8

Conclusion

The goal of this thesis was to study the stability of a system with high integration of power electronic converters. The system analyzed is composed of large offshore wind parks and HVDC links.

In the first part, the impact of wind events has been investigated. The wind events can greatly change the power flows as the wind parks are tightly grouped where the wind potential is the highest. When the wind speeds vary, the wind turbines adapt their active power setpoints to extract the maximum energy from the wind. Thus, changes in wind speed lead to large variations in power flows. It induces voltage deviations and enhances reactive power consumption or production. Thanks to power electronics, the converters can control their active and reactive power production. Therefore, they can provide voltage support.

Two wind events have been considered: the *Ramping event* and the *Storm event*. Both of them result from extreme wind conditions and last less than an hour. The *Ramping event* drives the voltages down as the system becomes more loaded because of the increase in wind speeds. The event has been analyzed with different wind park configurations. Indeed, wind parks can have different control strategies. They can be set in voltage control mode or reactive power control mode. The voltage control mode adapts the reactive power injection depending on the voltages. On the other hand, the reactive power mode sets the reactive power production of the converters, whatever the voltages. When the wind parks are in voltage control mode, the *Ramping event* did not pose a threat because the voltage support was sufficient. But, solutions have to be found for other wind park configurations. The conclusion was that the best solution is to monitor the power injections of the different converters. If a converter reaches its limits, the operator can be notified, or actions can be taken. The notified operator can, for instance, trip a shunt inductor. This solution can be coupled with the use of an automaton. The automaton can trip or connect shunt inductors based on voltage measurements. It has been shown that the automaton was sufficient for the *Storm event*. During the *Storm event*, the voltages rise because of the unloading of the system, and the automaton can connect a shunt inductor to prevent the voltage increase. There's no need for monitoring the converters for the *Storm event*.

In the first part, it has been highlighted that one should act on the system to prevent large voltage deviations. The wind events can occur rapidly, within an hour, and jeopardize the system if no action is taken. But, the solutions do not need to be based on fast corrective controls. A slow reaction time is accepted as the wind event is slow compared to the fast

dynamics of the system.

In the second part, the impact of transmission outages on the system's stability has been studied. The system, already stressed by the wind event, loses a line or an injector. Compared to wind events, one has to deal with faster dynamics. If no action is taken, the system collapses whatever the wind park configuration. To ensure the stability of the system, solutions that can be applied rapidly were found.

Three incidents have been considered. The first one is the loss of the green circuits after the *Ramping event*. The impedance of the system increases as the circuits are lost. Therefore, the power has to flow over the greater impedance path, driving the voltages down. The stability of the system is jeopardized, and the voltages collapse. Solutions based on active power reduction and reactive power injection were found to ensure a secure system. The goal was to maintain the wind parks connected. Thus, the wind turbine fault-ride through capability was used to verify if the voltage drop can be withstood. The solutions consist in active power setpoint reduction for the HVDC links and reactive power injection. To increase the reactive power injection, it has been decided to disconnect the shunt inductors or to add synchronous condensers. It has been observed that when the wind parks do not take part in voltage support, the volume of actions to be taken increases. It has been concluded that the configuration in which the wind parks are in reactive power control mode shouldn't be envisaged.

The second incident is the loss of the green circuits provoked by a three-phase short-circuit at TORPAH after the *Ramping event*. The effects of the short-circuit inhibit the voltage drop caused by the loss of the green circuits. Indeed, because of the short-circuit, the active power injections are reduced. When the green circuits are tripped, the power flows are already curtailed, and the voltage drop is limited. It has been observed that the voltage drop lasts longer when some of the wind parks are in reactive power control mode. The voltages take more time to restore when wind parks do not provide voltage support.

The last incident is the loss of HVDC-AB during the *Storm event*. HVDC-AB is injecting active power and consuming reactive power. Thus, losing HVDC-AB leads to a voltage rise. Indeed, it unloads the system, and its voltage support is lost. It has been seen that the voltage of CHOUFFE overreaches the maximum limit, but for 25 seconds, the time needed for the automaton to connect a shunt inductor. It has been concluded that the incident did not threaten the system.

The last part studied the impact of having HVDC-AC in grid following mode. The HVDC link is supposed to connect different control areas. Because one cannot have a grid forming converter at both ends of the link, HVDC-AC may be in grid following mode. In that part, the interests of a grid forming converter have been highlighted. With HVDC-AC in grid following mode, the voltage magnitudes and angles vary faster. Those variations can lead to sustained oscillations that are not wanted. Nevertheless, it has been shown that a synchronous condenser can limit the oscillations as it prevents high rate of change in phase angles.

For future works, a wind park controller could be modeled. In this thesis, three wind park configurations have been analyzed to get an overall picture. Nevertheless, a model of a wind park controller would lead to more accurate results. For the *Ramping event* scenario, one could also model the control logic that monitors the converters. The control

logic should be able to take specific actions according to the converters' data.

For the transmission outages, it has been highlighted that the phasor approximation method does not model all the dynamics. Indeed, to verify the solutions proposed, the use of EMTP software is needed. For the last part, when HVDC-AC is in grid following mode, the phasor approximation gives only clues about the system dynamics. The EMTP software could represent the interactions between the different converters and evaluate the importance of a grid forming converter.

Chapter 9

Appendix

9.1 Acronyms

AVR	Automatic Voltage Regulator
EMTP	Electromagnetic Transients Program
FRT	Fault-Ride Through
HVDC	High Voltage Direct Current
HWRT	High Wind Ride Through
LVRT	Low Voltage Ride Trough
LTC	Load Tap Changer
MPPT	Maximum Power Point Tracker
OEL	Over-Excitation Limiter
PCC	Point of Common Coupling
PLL	Phase-Locked Loop
PSS	Power System Stabilizer
RoCoF	Rate of Change of Frequency
SCR	Short-Circuit Ratio
TSO	Transmission System Operator
VSC	Voltage Source Converter

9.2 Power flows: *Ramping event*

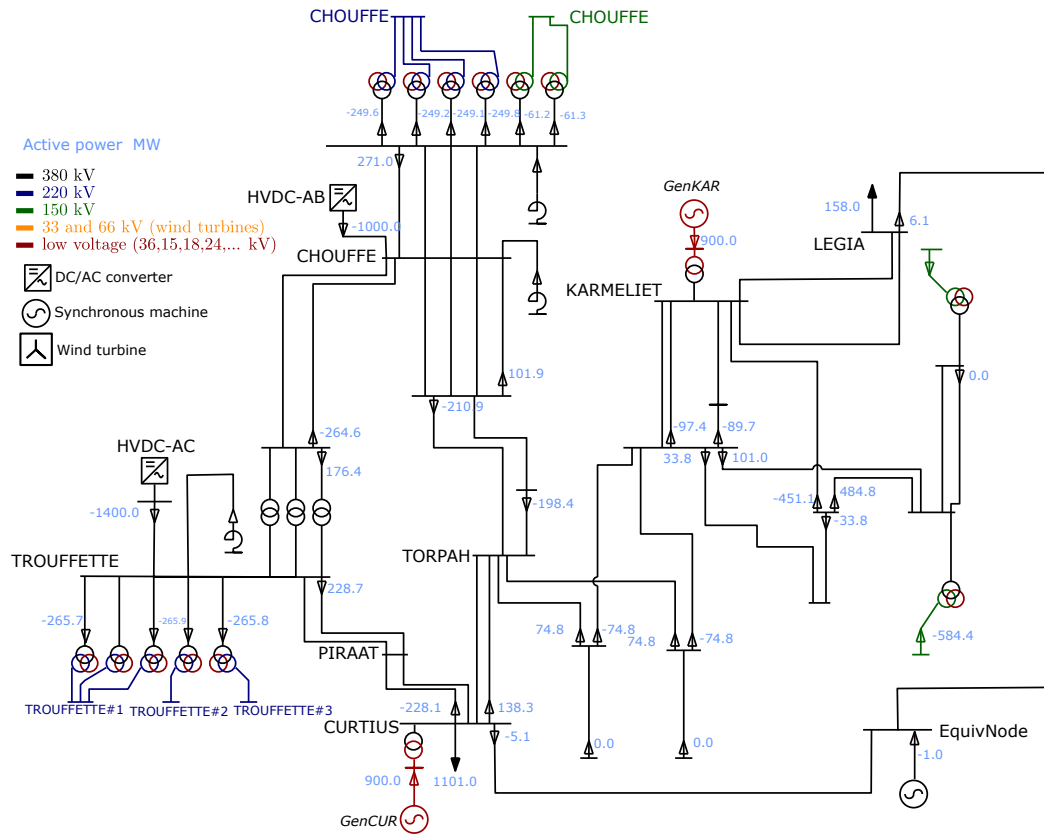


Figure 9.1: Detailed view of the 380kV network.

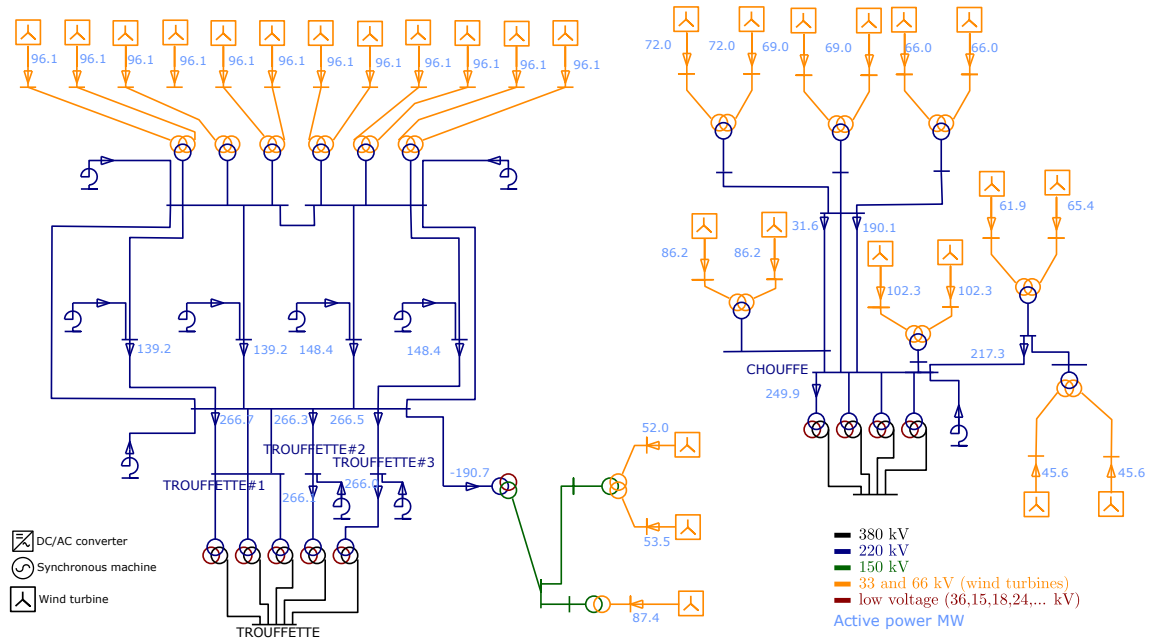


Figure 9.2: Detailed view of the 220kV network.

9.3 Power flows: *Storm event*

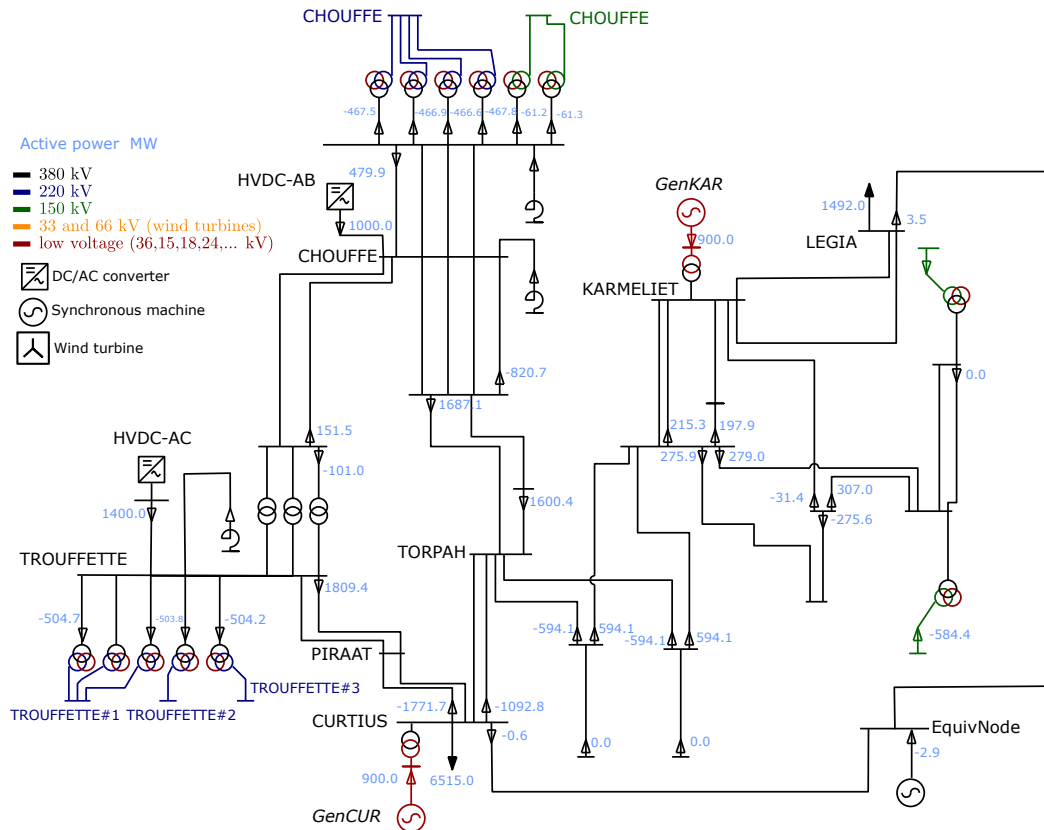


Figure 9.3: Detailed view of the 380kV network.

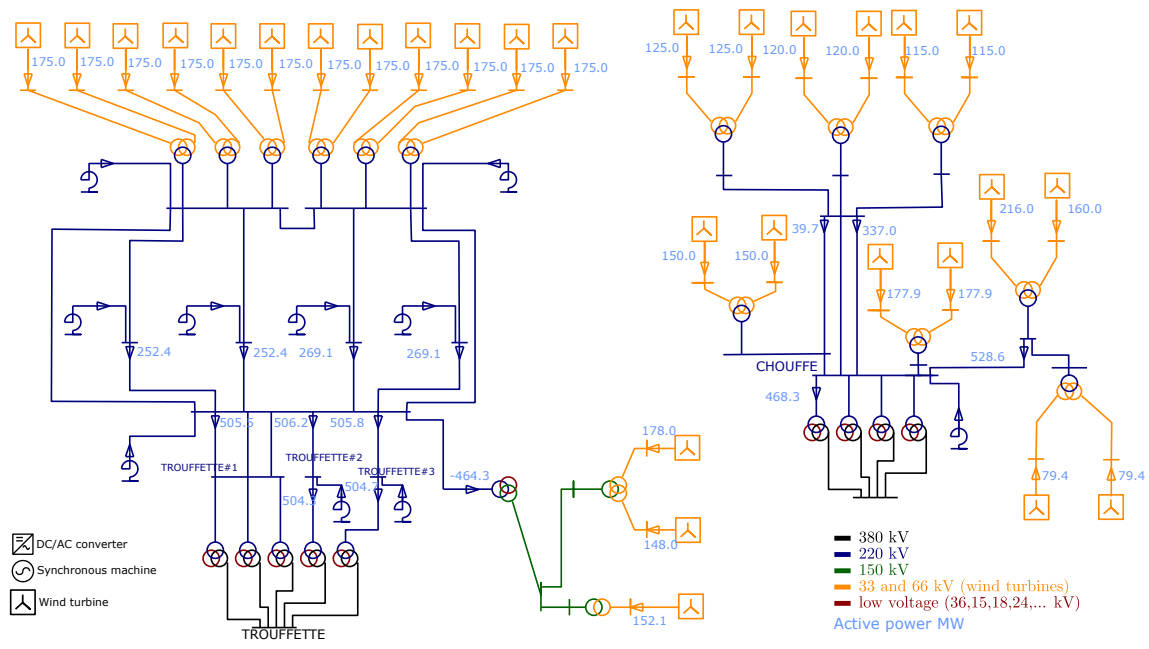


Figure 9.4: Detailed view of the 220kV network.

9.4 Configuration *Q+Automaton version 2*: HVDC-AC power shift variant

In this variant, the HVDC-AC active power setpoint is changed from -1400MW to 1000MW under 8 minutes and a half. The power shift starts at H-4min15s and ends at H+4min15s. The results shown in this section prove that a control logic only based on the current magnitude of HVDC-AC may be weak. Indeed, Figure 9.5 shows that the voltages collapse below the lower limit. One can observe in Figure 9.6 that the current magnitude of HVDC-AC has never reached 0.95pu and the quadrature current of HVDC-AB attains -0.3pu.

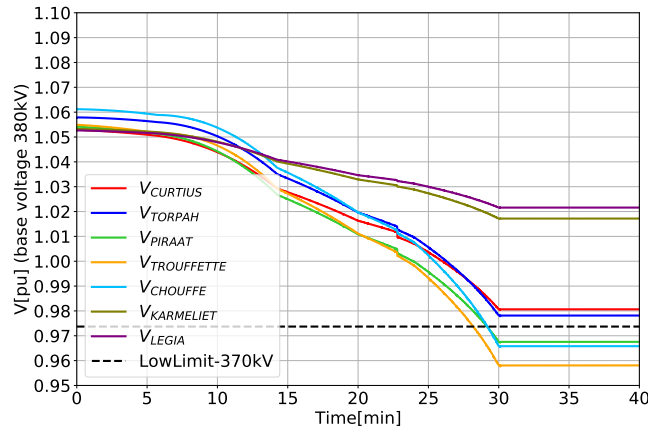


Figure 9.5: **Variant.** *Configuration Q+Automaton version 2*: Voltages at various 380kV buses.

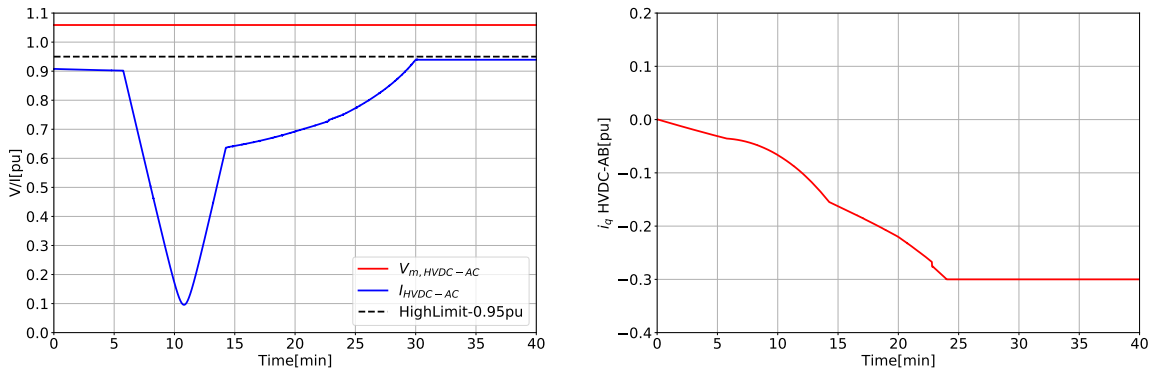


Figure 9.6: **Variant.** *Configuration Q+Automaton version 2*: Modulated voltage and current amplitude of HVDC-AC on the left. Quadrature current of HVDC-AB on the right.

9.5 Influence of the maximum current magnitude of HVDC-AC on the network stability post incident

The tests have been realized with the configuration of line *Post-10* from Table 6.2. The post-fault corrective controls are:

- Reduction of HVDC-AB active power setpoint: from 1000MW to 0MW in 500ms,
- Connection of 1000MVar of capacitor banks at TROUFFETTE,
- Tripping of 300MVar of shunt inductors connected to TROUFFETTE.

The pre-fault configuration is:

- The wind parks WP1 and WP2 are in reactive power control mode,
- There are 300MVar of shunt inductors connected to TROUFFETTE,
- HVDC-AC is in grid forming mode and HVDC-AB is in grid following mode,
- The HVDC links import their nominal active power and the wind parks produce their full active power.

The maximum current magnitude of HVDC-AC has been boosted. Two HVDC-AC configurations are analyzed. The *boosted* HVDC-AC has a maximum current magnitude $I_{max} = 1.015pu$. The *normal* HVDC-AC has a maximum current magnitude $I_{max} = 1pu$. The *boosted* configuration permits the converter to recover the voltage control for a greater current magnitude. One can see in Figure 9.7 that the voltages are restored for the *boosted* HVDC-AC whereas the voltages collapse for the *normal* HVDC-AC. Figure 9.8 shows that the *boosted* HVDC-AC recovers its voltage control for a maximum current magnitude of $1.015pu$. A greater maximum current magnitude allows the converter to control its voltage more quickly and prevents the voltage drop.

The results give indications on the important parameters that can influence the operating point reached after the incident. For a better comprehension, further studies should be done.

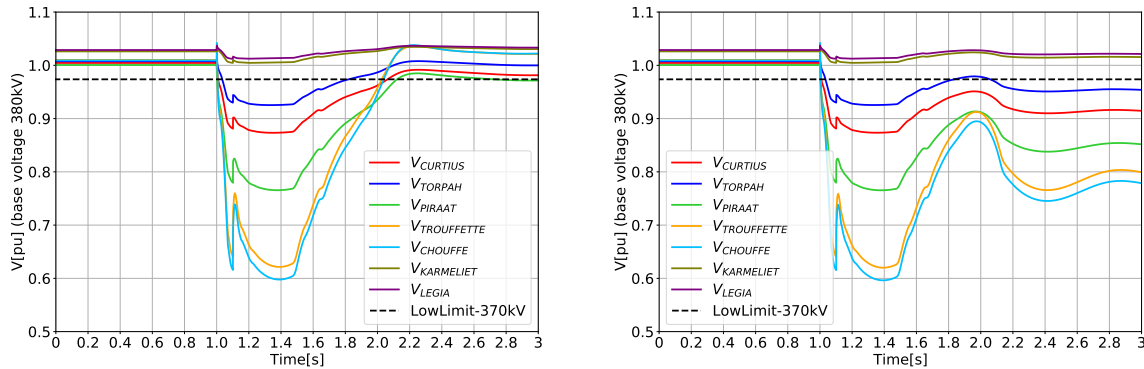


Figure 9.7: Voltages at various 380kV buses. The figure on the left corresponds to the *boosted* HVDC-AC. The figure on the right corresponds to the *normal* HVDC-AC.

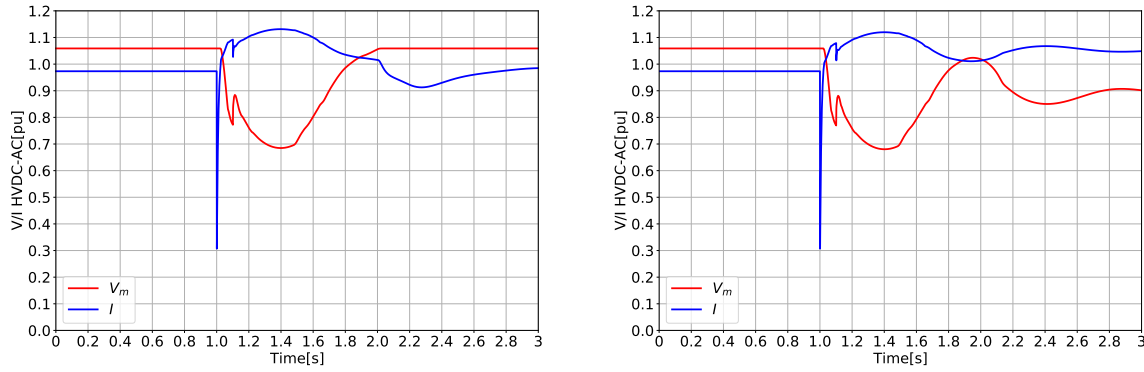


Figure 9.8: Modulated voltage and current magnitude of HVDC-AC. The figure on the left corresponds to the *boosted* HVDC-AC. The figure on the right corresponds to the *regular* HVDC-AC.

9.6 *Scenario 1*: Influence of HVDC-AC synthetic inertia on the active power production and voltage phasors

Figure 9.9 shows that for smaller synthetic inertias, the active power production reaches more quickly 0MW. It attained 0MW under 800ms as expected for $H=0.01s$.

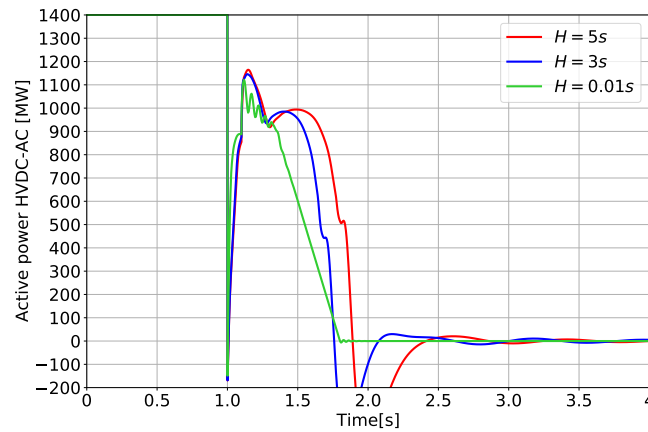


Figure 9.9: **Influence of synthetic inertia H .** *Scenario 1*: Active power production of HVDC-AC.

One can observe in Figure 9.10 that, for smaller synthetic inertias, the voltage magnitude is restored in less time. On the other hand, it drops faster, and some oscillations can be seen. The voltage angle increases more steeply, and some oscillations appear. In the tests realized, the system does not suffer from the loss of inertia. Nevertheless, further studies with EMTP software should be done to ensure the stability of every network component. The oscillations seen for low synthetic inertia may be amplified if the simulations are done with more detailed models.

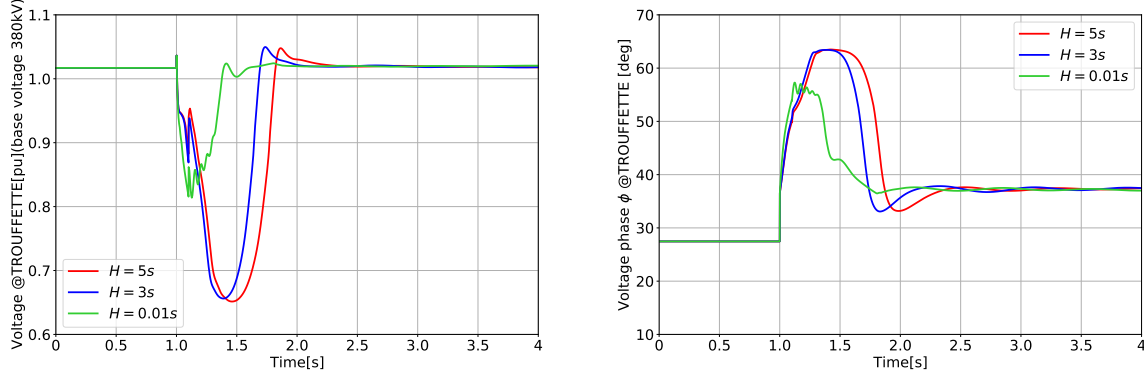


Figure 9.10: **Influence of synthetic inertia H .** *Scenario 1:* Amplitude and phase angle of the TROUFFETTE voltage.

9.7 *Scenario 3:* Influence of the maximum ramping rate of HVDC-AB direct current and the value of the synchronous condensers gain on the voltages of the wind parks

Figure 9.11 shows that for a larger synchronous condenser gain, the voltages of the wind parks remain within the FRT. For the same voltage drop, the synchronous condensers reaction are stronger with a greater gain.

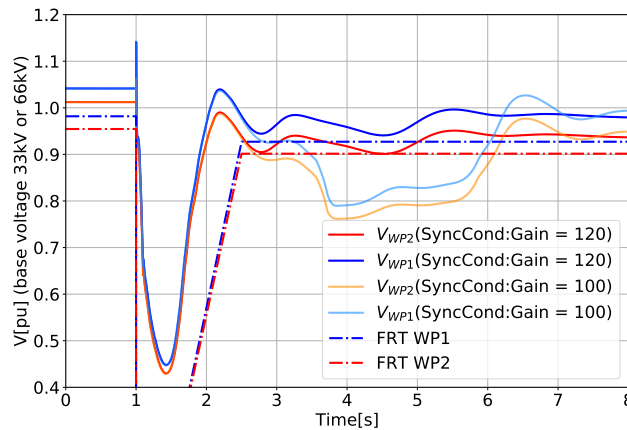


Figure 9.11: **Influence of the synchronous condensers gain.** *Scenario 3:* Voltages of the wind parks.

Figure 9.12 illustrates the impact of $\frac{di_d}{dt}^{max}$. The active power of HVDC-AB is more quickly restored for a larger ramping rate. It leaves less time for the converters to adjust their reactive power output as the system is quickly reloaded. Thus, it is more difficult to restore the voltages.

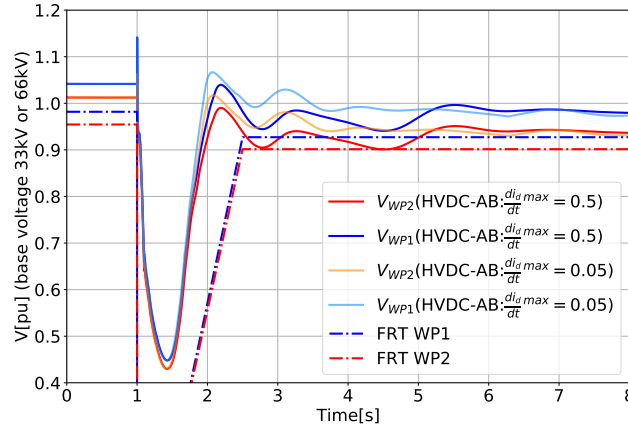


Figure 9.12: **Influence of the maximum ramping rate of HVDC-AB direct current.** *Scenario 3:* Voltages of the wind parks.

9.8 Network post *Ramping event*: Preventive actions to ensure a safe system

Table 9.1 shows the active power reductions that are to be applied before the incident to ensure a safe system. For the wind parks in voltage control mode, the preventive actions may be small enough to limit the cost. Indeed, there is a cost associated with those actions. Constraining the active power injection of the HVDC links increases the cost of electricity in the different control areas. The loss of the green circuits is a rare incident, but one should realize the preventive actions every time the system is highly loaded, which is frequent. A cost-benefit analysis should answer the question: *Could the cost of the preventive actions mitigate the cost associated with the loss of the green circuits?*

The preventive actions should also be compared with the post-fault corrective controls. What is the cost associated with the post-fault corrective controls, and what are the chances for them to fail? They are more chances to make the system collapses with the post-fault corrective controls. They are more likely to fail than preventive actions. The preventive actions thus increase the security margin but with an extended cost. The preventive actions are too costly for the wind parks in reactive power control mode and voltage control mode. For an active power reduction of HVDC-AB, one should preventively limit the power injection to 0MW, which is not conceivable.

Finally, the table shows only some preventive actions for specific scenarios. Contingency analysis has to be frequently realized to determine the necessary preventive actions.

ΔQ^{nom} injected at TROUFFETTE[MVar]	ΔQ^{nom} injected at CHOUFFE[MVar]	ΔP HVDC-AC [MW]	ΔP HVDC-AB [MW]
900	300	-200	0
900	300	0	-200
300	300	-800	0
300	300	0	-1000

Table 9.1: Wind park configurations are defined as following: Voltage control, WP1 in reactive power control, WP2 in voltage control.

Chapter 10

Bibliography

- [1] A. G. Abo-Khalil. Impacts of wind farms on power system stability. *Modeling and Control Aspects of Wind Power Systems*, pages 133–51, 2013.
- [2] A. Adib, B. Mirafzal, X. Wang, and F. Blaabjerg. On stability of voltage source inverters in weak grids. *Ieee Access*, 6:4427–4439, 2018.
- [3] A. Buatois, M. Gibescu, B. G. Rawn, and M. A. Van der Meijden. Analysis of north sea offshore wind power variability. *Resources*, 3(2):454–470, 2014.
- [4] N. A. Cutululis, N. K. Detlefsen, and P. E. Sørensen. Offshore wind power prediction in critical weather conditions. In *10th International Workshop on Large-Scale Integration of Wind Power into Power Systems as well as on Transmission Networks for Offshore Wind Farms*. Energynautics GmbH, 2011.
- [5] T. Demiray. *Simulation of power system dynamics using dynamic phasor models*. PhD thesis, ETH Zurich, 2008.
- [6] E. Ela and B. Kirby. Ercot event on february 26, 2008: Lessons learned. Technical report, National Renewable Energy Lab.(NREL), Golden, CO (United States), 2008.
- [7] Elia. Rfg requirements of general application. Elia.be, Aug. 2019. [Online; accessed 29-May-2021].
- [8] ELIA and 3E. Study report on offshore integration. Elia.be, 2018. [Online; accessed 8-January-2021].
- [9] C. Eping, J. Stenzel, M. Pöller, and H. Müller. Impact of large scale wind power on power system stability. In *Proceedings of the 5th International Workshop on Large-Scale Integration of Wind Power and Transmission Networks for Offshore Wind Farms*, pages 1–9, 2005.
- [10] C. Ferreira, J. Gama, L. Matias, A. Botterud, and J. Wang. A survey on wind power ramp forecasting. Technical report, Argonne National Lab.(ANL), Argonne, IL (United States), 2011.
- [11] C. Gallego-Castillo, A. Cuerva-Tejero, and O. Lopez-Garcia. A review on the recent history of wind power ramp forecasting. *Renewable and Sustainable Energy Reviews*, 52:1148–1157, 2015.

- [12] P. S. Georgilakis. Technical challenges associated with the integration of wind power into power systems. *Renewable and Sustainable Energy Reviews*, 12(3):852–863, 2008.
 - [13] F. Gonzalez-Longatt, E. Chikuni, and E. Rashayi. Effects of the synthetic inertia from wind power on the total system inertia after a frequency disturbance. In *2013 IEEE International Conference on Industrial Technology (ICIT)*, pages 826–832. IEEE, 2013.
 - [14] I. W. Group et al. Ieee guide for planning dc links terminating at ac locations having low short-circuit capacities, 1997.
 - [15] T. Guardian. Wind power generates 140 <https://www.theguardian.com/environment/2015/jul/10/denmark-wind-windfarm-power-exceed-electricity-demand>, July 2015. [Online; accessed 28-May-2021]].
 - [16] Q. Guo, H. Sun, B. Wang, B. Zhang, W. Wu, and L. Tang. Hierarchical automatic voltage control for integration of large-scale wind power: Design and implementation. *Electric Power Systems Research*, 120:234–241, 2015.
 - [17] A. D. Hansen and G. Michalke. Fault ride-through capability of dfig wind turbines. *Renewable energy*, 32(9):1594–1610, 2007.
 - [18] N. Hatziaargyriou, J. Milanovic, C. Rahmann, V. Ajjarapu, C. Canizares, I. Erlich, D. Hill, I. Hiskens, I. Kamwa, B. Pal, et al. Definition and classification of power system stability revisited & extended. *IEEE Transactions on Power Systems*, 2020.
 - [19] H. Ibrahim, M. Ghandour, M. Dimitrova, A. Ilinca, and J. Perron. Integration of wind energy into electricity systems: technical challenges and actual solutions. *Energy Procedia*, 6:815–824, 2011.
 - [20] P. C. Kalverla, G.-J. Steeneveld, R. J. Ronda, and A. A. Holtslag. An observational climatology of anomalous wind events at offshore metemast ijmuiden (north sea). *Journal of Wind Engineering and Industrial Aerodynamics*, 165:86–99, 2017.
 - [21] B. Karthikeya and R. J. Schütt. Overview of wind park control strategies. *IEEE Transactions on Sustainable Energy*, 5(2):416–422, 2014.
 - [22] G. Li, X. Hu, Y. Li, G. Yang, and L. Bai. Influences of large scale wind farm centralized access on power system voltage stability. In *2020 IEEE 5th Information Technology and Mechatronics Engineering Conference (ITOEC)*, pages 1395–1399. IEEE, 2020.
 - [23] Y. Li, Y. Chi, Z. Wang, et al. Study on lvrt capability of d-pmsg based wind turbine. In *Power Engineering and Automation Conference (PEAC)*, pages 154–157, 2011.
 - [24] J. O. S. . P. B. Meridian. Performance upgrades of operational wind turbines, 2014.
 - [25] M. P. Palsson, T. Toftevaag, K. Uhlen, and J. O. G. Tande. Large-scale wind power integration and voltage stability limits in regional networks. In *IEEE Power Engineering Society Summer Meeting*, volume 2, pages 762–769. IEEE, 2002.
-

- [26] M. Paolone, T. Gaunt, X. Guillaud, M. Liserre, S. Meliopoulos, A. Monti, T. Van Cutsem, V. Vittal, and C. Vournas. Fundamentals of power systems modelling in the presence of converter-interfaced generation. *Electric Power Systems Research*, 189:106811, 2020.
- [27] L. Papangelis, M.-S. Debry, T. Prevost, P. Panciatici, and T. Van Cutsem. Stability of a voltage source converter subject to decrease of short-circuit capacity: A case study. In *2018 Power Systems Computation Conference (PSCC)*, pages 1–7. IEEE, 2018.
- [28] T. Qoria. Grid-forming control to achieve a 100% power electronics interfaced power transmission systems.electric power. hesam université. english. nnt:2020hesae041. tel-03078479. 2020.
- [29] T. Qoria, E. Rokrok, A. Bruyere, B. François, and X. Guillaud. A pll-free grid-forming control with decoupled functionalities for high-power transmission system applications. *IEEE Access*, 8:197363–197378, 2020.
- [30] R. Rosso, M. Andresen, S. Engelken, and M. Liserre. Analysis of the interaction among power converters through their synchronization mechanism. *IEEE Transactions on Power Electronics*, 34(12):12321–12332, 2019.
- [31] X. Wang, F. Blaabjerg, and W. Wu. Modeling and analysis of harmonic stability in an ac power-electronics-based power system. *IEEE Transactions on Power Electronics*, 29(12):6421–6432, 2014.
- [32] Y. Wang, Z. Li, and F. Lu. Research on the impact of wind power integration on power system voltage stability. In *2019 IEEE Innovative Smart Grid Technologies-Asia (ISGT Asia)*, pages 1683–1687. IEEE, 2019.
- [33] WindEurope. Wind energy in europe in 2019 - trends and statistics. <https://windeurope.org/data-and-analysis/product/wind-energy-in-europe-in-2019-trends-and-statistics/#overview>, accessed on 03 November 2020.
- [34] J. Z. Zhou, H. Ding, S. Fan, Y. Zhang, and A. M. Gole. Impact of short-circuit ratio and phase-locked-loop parameters on the small-signal behavior of a vsc-hvdc converter. *IEEE Transactions on Power Delivery*, 29(5):2287–2296, 2014.